Permissive and decisive roles of *Hox* code genes in limb induction

Dissertation

zur

Erlangung des Doktorgrades (Dr. rer. nat.)

der

Mathematisch-Naturwissenschaftlichen Fakultät

der

Rheinischen Friedrich-Wilhelms-Universität Bonn

vorgelegt von

Yajun Wang

aus Shandong, China

Bonn 2022

Angefertigt mit Genehmigung der Mathematisch-Naturwissenschaftlichen Fakultät der Rheinischen Friedrich-Wilhelms-Universität Bonn

1. Gutachter: Prof. Dr. med. Ruijin Huang

2. Gutachter: Prof. Dr. Thomas Bartolomaeus

Tag der Promotion: 20. Juli 2022

Erscheinungsjahr: 2022

Table of contents

Index of Tables and Figures

Tables

Figures

Abbreviations

AER	apical ectodermal ridge
AP	anterior-posterior
AP	alakaline phosphatase
bp	base pair
C	cervical
CDS	coding DNA sequence
DEPC	diethylpyrocarbonate
DIG	Digoxigenin
DMSO	dimethylsulfoxide
DV	dorsal-ventral
EGFP	enhanced green fluorescent protein
EMT	epithelial-to-mesenchymal transition
FGF	fibroblast growth factor
Fig.	Figure
HH	Hamburger and Hamilton
HOS	Holt-Oram Syndrome
Hox	homeobox
IM	Intermediate mesoderm
ISH	In Situ Hybridization
L	lumbar
LPM	lateral plate mesoderm
M	Molar weight
µl	microliter
µg	microgram
ml	milliliter
mm	micro meter
ms	millisecond
NT	Neural tube
PBS	phosphate buffered saline
PBS	Phosphate Buffered Saline
PCR	Polymerase chain reaction

PD	Proximal-distal
PFA	Paraformaldehyde
PG	Paralogue group
PS	Primitive streak
RA	Retinoic acid
Raldh2	Retinaldehyde dehydrogenase-2
RNA-seq	RNA sequencing
RPKM	Reads Per Kilobase of transcipt per Million mapped reads
RQN	RNA Qulity Numbers
Shh	Sonic hedgehog
SSC	Standard saline citrate
T	Thoracic
V	Volt
ZPA	Zone of polarizing activity

Summary

Vertebrates display positional identities along the head-to-tail axis. The forelimb is one of the characteristics among them that shows its specific position at the interface between the cervical and thoracic region independent of the length of the neck of animals. The axial identities, including limb positioning, are determined by the temporal and spatial collinearity expression pattern of *Homeobox* (*Hox*) genes. This can be realized through their collinearity activation during gastrulation. *Hox PG 4-5* genes, whose down-regulation in mice induces homeotic transformations in the cervical-thoracic interface, activate *Tbx5* transcription. *Tbx5* is the first factor to initiate forelimb bud formation from the dorsal layer of the lateral plate mesoderm. The expression of *Hox PG 9* inhibits *Tbx5* expression, thus limiting the posterior boundary of the forelimb. However, which *Hox* genes determine the anterior boundary of the forelimb is still not clear. Considering the expression pattern of *Hox PG 6-7* genes during forelimb induction, I hypothesized that *Hox PG 6-7* genes participate in regulating the anterior forelimb boundary. The hypothesis was experimentally performed in chick embryos. Before manipulating gene expression, I first identified the prospective wing region using DiI and EGFP labeling approaches and found that the wing-forming mesoderm maintains its axial level from generation to differentiation. The anterior boundary of the wing bud is located at the level of the prospective somite 15/16. Then, I electroporated constructs expressing *Hox PG 6-7* into the dorsal lateral plate mesoderm anterior to the prospective wing region. This ectopic expression caused additional wing buds formation anterior to the endogenous ones. *In situ* hybridization and mRNA sequencing data indicated that the ectopic wing buds have partial similarities to the normal wing bud. Hence, *Hox PG 6-7* are sufficient to induce forelimb buds. To demonstrate the functional correlation of *Hox PG 4-5* and *Hox PG 6-7* genes, the dominant-negative form of *Hoxb4* was electroporated into the prospective wing mesoderm, resulting in a flattened wing bud. This observation identified the necessity of *Hox PG 4-5* genes in forelimb induction. In summary, the anterior boundary of the forelimb is regulated by two functionally distinct *Hox* gene groups. While *Hox PG 4-5* genes initiate *Tbx5* expression, *Hox PG 6-7* genes maintain *Tbx5* expression to instruct the forelimb formation. This permissive and decisive induction would be a general mechanism for the combinatory functions of a *Hox* code for morphogenesis and organogenesis.

1 Introduction

The term ‘axial identity’ describes the fact that tissues and organs are specified in a region-specific manner along the anterior-to-posterior or head-to-tail axis of the human or animal body (Jeannotte et al., 1993). This is most obvious by comparing the vertebrae of the spinal column. Axial identity is regulated by a set of genes, with a specific cluster, the *homeobox* (*Hox*) genes, being of particular importance (Kessel and Gruss, 1991). *Hox* genes, a family of transcription factors characterized by the ‘homeo-box’, are expressed with defined segmental anterior borders along the body axis (Kessel and Gruss, 1990). This holds true for both invertebrates and vertebrates. Originally performed in *Drosophila melanogaster*, numerous studies on the developmental regulation of axial identity are now carried out in vertebrates (Nüsslein-Volhard and Wieschaus, 1980; Nüsslein-Volhard et al., 1984). The most common methods are experimental micro-manipulations and reverse genetic approach. Chicken and mouse embryos are vertebrate models for the investigation of axial development, including the positioning of the extremities. The forelimb and hindlimb also have their specific axial levels. The posterior (caudal) boundary of the forelimb is regulated by paralogous *Hox4* and *Hox9* genes (Moreau et al, 2019). However, it is yet unknown yet how the anterior (cranial) boundary is determined. In this study, I focused on wing bud induction in chicken embryos, aiming to identify *Hox* genes that determine the anterior boundary of the forelimb.

1.1 Axial identities

1.1.1 Determination of axial identities during gastrulation

The best example to describe axial identity is the specific morphology of vertebrae along the anterior-posterior (AP) axis of the body. During development, the first five somites are incorporated into the occipital region of the skull (Lim et al, 1999). The following somites are included in the development of the trunk and form cervical, thoracic, lumbar, sacral, and coccygeal/caudal vertebrae (Burke, 2000; Nowicki and Burke, 2000). Accordingly, each vertebra is formed from two adjacent somites. The anterior half of the vertebra is derived from the posterior half of the somite and its posterior half from the anterior half of the next caudal somite (Burke et al., 1995). For example, the first cervical vertebrae is developed from the posterior half of somite 5 and the anterior half of somite 6 (Fig. 1).

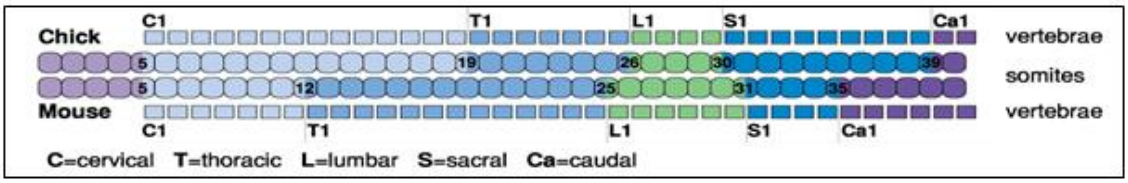

Fig. 1: Diagram for body plan with vertebrae and related somites in the chick and mouse (Burke et al., 1995). Somites and vertebrae levels are shown by number.

Different vertebrate classes have distinct vertebrae formulas. Chicken have 14 cervical, 7 thoracic, 12-13 lumbosacral, and 5 coccygeal/caudal vertebrae. Mice have 7 cervical, 13 thoracic, 6 lumbar, 4 sacral, and a variable number of coccygeal/caudal (20+) vertebrae (Fig. 1) (Burke et al., 1995). The pectoral fin in zebrafish is the homologous organ to the forelimb in mouse or the wing in chicken. The axial level of the forelimb among vertebrate classes is highly conserved and always located at the region of the cervical-thoracic interface or the anterior tip of the trunk (Fig. 2) (Burke et al., 1995; Molven et al., 1990).

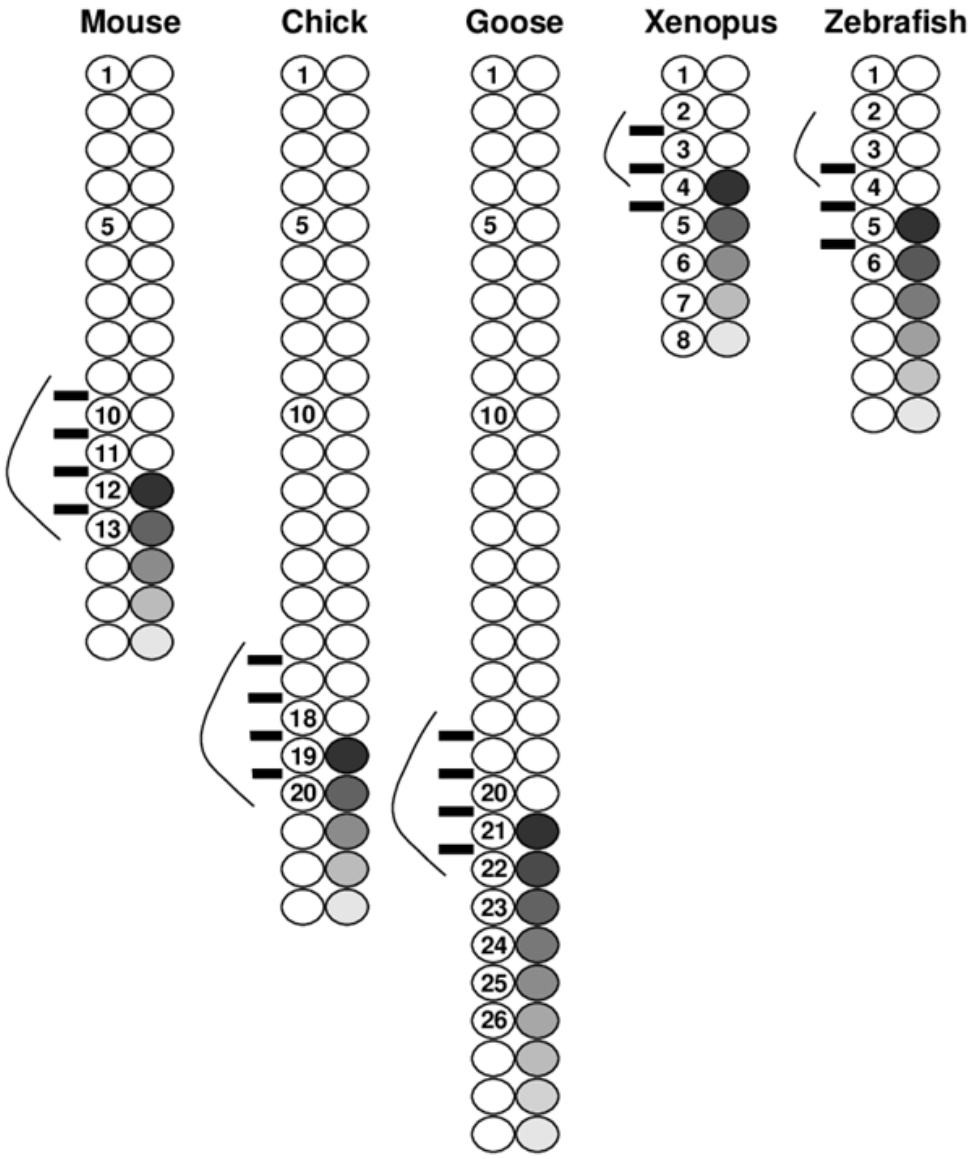

Fig. 2: Diagram for somites and related *Hox* genes (Burke et al., 1995). The spinal nerves are indicated by black bars. The limb bud or fin bud is indicted by curved line. The expression level of Hoxc6 is shown by shaded circles. Somites levels are shown by numbers.

The blueprint of the embryonic body plan and its subsequent morphogenesis is laid down during the progression of gastrulation (Tam and Behringer, 1997). It consists of the ingression of the prospective mesoderm and endoderm and the migration of cells to their ultimate positions (Chuai and Weijer, 2008, 2009; Downs, 2009; Mikawa et al., 2004). Ingression mainly occurs in the primitive streak (PS), which is formed in the midline region of the gastrula (Lawson et al., 2001), and the Hensen's node (Charrier and Teillet, 1999; DeRuiter, Corinne, 2011). At the end of gastrulation, most embryonic cells are determined for their final fates. During further differentiation, the axial skeleton-muscular system, including the

vertebral column and the muscles of the back, become distinct along the AP axis (Bellairs and Osmond, 2005). This ‘rule’ is also true for the spinal cord, gut, heart and other organs which are specified along the AP axis during embryonic development (Bellairs and Osmond, 2005).

The three germ layers, derived from epiblast and hypoblast, are the definitive ectoderm, mesoderm and endoderm (Fig. 3) (Bellairs and Osmond, 2005). The ectoderm mainly gives rise to the epidermis and neural tissues. Beneath the ectoderm is mesoderm, which can be subdivided into axial notochord, paraxial mesoderm (somites), intermediate mesoderm (IM) and lateral plate mesoderm (LPM) (Fig. 3) (Bellairs and Osmond, 2005). The somites are the first segmental structures, arranged on the left and right sides of the notochord (Chuai and Weijer, 2009). The first pair of somites in chicken is formed during HH-stage 7 (after 24 h of incubation; according to Hamburger and Hamilton, 1951) (Hamburger and Hamilton, 1951) and others are formed successively in an anterior-to-posterior order. The region posterior to the last newly-formed somite is the presomitic mesoderm (PSM) for pre-segmented somite formation (Bellairs and Osmond, 2005).

The LPM is located laterally to the IM and consists at first of one layer of cells, which is then subsequently separated into two layers. The dorsal layer, beneath the ectoderm, is the somatic LPM and the ventral layer is the splanchnic LPM adjacent to the endoderm (Fig. 3) (Bellairs and Osmond, 2005). Between the two layers is the coelom, which gives rise to the body cavity. Forelimb and hindlimb become visible by a thickening of the somatic LPM at specific axial levels (Tickle, 2015). Endodermal cells generate the lining of the gastrointestinal and respiratory tracts (DeRuiter, Corinne, Doty, 2011).

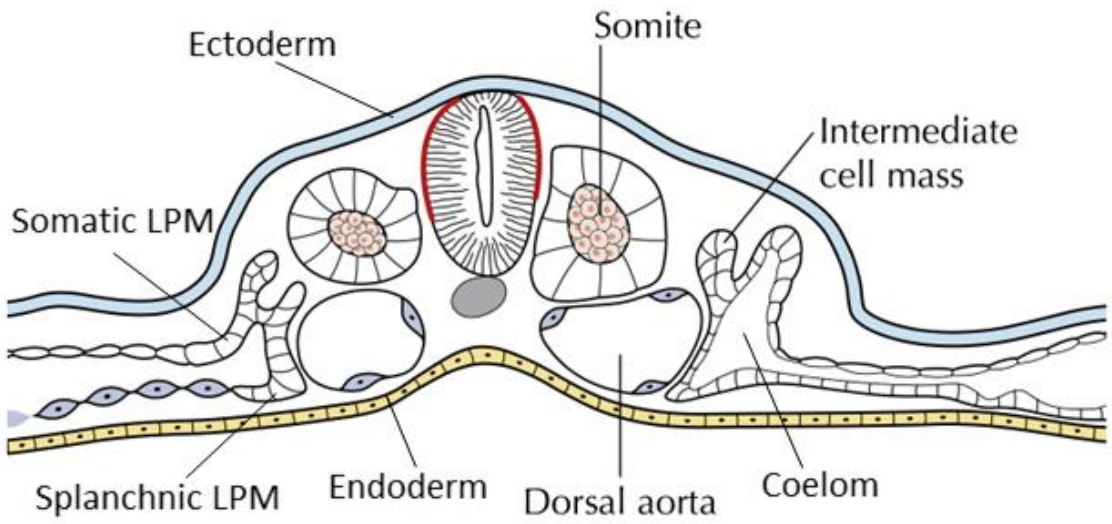

Fig. 3: Diagram showing the anatomy of embryo by transverse section (Bellairs and Osmond, 2005).

Due to the easy access, chicken embryos are amendable by molecular techniques (genetic manipulations) and *in ovo* and *ex ovo* manipulations, as well as observable by live imaging techniques (Vilches-Moure, 2019). The standard description of chick embryonic development is by Hamburger and Hamilton (1951) (Hamburger and Hamilton, 1951). Gastrulation of chick embryos starts at HH-stage 2 and proceeds to HH-stage 11, when the prospective limb fields can be determined (Moreau et al., 2019).

As discussed above, during gastrulation precursor cells are formed along the AP axis for e.g. the neural tube, paraxial mesoderm, LPM and extraembryonic mesoderm (Fig. 4). This takes place in a collinear fashion of the activation of *Hox* genes (Iimura and Pourquie, 2006). The forelimb precursor cells and their axial position are specified by the same process (Moreau et al., 2019).

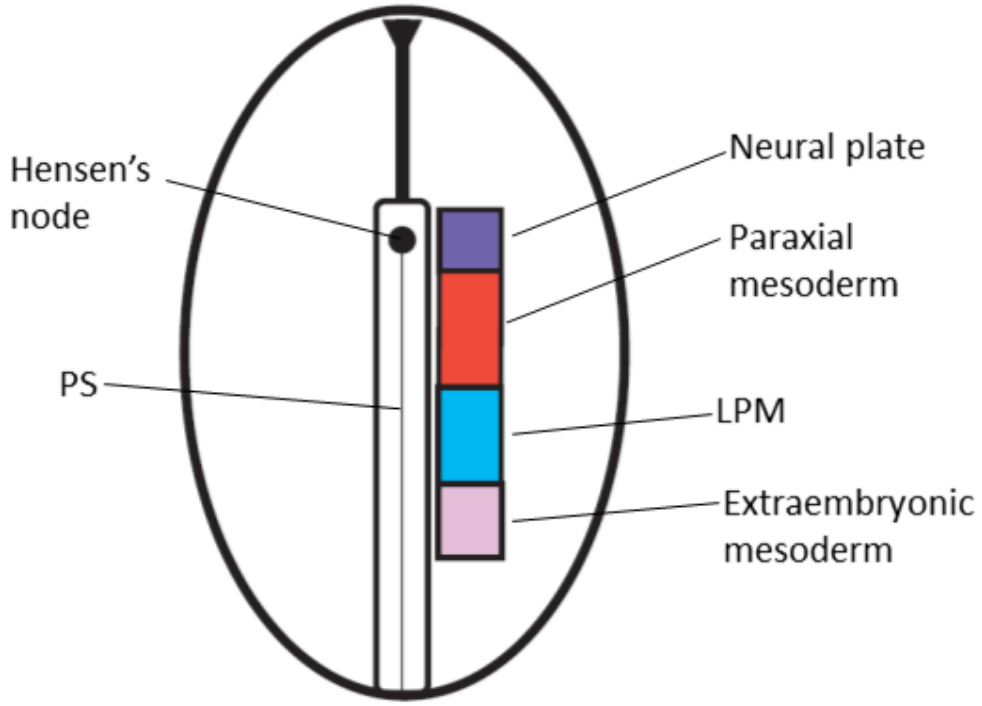

Fig. 4: Diagram showing a fate map of epiblast cells (Iimura and Pourquie, 2006).

1.1.2 Regulation of axial identities through *Hox* genes

Regionalization of the body in various vertebrate classes is regulated by homologous mechanisms although their morphologies are distinct; e.g. the mouse has a short neck and the chicken a long neck. Regionalization is controlled by a specific pattern of *Hox* genes and each somite has a nested *Hox* gene pattern (McIntyre et al., 2007). The combined activity of *Hox* genes relates to distinct cell behavior and morphogenesis by gene regulation, which remains incompletely understood (Böhmer, 2017; Böhmer et al., 2015a, b). Patterning by *Hox* genes is found in various organ systems including gut, urogenital, as well as the nervous system (Barak et al., 2012; Wellik, 2007).

1.1.2.1 The expression pattern of *Hox* genes

Homeobox (*Hox*) genes, first discovered in *Drosophila* (Lewis, 1978), encode a family of transcription factors which regulate the morphogenesis of embryonic tissues (Zakany and Duboule, 2007). Mutations of *Hox* genes, including gain-of- and loss-of-function, can result in 'homeotic transformations' of vertebrae in mice (Mallo, 2018; Mallo et al., 2010). Overexpression or negative expression can induce positional shifting along the AP axis in chicken (Cohn et al., 1997; Moreau et al., 2019; Nelson et al., 1996).

Hox genes are named after their conserved homeodomain (homeobox), which is a region of 183bp, encoding a highly conserved DNA-binding domain of 61 amino acids (Kessel and Gruss, 1990; Pick, 2016). There are 39 *Hox* genes organized in 4 clusters (A, B, C, D) (Fig. 5). Each cluster is located in one chromosome, including chromosomes 6, 11, 15 and 2, and has up to 13 paralogue groups (*Hox PG 1-13*) (Fig. 5) (Gaunt and Strachan, 1996). Each PG is located at the same homologous region in different clusters and has redundant functions (Burke, 2000). Each *Hox* gene has its specific expression domain, but the exact level of the expression domain may differ in different organ anlagen, such as in the NT, somite, IM, and LPM cells at a particular developmental stage (Barak et al., 2012; Cohn et al., 1997). Furthermore, their expression domains are not fixed during embryonic development, such that 5' *Hox* genes can show regression of their expression pattern in the NT. Furthermore, the expression patterns of 3' genes and 5' genes have distinct reactions to different signaling treatment (Bel-vialar et al., 2002).

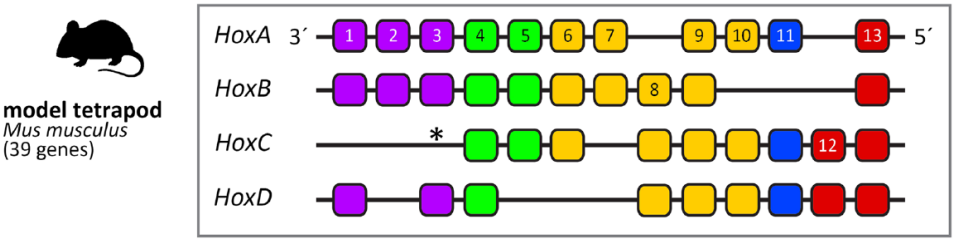

Fig. 5: *Hox* genes in mice (Boehmer et al., 2015b). Occipital: purple; cervical: green; thoracic: orange; scral: blue; caudal: red. *Hoxc3 exists in lizards and snakes, but not in birds and placental mammals.

In general, *Hox* genes show temporal and spatial collinearity of their expression patterns in vertebrates (Bel-Vialar et al., 2002; Duboule and Dollé, 1989; Kessel and Gruss, 1990; Kessel and Gruss, 1991). The temporal collinearity means that Hox genes are sequentially activated in a 3' to 5' direction along their chromosomal sequence and *Hox* genes in 3' location are activated earlier than those in the 5' position. In chick embryos for example, expression of the *Hoxb* cluster is initiated at HH-stage 3 with *Hoxb1*, followed at HH-stage 3+ by *Hoxb2*, HH-stage 4 by *Hoxb3*, HH-stage 5 by *Hoxb5*, and HH-stage 6 by *Hoxb8* (Barak et al., 2012). The spatial collinearity indicates that early activated *Hox* genes are expressed at a more anterior/cranial level along the AP axis, whereas later activated *Hox* genes are expressed in a more posterior/caudal region; e.g. *Hox PG 1-3* genes are expressed in the head region and

Hox PG 13 genes in the tail bud (Fig. 6). Usually the anterior expression boundary is used to define the expression domain, for example in chicken embryos, *Hoxb4* at somite level 6-7, *Hoxb6* at somite level 19-20 and *Hoxb9* at somite level 21-22 (Fig. 6) (Barak et al., 2012; Bel-Vialar et al., 2002; Burke et al., 1995;). Although the dynamic collinear expression of *Hox* genes is exemplified, there are a few exceptions of independent expression, as in the IM (Barak et al., 2012).

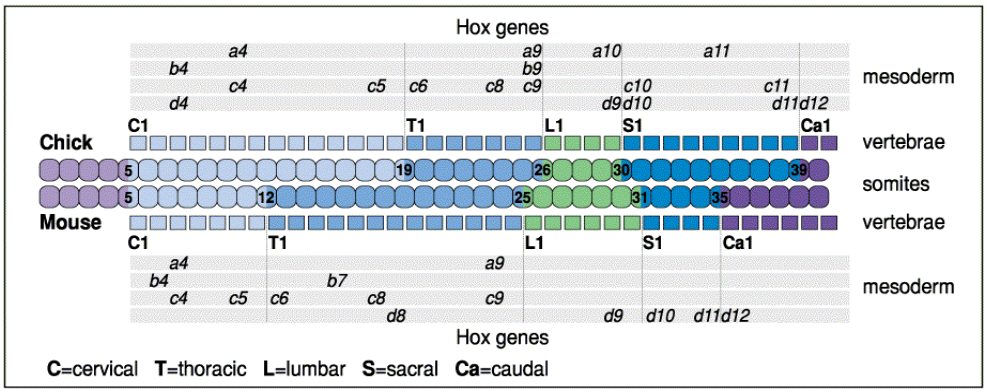

Fig. 6: Diagram of vertebrae and related *Hox* genes in chick and mouse (Burke et al., 1995). The levels of the anterior expression boundaries of *Hox* genes in the somites are shown by their names. The somite level is shown by number.

1.1.2.2 Occipital skull shows *Hox PG 1-3* expression

Hoxa1 is the first gene to be detected at HH-stage 3 in chicken embryos. Its expression covers the posterior two-thirds of the PS during gastrulation (Barak et al., 2012). *Hoxb1* is first detected at HH-stage 4 and expressed along the entire PS of HH-stage 5, except for the Hensen's node (Gaunt and Strachan, 1996). *Hoxb2* is expressed in the posterior PS of HH-stage 3 and then mainly in the neural plate and NT. *Hoxb3* expression is initiated at HH-stage 4 in the posterior half of the PS and in the PSM and neural plate at HH-stage 8 (Gouveia et al., 2015). *Hoxd3* is first expressed at HH-stage 3, but only weakly in the posterior PS around HH-stage 4; however, at HH-stage 10, *Hoxd3* is expressed strongly in the entire NT without any expression in the IM or LPM (Barak et al., 2012). In general, *Hox PG 1-3* genes are activated in the earlier stages and located in the most anterior parts of the embryos. Their expression has anterior boundaries in the head region and they have the strongest expression in the NT. They mainly regulate the hindbrain formation (Krumlauf, 2016; Wellik, 2009).

1.1.2.3 The cervical vertebrae show *Hox PG 4-5* expression

In chicken embryos, *Hoxa4* and *Hoxb4* are first detected at HH-stage 4 covering two-thirds of the PS (Barak et al., 2012). *Hoxc4* is first detected at HH-stage 9 with the expression from the level of somite 2 posteriorly in the NT. *Hoxd4* is maintained strongly in the NT at the level of somite 1-9; in the somites, its anterior boundary is somite 6/7 and it is faintly expressed in the LPM (Barak et al., 2012; Burke et al., 1995). The expression pattern of *Hox PG 4* in mice is different from those in chicken because of the different length of their necks. After formation of forelimb and wing in mice and chicken, respectively, *Hoxa4* and *Hoxc4* share the same anterior boundary, at somite 7-8 (cervical 3, C3) in mice and somite 10-11 (C6) in chicken. Similarly, *Hoxb4* and *Hoxd4* have the same anterior expression boundary at somite 6-7 (C2) in mice but somite 7-8 (C3) in chicken (Burke et al., 1995). *Hox PG 4* is conserved in the formation of cervical vertebrae (Burke et al., 1995). Overexpression of *Hoxa4* and *Hoxd4* induce cervical vertebrate transformation (Horan et al., 1994; Horan et al., 1995b). Both *Hoxb4* and *Hoxd4* single mutant mice show an anterior transformation of C2 to C1 and even an anterior transformation of C3 to C2 (Horan et al., 1995b; Ramfrez-Solis et al., 1993). *Hoxa4* also has an effect on the dorsal-ventral aspect of the cervical vertebrae (Horan et al., 1994; Kostic and Capecchi, 1994). Besides the homeotic transformations at C1 to C3, *Hox PG 4* single mutation also causes a more posterior transformation at the cervical-thoracic interface at the level of C7 and T1 (Horan et al., 1994; Horan et al., 1995b). Furthermore, there is a dose-dependent increase of transformations in the C1-C3 region from the single mutant to double and triple mutants of *Hox PG 4* genes (Horan et al., 1995a). The dose-dependent increase in transformation also exists in the cervico-thoracic region, when comparing the *Hoxb4* and *Hoxd4* double mutant with the additional *Hoxa4* triple mutant, resulting in shortened cervical vertebrae (Horan et al., 1995a). Hence, *Hox PG 4* genes are necessary for the morphogenesis of the entire cervical vertebrae.

Hox PG 5 genes are expressed posterior to *Hox PG 4* and thus located at the posterior part of the cervical region in chicken, mice and crocodiles (Böhmer et al., 2015a; Burke et al., 1995). *Hoxa5* is restricted at C8-C14 of chicken and *Hoxc5* expression starts posteriorly from C13 (somite 17/18) in chicken, C6 (somite 10/11) in mice and the penultimate cervical vertebrae in the Nile crocodile (Böhmer et al., 2015a; Burke et al., 1995). *Hoxb5* is first detected at HH-stage 4 at the posterior edge of PS and extends anteriorly in LPM precursor cells, as well as in the extraembryonic mesoderm (Gouveia et al., 2015). *Hoxb5* is expressed posteriorly from C2

in chicken, mice and Nile crocodiles (Böhmer et al., 2015a, b). *Hoxa5* has potential in the specification of axial identity and regulates rib repression and/or cervical-thoracic transition (Böhmer et al., 2015a; Chen et al., 2013; Jeannotte et al., 1993; McIntyre et al., 2007). Down-regulation of *Hoxa5* at HH-stage 11-12 of chicken embryos induces cartilage reduction (Chen et al., 2013). Hence, Hox PG 5 genes are related to the formation of posterior cervical vertebrae.

1.1.2.4 The thoracic vertebrae with *Hox PG 6-7* expression

There is no expression of Hoxa6 until HH-stage 6 in chicken embryos (Barak et al., 2012). At HH-stage 12, *Hox PG 6* expression is mainly in the posterior part of the embryo from somite 12 level onwards in the NT, somites and LPM (Bel-Vialar et al., 2002; Gaunt and Strachan, 1996). *Hoxa6*, *Hoxb6* and *Hoxc6* expression have the same anterior boundary at T1 in vertebrate animals, like birds, mice and frogs (Burke et al., 1995). *Hox PG 6* mutation causes the transformation of vertebrae around the cervical-thoracic interface (McIntyre et al., 2007). *Hoxa6* mutation results in a posterior transformation of C7 to T1 (Kostic and Capecchi, 1994). *Hoxb6* mutants show an anterior shift of cervical-thoracic vertebrae from C6 through T1 (Rancourt et al., 1995). *Hoxc6* has a role in the determination of the morphology of thoracic vertebrae in mice (Garcia - Gasca and Spyropoulos, 2000). Hence, the morphogenesis of the cervical-thoracic vertebral region has relations to the function of *Hox PG 6* genes.

The expression of *Hox PG 7* is restricted to the thoracic vertebrae. *Hoxa7* starts at T2 in crocodiles and chicken while at T1 in mice (Burke et al., 1995). At HH-stage 16 of chicken embryos, *Hoxb7* is expressed in the neural crest and in the LPM, including the preliminary wing region (Coelho et al., 1992). *Hoxb7* mutant mice show fusion of the first with the second rib and *Hoxb7* and *Hoxa7* double knockout mice show increased penetrance of this fusion. *Hoxa7* and *Hoxb7* regulate morphogenesis of thoracic vertebrae in a dose-dependent manner (Chen et al., 1998).

1.1.2.5 The lumbar-sacral vertebrae with *Hox PG 8-10* expression

Hoxb8 is expressed in the whole length of PS at HH-stage 4 in chicken embryos (Barak et al., 2012; Gouveia et al., 2015). At HH-stage 11, *Hoxb8* shows a strong expression in LPM posterior to the level of somite 11. *Hoxc8* expression in LPM is very similar.

The anterior *Hoxc8* expression boundary is at T5 in chicken, at T6 in mouse, and at T1 in crocodiles (Böhmer, 2017). Mutations of *Hoxb8*, *Hoxc8*, and *Hoxd8* induce transformations of vertebrae in the thoracic-lumbar region with functional redundancy (van den Akker et al., 2001).

Hox PG 9 is expressed along the AP axis posteriorly from the last thoracic vertebrae of HH-stage 24 chicken embryos, contributing to the thoracic-lumbar transition (Burke et al., 1995). The quadruple mutant of *Hox PG 9* shows an anterior transformation from T8 - L2 into a T7-like phenotype; in the anterior lumbar region, there are fusions of the anterior-most ribs even formation of extra ribs (McIntyre et al., 2007).

The expression of *Hox PG 10* contributes to the transition of lumbar-to-sacral vertebrae in chicken and mice embryos (Burke et al., 1995). *Hoxa10* expression starts at the last thoracic, while *Hoxc10* and *Hoxd10* start at the first sacral vertebrae of chicken embryos; in mice, *Hoxd10* has the same anterior boundary at the first sacral vertebrae (Burke et al., 1995). Mutation of *Hox PG 10* results in an anterior transformation of the lumbar-sacral region to a thoracic-like phenotype with ribs (McIntyre et al., 2007). Together, *Hox PG 8-10* genes are expressed in the thoracic to sacral region and maintain the vertebrae phenotype.

1.1.2.6 Caudal vertebrae show *Hox PG 11-13* expression

Hox PG 11-13 genes are expressed in the posterior part of the embryo and are essential for the posterior trunk formation (Aulehla and Pourquie, 2009). *Hox PG 11* genes are expressed in the sacral vertebra region (Burke et al., 1995; McIntyre et al., 2007). Mutation of *Hox PG 11* causes the entire sacral region to transform into a lumbar-like morphology (Wellik and Capecchi, 2003). Precocious expression of *Hox PG 13* reduces the vertebrae number in the tail bud region (Young et al., 2009). *Hox PG 11-13* genes are important for the body's posterior extension.

1.2 Forelimb development

The early limb bud formation can be characterized by four phases: specification/determination, induction, initiation, and outgrowth (Fig. 7). Regulation of the formation of the forelimb bud during these four phases is described below.

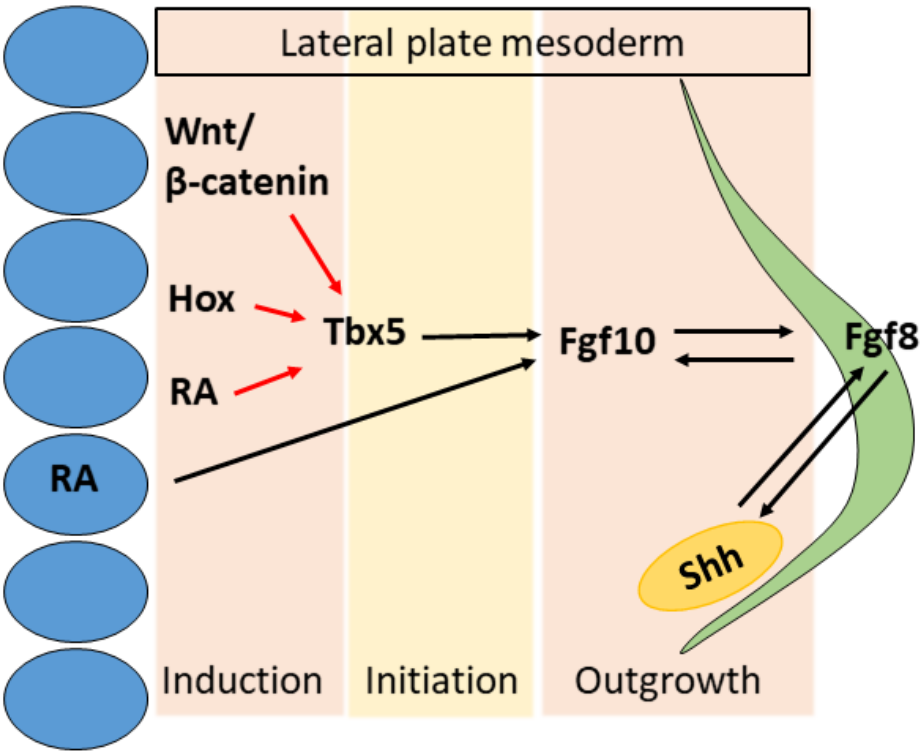

Fig. 7: Diagram showing formation of the early forelimb bud (Nishimoto et al., 2015). Somites are depicted as blue circles. Ectoderm or AER in light green. ZPA as orange circle.

1.2.1 Specification and Determination

The process by which a cell or tissue is committed to developing a specific fate is called determination (Bellairs and Osmond, 2005). The initial, labile determination or the 'presumptive fate' is known as specification (Bellairs and Osmond, 2005). The prospective wing is located at the level posterior to Hensen's node at HH-stage 7-8 of chicken embryos (Chaube, 1959). The wing precursor cells are generated around HH-stage 4-5 when *Hoxb4* is activated (Moreau et al., 2019). The temporal collinearity expression of *Hox PG 4/7/9* genes and their activation or repression determines the position of the wing during gastrulation (Fig. 8) (Moreau et al., 2019). The interface of *Hoxb4* and *Hoxb9* is consistent with the wing positioning in different avian species (Moreau et al., 2019). However, there are still many open questions concerning the position of the forelimb and the regulation of *Hox* genes. In this study, I addressed this question and provide a detailed analysis of this relationship.

Hox PG 4 genes are expressed in the entire neck region, while *Hox PG 5* genes are specifc for the posterior neck region (Burke et al., 1995). Their mutation in mice induce the transformation of cervical vertebrae, especially at the cervical-thoracic interface (Horan et al., 1995a; Horan et al., 1994).

Hoxb5 mutation results in a rostral shift of the shoulder girdle (Rancourt et al., 1995). Furthermore, deletion of all three of *Hox PG 5* genes in mice causes a skeletal defect of the anterior forelimb (Xu et al., 2013). There is a high level of redundancy among *Hox PG 4* and *Hox PG 5* genes in forelimb development (Xu et al., 2013). Negative expression of *Hoxb4* shortens the expression region of *Tbx5* resulting in a truncated HOXB4 protein. This protein retains its binding to paralog-specific co-factors but cannot to bind to target DNA, acting by competing for co-factors (Denans et al., 2015; Gehring et al., 1990). *Hox PG 4-5* genes are activators of forelimb induction thorough initiating *Tbx5* expression (Fig. 8) (Minguillon et al., 2012). However, *Hoxc9* stops the activation of *Tbx5* and determines the posterior boundary of the forelimb (Fig. 8) (Cohn et al., 1997; Nishimoto et al., 2014). *Hoxc9* negative expression in the flank with *Hoxb4* overexpression induces a posterior extension of the forelimb (Moreau et al., 2019). Therefore, the function of *Hox PG 9* is to stop forelimb induction.

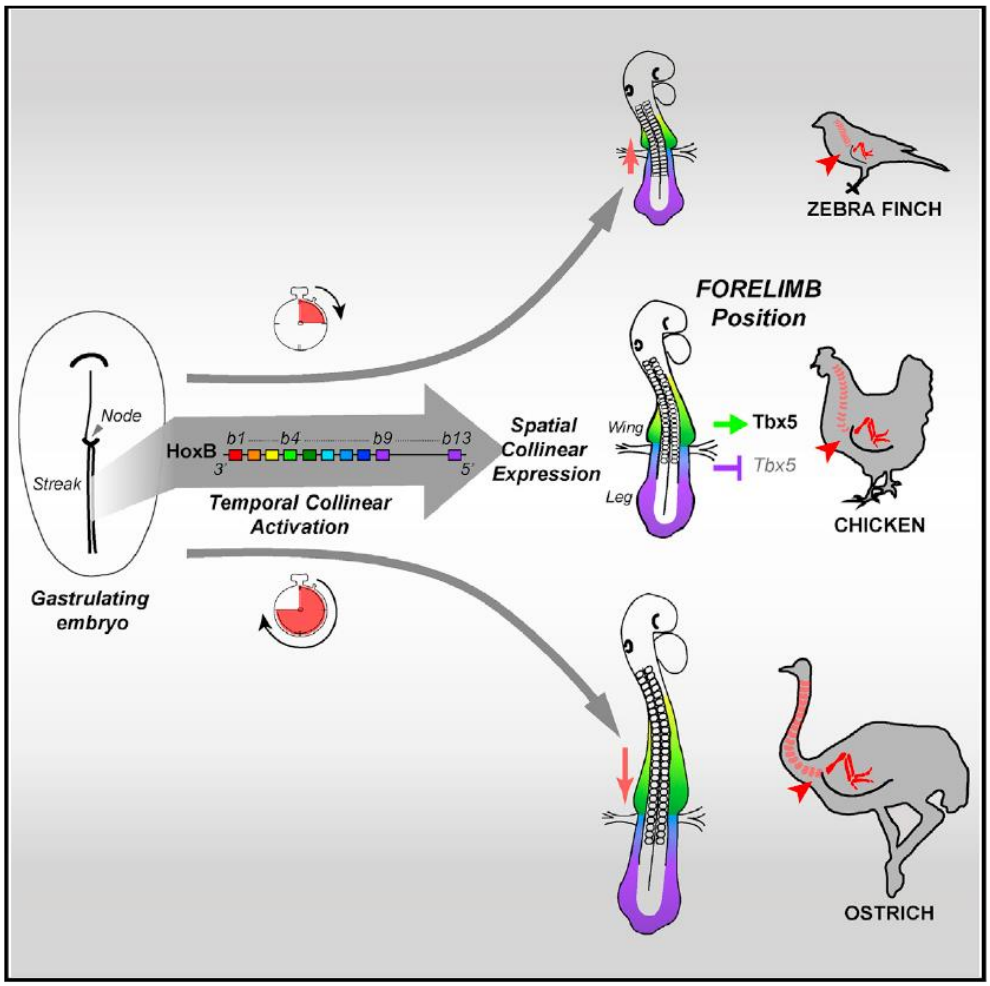

Fig. 8: Temporal collinear expression of *Hox* genes during gastrulation determines wing position (Moreau et al., 2019). *Hoxb4* (light green) induces *Tbx5* expression for the wing formation, while *Hoxb9* (purple) inhibits *Tbx5* expression. Activation of *Hoxb4* among three avian species is shown. Activation of *Hoxb9* in the zebra finch is earlier than in chick, therefore, the level of its wing is anterior to that of chick. Activation of *Hoxb9* in the ostrich is later than in chick, and the level of its wing is posterior to that of chick.

The expression of *Hox PG 6* and *Hox PG 7* at T1/T2 is also related to the morphogenesis of the cervico-thoracic region (Garcia - Gasca and Spyropoulos, 2000; Kostic and Capecchi, 1994). *Hoxb7* expression is related to the specification of the wing field and cooperates with *Hoxb4* and *Hoxb9* (Moreau et al., 2019). Accordingly, we hypothesized that *Hox PG 6-7* genes may be related to forelimb development, and forelimb positioning would be determined by the combination of *Hox PG 4/7/9* genes. Thus, Hox genes may contribute not only to the determination of the forelimb position but also to forelimb induction.

1.2.2 Induction

The early limb bud develops from undifferentiated mesenchymal cells derived from the somatic LPM (Burke, 2000). During the induction phase, signaling molecules secreted from adjacent NT, somites, and IM, such as Wnt/β-catenin and retinoic acid (RA), and transcription factors, like Hox proteins, act in concert to induce Tbx5 transcription (Minguilon et al., 2012). Tbx5 is expressed in the prospective wing LPM mesoderm of HH-stage 13 chicken embryos (Sheeba et al., 2016). The effects of Wnts during limb bud formation are mediated intracellularly by β-catenin. The β-catenin mutant mice have reduced Tbx5 expression (Nishimoto et al., 2015).

Tbx5 and Tbx4

Tbx5 is a member of the T-box family and is required for the induction and initiation of the forelimb (Minguillon et al., 2012). Another member of the T-box family, *Tbx4*, is expressed in the hindlimb bud, and the two can be used as the forelimb and hindlimb markers, respectively (Gibson-Brown et al., 1996; Minguillon et al., 2012; Rallis et al., 2003). The characteristic disease for TBX5 mutation in humans is the Holt-Oram Syndrome (HOS) with upper limb truncation (Basson et al., 1997). Deletion of *Tbx5* in mice results in complete failure of forelimb formation (Agarwal et al., 2003; Rallis et al., 2003). Negative expression of *Tbx5* or *Tbx4* in HH-stage 7-10 chicken embryos results in wingless or legless animals, respectively, and the functions turns out to be stage-dependent (Hasson et al., 2007; Rallis et al., 2003; Takeuchi et al., 2003). Another T-box transcription factor, *Tbx3*, has the redundant functions in limb formation and body size determination. The mutation of its enhancer in mice results in shorter limbs (Liu et al., 2022). Hence, T-box factors, especially *Tbx5* and *Tbx4*, are necessary and indispensable for limb induction.

Retinoic acid

Retinoic acid (RA), an inductive signal in somatic mesoderm, is essential for forelimb induction (Chambers et al., 2007). Retinaldehyde dehydrogenase-2 (Raldh2) is an enzyme to oxidize retinal to RA. Mutation of Raldh2 in zebrafish results in the lack of pectoral fins (Begemann et al., 2001). Inhibition of RA synthesis in chicken or deletion of Raldh2 in mice results in failure of the forelimb formation (Stratford et al., 1996). Recently, RA was identified to have a general role in the timing and size determination during avian wing development (Stainton and Towers, 2022). Hence, RA has a vitally important role in forelimb induction.

1.2.3 Initiation

Limb initiation starts with fibroblast growth factor (Fgf) 10 expression in the limb mesoderm (Fig. 9 B, B'). From HH-stage 14 (Fig. 9 A, A') to HH-stage 15 of chicken embryos, the wing bud mesenchyme is formed locally by epithelial-to-mesenchymal transition (EMT) within the wing field (Gros and Tabin, 2014; Ng et al., 2002). With constant expression of *Fgf10* induced by *Tbx5*, proliferation of forelimb cells remains high from HH-stage 15 to 18, while it decreases in flank cells after HH-stage 16. The prospective limb LPM with sustained EMT generates the limb primordium and therefore differs from the flank (Gros and Tabin, 2014; Ng et al., 2002). The expression of *Tbx5* and *Fgf10* are induced by forelimb mesenchymal cells, which is the core of the forelimb bud initiation (Gros and Tabin, 2014; Ohuchi et al., 1997). RA also forms a feed-forward loop with *Tbx5* to regulate *Fgf10* expression (Nishimoto et al., 2015). Wnt2b is expressed in the IM and LPM restricted to the forelimb region and it is required for *Fgf10* activation with *Tbx5* induction. Canonical Wnt signaling via β-catenin is a key regulator of limb bud initiation (Kengaku et al., 1998; Sweetman et al., 2008; Takeuchi et al., 2003). The ectopic expression of β-catenin and Wnt2b in the flank region induce Fgf10 ectopic expression and ectopic limb buds formation (Kawakami et al., 2001).

Fgf10

Ectopic *Fgf10* expression in the flank of chicken embryos causes the formation of extra limb buds (Min et al., 1998). *Fgf10* knock-out mice show initiation of limb buds but no outgrowth, and the fetuses show no forelimb and hindlimb formation (Sekine et al., 1999). Recently, a comparison between the chick and the emu, which has delayed and reduced forelimbs, also indicates the importance of *Fgf10* during limb initiation. The ectopic expression of *Fgf10* in emu embryos can cause a precocious limb formation (Young et al., 2019). This difference between limb development of chick and emu embryos indicates that *Fgf10* is essential for time dependent limb initiation.

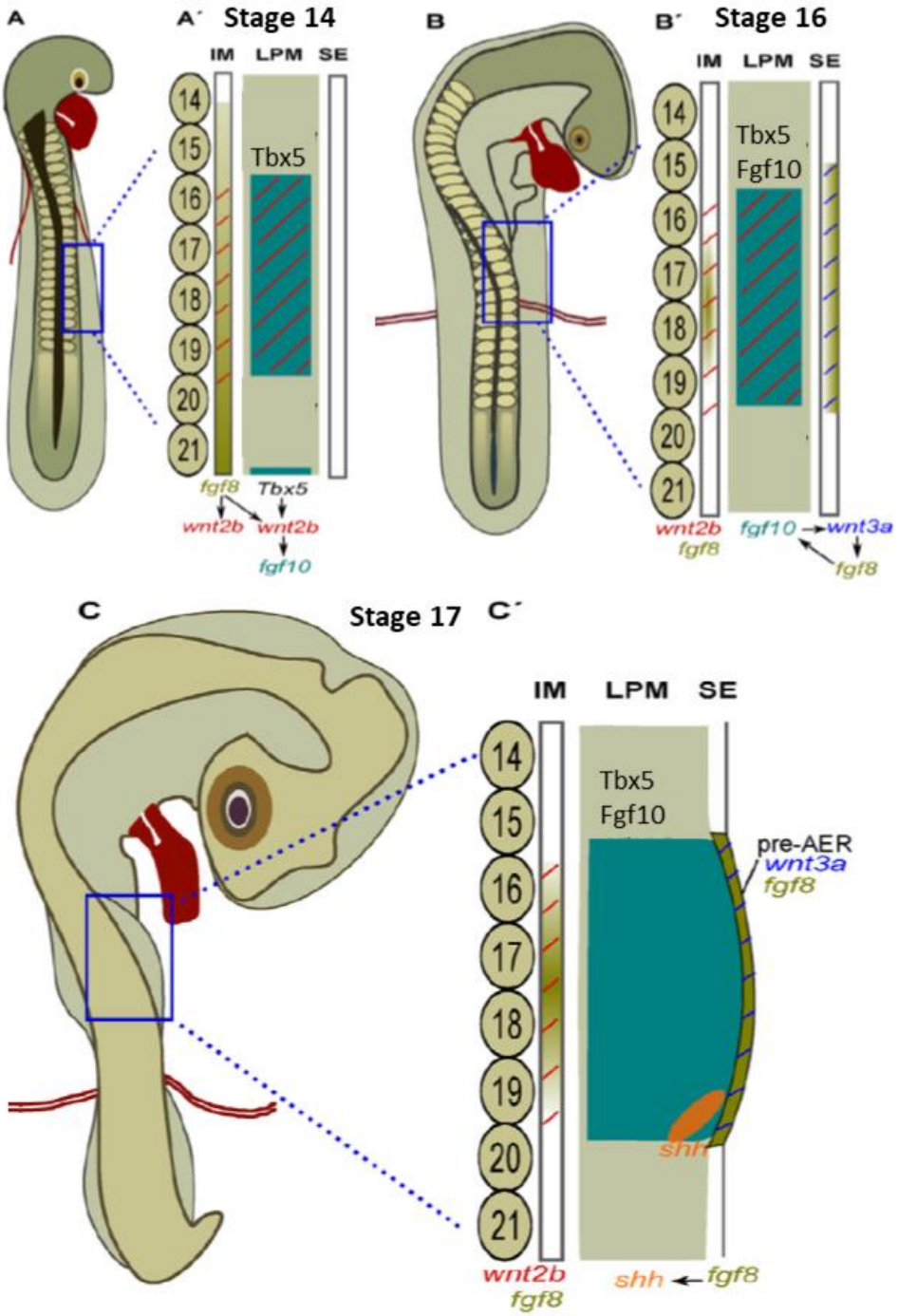

Fig. 9: Signaling interaction during limb bud initiation (Sheeba et al., 2016). The cyan box in A-C represents the prospective forelimb field. A'- C' represent enlarged views of the prospective forelimb region.

1.2.4 Outgrowth

The middle part of the ectoderm covering the prospective limb field forms the apical ectodermal ridge (AER) with high *Fgf8* expression (Crossley et al., 1996; Tickle, 2015). AER is a thickened epithelium at the tip of the limb bud. Limb bud outgrowth requires AER and Fgf10-Fgf8 loop formation, whereas the Fgf10-Fgf8 loop is also the key for AER formation (Boulet et al., 2004; Fernandez-Teran and Ros, 2008). *Fgf8* expression is activated by *Fgf10* from limb mesoderm through Wnt3a and in turn, *Fgf8* maintains *Fgf10* expression, constituting a positive feedback loop ((Barrow et al., 2003; Boulet et al., 2004; Jin et al., 2018; Kawakami et al., 2001). Ectopic *Fgf8* can induce ectopic limb bud formation in the flank, which has also been shown for Fgf1, Fgf2, and Fgf4 (Cohn et al., 1995). Ectopic *Fgf2* expression in the flank down-regulates *Hoxc9* and induces an elongated forelimb (Cohn et al., 1997; Vogel et al., 1996). In summary, the experiments demonstrate that Fgfs are essential for limb bud initiation and outgrowth (Crossley et al., 1996; Mahmood et al., 1995; Min et al., 1998).

1.2.5 Patterning

The patterning of the limb bud is established along the three axes of the adult limb. These three axes are the anterior-posterior (AP), the dorsal-ventral (DV), and the proximal-distal (PD).

The AP patterning is determined by the zone of polarizing activity (ZPA) with sonic hedgehog (Shh) expression, as well as Bmp2 and RA (Riddle et al., 1993; Tickle, 2002). Shh, related to the Drosophila segment polarity gene hedgehog, is specifically expressed in the ZPA (Riddle et al., 1993). It is induced by *Fgf8* from the AER and located in the posterior boundary of the limb bud mesoderm. Transplantation of ZPA or Shh-containing micro-bead to the anterior margin of the wing bud causes a mirror-image duplication and a loss of anterior polarity (Riddle et al., 1993; Xu et al., 2013). Loss of *Shh* in mice and chicken results in the malformation of digits (Ros et al., 2003). Establishment of ZPA-Shh requires not only *Fgf8* from the AER but also *Wnt7a* to maintain Shh expression (Sheeba et al., 2016). In turn, *Shh* is required for the regular formation of AER (Neumann et al., 1999). It also induces the activation of *Hoxd* genes necessary for the limb AP patterning of the limb (Marigo et al., 1996).

The DV patterning takes place during thickening of the wing-forming mesoderm and the ventral folding of LPM (Michaud et al., 1997). For the DV polarity, *Wnt7a* is of great importance and starts to be expressed in the dorsal ectoderm at HH-stage 15 of chick embryos. *Wnt7a* activates *Lmx1* (Lmx1b in mouse) expression in the dorsal mesoderm (Altabef et al., 1997; Tickle, 2002), while BMP in the ventral ectoderm induces *En1* expression (Chen and Johnson, 2002; Sheeba et al., 2016). These signals maintain the DV polarity of the limb bud.

The PD patterning is established by signals secreted by the AER, especially *Fgf8*. The feedback loop between *Fgf10* and *Fgf8* is the first step contributing to AER formation and maintenance (Boulet et al., 2004; Mahmood et al., 1995). Besides *Fgf8* in AER, *Fgf2*, *Fgf4*, *Fgf9*, and *Fgf19* have similar functions (Cohn et al., 1995). However, *Fgf8* is expressed for the longest time and in the entire AER, whereas the other family members are express in the later periods and only in the posterior part of the AER (Fernandez-Teran and Ros, 2008).

Establishment of PD polarity is a complex process regulated by gradients of signals extending from the adjacent flank to the AER. These signals are determined by *Hox PG 9-13* genes (Fig. 10) (McQueen and Towers, 2020; Nelson et al., 1996; Zakany and Duboule, 2007). Starting at HH-stage 18 of chick embryos, *Hoxd9* to *Hoxd13* are expressed in the posterior distal part of the limb bud. Until HH-stage 22/23, *Hoxd9* to *Hoxd13* are expressed in the limb bud from the proximal to distal part (Tickle, 2002; Zakany and Duboule, 2007). The paralogous genes *Hoxa9* to *Hoxa13* have a similar expression pattern. *Hoxa9* and *Hoxd9* double mutation results in defects of the *stylopodium* (Fromental-Ramain et al., 1996a; McIntyre et al., 2007; Xu and Wellik, 2011). In zebrafish, *Hox PG 13* knockout causes the loss of fin rays (Nakamura et al., 2016). *Hox PG 9-10* determins the formation of the *stylopodium* (stylopod) (Fromental-Ramain et al., 1996a), *Hox PG 11* the *zeugopodium* (zeugopod) (Wellik and Capecchi, 2003), and *Hox PG 12-13* the *autopodium* (autopod) (Fromental-Ramain et al., 1996b) (Fig. 10). Double mutation of Hoxa13 and Hoxd13 in mice causes complete loss of digits (Fromental-Ramain et al., 1996b; Scotti et al., 2015). HOXA13 mutation in humans causes the hand-foot-genital syndrome and malformations of tail and hindgut in chicks (de Santa Barbara and Roberts, 2002; Mortlock and Innis, 1997).

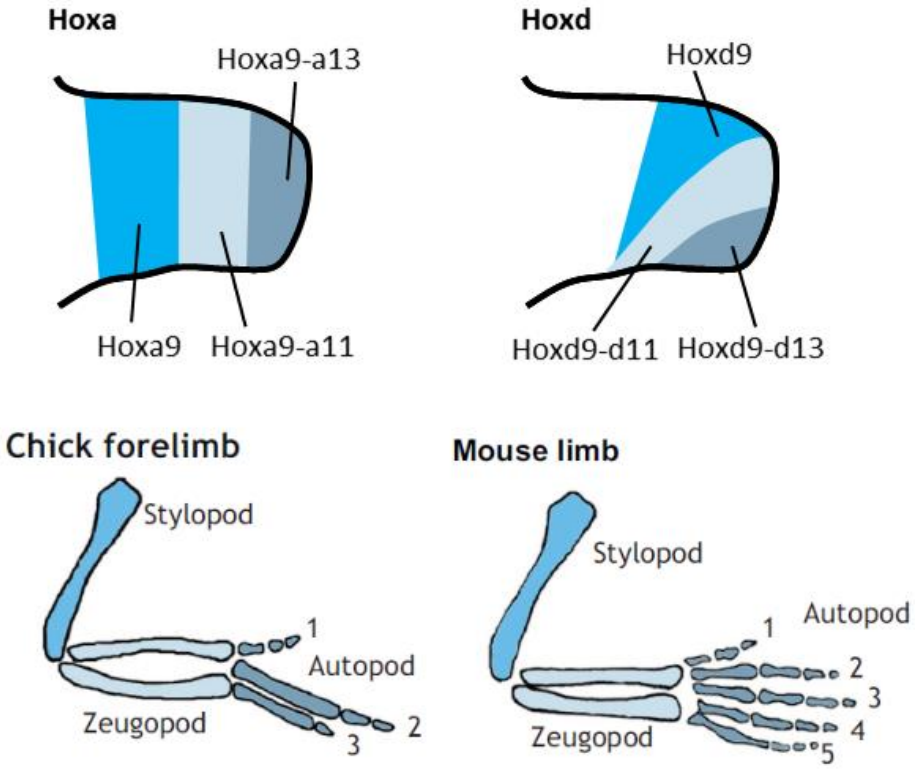

Fig. 10: Hoxa and Hoxd genes during limb patterning (Mcqueen and Towers, 2020). Top row shows the expression pattern of Hoxa9-a13 and Hoxd9-d13 in the early limb bud of chick. Bottom row shows the limb anatomy of chicken forelimb and mouse limb.

1.3 Questions

As described above, determination of the posterior boundary of the forelimb has already been studied. Restriction of the forelimb-forming region is by *Hox PG 9* genes, which repress the limb-forming activity of *Tbx5*. Before, *Tbx5* is induced by *Hox PG 4* genes. However, it is not known how the anterior boundary of the forelimb is determined. *Hox PG 4* genes cannot be involved in the process, since their anterior expression boundary is located anterior to the forelimb field. I hypothesized that other *Hox* genes might be involved in this pattern formation and asked which paralogous group of *Hox* genes might determine the anterior boundary of the forelimb. My primary choice was the *Hox PG 6-7* genes although single mutations have not yet provided evidence for defects in forelimb formation. Since my investigations revealed evidence for involvement of the *Hox PG 6-7* genes, I further investigated how the *Hox PG 6-7* genes interact with *Hox PG 4* genes during forelimb induction.

2. Materials and Methods

2.1 Materials

2.1.1 List of Laboratory Equipments

Name	Supplier
Disposable syringes (2 ml)	BD Biosciences
Egg Incubator	Grumbach
EP21 Current Amplifier	Intracel
Fiber Illuminator	Nikon
Fluorescence Microscope (SM21500)	Nikon
Forceps (microsurgical)	Fine Science Tools
Glass Pasteur pipettes (150 mm)	Brand
Light Microscope (SMZ1000)	Nikon
Ovodyne TSS20 Electroporator	Intracel
pH-Meter	Hanna Instruments
PCR strip tubes (0.2 ml)	Fermantas
Round bottom tubes (12 x75 mm)	Greiner Bio-one
Scissors (microsurgical)	Fine Science Tools
Serological pipettes (5 ml, 10 ml, 25 ml)	Falcon
Tubes (0.5 ml, 1.5 ml, 2 ml, 15 ml, 50 ml)	Nerbeplus

2.1.2 Preparation of micro-manipulation tools

Tungsten needle

Sharpened tungsten needles were the main tool for the isolation of wing buds from the surrounding mesenchyme. Accordingly, a 20 mm tungsten wire was inserted into the anterior opening of a glass Pasteur pipette whose thin nozzle had been removed with a diamond knife. The glass around the wire was heated over the flame of a Bunsen burner and removed when it began to melt. It was then pressed with the forceps and the tungsten wire was fixed in the anterior end of the Pasteur pipette. The tip of the tungsten wire was sharpened by electrolysis in saturated $NaNO_3$ solution.

Dye tip

Since staining of the translucent embryonic tissue helps to improve its visibility, dye tip is one of the prerequisites for microsurgery. The center of the narrow end of a Pasteur pipette was melted over the flame of a Bunsen burner until it began to melt. Then the anterior end of the pipette was removed from the flame and quickly pulled off to form a long thread. The sharpened end of the glass thread was shortly heated over the flame till it formed a small bulb (0.5-1 mm). Dye solution with 2.5% agarose and 1% Nile blue sulfate was placed on a heating block and stirred repeatedly to keep it in the liquid state. The small bulb of the glass pipette was dipped into the dye solution several times to coat it with the blue dye.

Glass capillary

The glass Pasteur pipettes were used to prepare glass capillaries. The narrow end of the glass pipette was flame heated over the Bunsen burner until it starts to melt. Immediately, the tip was pulled off with the forceps to form a very fine capillary. Following which, the blind end at the tip of the capillary was opened with the fine forceps. Another method that was used for preparing the glass capillary for injection was by an appropriate machine, NARISHIGE (model PC-100 (NARISHIGE CO., LTD). The capillary needed for this machine is from GB150T-10 (SCIENCE PRODUCTS GmbH). And the procedure is by two-step model with 100℃ at first and 93℃ at second time.

2.1.3 List of Chemicals, Reagents and Supplements

Name	Supplier
Agarose	Sigma
Anti-Digoxigenin-AP, Fab fragments	Roche
Blocking reagent	Roche
$CaCl_2.2H_20$ (Calcium chloride dehydrate)	Sigma
DEPC (Diethylpyrocarbonate)	Sigma
DNA ladder (100 bp, 1 kb)	Fermantas
DMSO (Dimethylsulfoxide)	Merck
EDTA (Ethylenediaminetetraacetic acid)	Fluka
EGFP (Enhanced green fluorescent protein)	R&D systems
Ethanol	Merck

Ethidium bromide	Carl Roth
Fast Green FCF	Sigma
FCS (Fetal calf serum)	Invitrogen
Formamide	Sigma
Gluteraldehyde solution (25%)	Sigma
Glycerol	Sigma
HCl (Hydrochloric acid)	Merck
Heparin	Sigma
H_2O_2 (Hydrogen peroxide)	Merck
India ink	Pelikan
KCl (Potassium chloride)	Merck
KH_2PO_4 (Potassium dihydrogen phosphate)	Merck
LB Agar	Sigma
Maleic acid ($C_4H_4O_4$)	Merck
Methanol	Applichem
$MgCl_2$ (Magnesium chloride)	Merck
Mowiol	Merck
NaCl (Sodium chloride)	Merck
Na_2HPO_4 (Disodium hydrogen phosphate)	Merck
NaOH (Sodium hydroxide)	Merck
$NaHCO_3$ (Sodium bicarbonate)	Merck
Nile blue sulfate	Merck
Paraformaldehyde	Merck
Penicillin-G sodium salt	Sigma
Proteinase-K	Roche
Sodium azide	Merck
Sodium citrate	Merck
Sucrose	Merck
Tissue Tek (O.C.T.)	Sakura Fintek
Tris	Carl Roth
Tris-HCl (Tris hydrochloride)	Sigma
Triton-X100	Sigma
Tryptone	Fluka

Tween-20	Dako
Yeast extract	Sigma

2.1.4 Buffers, Solutions and Media

Alakaline phosphatase (AP) buffer

5 ml of Tris 1M pH 9.5, 2.5 ml of 1M $MgCl_2$, 1 ml of 5M NaCl, and 2 ml of 25% Triton X-100 with the final volume adjusted to 50 ml with distilled water. For optimal results, this buffer was prepared immediately before use.

AP staining solution

NBT/BCIP was mixed well in AP buffer (20 μl/ml) and used to prepare the staining solution.

10% CHAPS

10g CHAPS powder was dissolved in 100 ml of DEPC-treated water. Solution was stored at 4°C.

DEPC-treated water

0.5 ml DEPC was added to 500 ml distilled water and allowed to sit for a minimum of 2 hour before sterilization by autoclaving.

Hybridization buffer

250 ml deionized formamide, 125 ml 20X SSC, 2.5 g CHAPS, 0.5ml Triton X-100, 5 ml 0.5M EDTA, 25 mg heparin powder, 500 mg tRNA, 10 g blocking reagent were added and made up to 500 ml with DEPC-treated water. Solution was heated at 65ºC to dissolve all ingredients. Hybridization buffer was stored at –20ºC in 50 ml tubes.

KTBT buffer

8.8 g NaCl, 1.5 g KCl, 10 ml Tween-20 and 25 ml 1M Tris pH 7.3 were dissolved in 965 ml of distilled water and the solution was sterilized by autoclaving.

LB medium

5 g yeast extract, 10 g Tryptone and 10 g sodium chloride were added to prepare 1 liter of LB medium. The pH was adjusted to 7.0 by adding NaOH and the medium was sterilized by autoclaving.

Magnesium chloride (1 M $MgCl_2$)

101.5 g $MgCl_2$ was made up in a final volume of 500 ml of distilled water. The solution was sterilized by autoclaving.

4% paraformaldehyde in PBS

20 g of paraformaldehyde powder was dissolved in a final volume of 500 ml of DEPC-treated PBS, heated to 65ºC and shaken periodically to dissolve. Solution was stored in 50 ml tubes at -20°C.

Phosphate buffered saline (PBS)

8 g NaCl, 0.2 g KCl, 1.15 g Na_2HPO_4 and 0.1 g KH_2PO_4 were dissolved in 1000 ml of distilled water and the pH was adjusted to 7.4. The solution was sterilized by autoclaving.

PBT

0.1% Tween-20 was added to PBS and stored at room temperature.

Proteinase-K

100 mg of Proteinase-K powder was dissolved in DEPC-treated water (20 μg/μl), vortexed and aliquoted into 50 μl. The aliquots were stored at -20°C and thawed on ice immediately before use.

Standard saline citrate buffer (SSC, 20X)

175 g Sodium chloride and 88 g Sodium citrate was made up to 1000 ml with distilled water. The pH was adjusted to 7.0 and the solution autoclaved and stored at room temperature.

Sucrose/PBS Solutions

2.5 g, 7.5 g and 15 g sucrose were dissolved in PBS to make 50 ml of 5%, 15% and 30% sucrose solutions, respectively. The solutions were freshly prepared before use.

TAE buffer (50X)

2 M Tris, 50 mM EDTA (pH 8.0), and 1 M glacial acetic acid were mixed well and stored at room temperature.

Tris buffer (pH 9.5 and 7.3)

121.12 g Tris base was dissolved in 800 ml of distilled water. The pH was titrated to 9.5 or 7.3 with concentrated HCl. Distilled water was added to a final volume of 1 liter. The solution was autoclaved and stored at room temperature.

2.1.5 DNA Plasmids and RNA Probes

DNA plasmids for electroporation

DNA plasmids were bought from a company (Dongzebio co.Ltd). Thereby, Hoxa6 (693bp), b6 (675bp), c6 (735bp), a7 (657bp), and b7 (651bp) coding sequences were inserted into pCAGGS-P2A-EGFP plasmid between EcoRI and XhoI restriction enzymes (Fig. 11). The dominant-negative form of Hoxb4 plasmid was produced using the same method, with its coding sequence lacking 144bp at the most C-terminal. The sequences were obtained from NCBI as shown in Table 1.

Table 1: *Hox* genes for chicken

Hoxb4	NCBI Reference Sequence: NM_205293.3
Hoxa6	NCBI Reference Sequence: NM_001030987.4
Hoxb6	NCBI Reference Sequence: NM_001396636.1
Hoxc6	NCBI Reference Sequence: XM_015300352.2
Hoxa7	NCBI Reference Sequence: NM_204595.2
Hoxb7	NCBI Reference Sequence: XM_040691977.1

RNA probes

The plasmids for *in situ* hybridization were a kind gift from O. Pourquie, H. Ohuchi and C. Tabin. Restriction enzymes for probe production are shown in a Table 2.

Table 2: RNA probes for chicken

Tbx5-T7	PF: TACTGGAGCCCACTGGATGA PR: ATGCTCGGTGGTGGAACATT		
Hoxb4-T7	PF: ACCAAGCAGCGGTGTTATCC PR: CTGGAAGGGTTGGACCTGAT		
Hoxa6-T7	PF: GTCCAACACCGTCATTGCTT PR: CTCCCCTGACTTTTCCTCTGTT		
Fgf8	EcoR I	**T7**	O. Pourquie
Fgf10	Nco I	**SP6**	H. Ohuchi
Shh	Hind III	**T3**	C. Tabin
Lmx-1	Not I	**T7**	C. Tabin

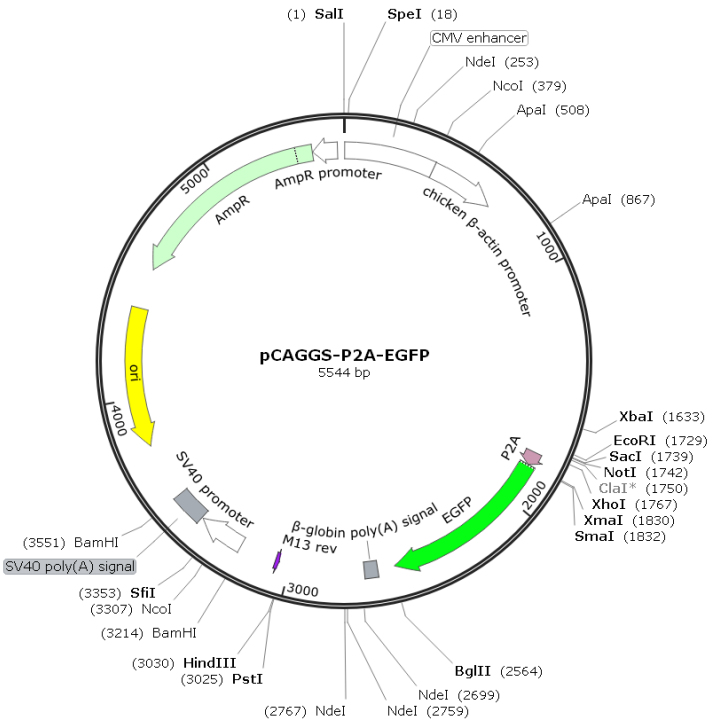

Fig. 11: The diagram for the map of the pCAGGS-P2A-EGFP plasmid.

2.2 Methods

2.2.1 Eggs for operation

Fertile chicken eggs were obtained from the farm maintained by the Institute of Animal Sciences, the Agricultural Faculty at the University of Bonn, Germany. The eggs were incubated in a humidified incubator at 38°C for the desired time and stages based on the description of Hamburger and Hamilton (HH), 1951. After the required period of incubation and checked by transmitted light, eggs were rinsed with 70% ethanol and windowed above the embryo for electroporation. After electroporation and re-incubation till the desired HH-stages were reached, the embryos were separated from the shells, transferred into PBT and cleaned from their attached membranes using fine surgical scissors and forceps. The processed samples were then used for fixation with 4% PFA.

2.2.2 DiI injection into chicken embryos

DiI original powder was dissolved in 100% ethanol to 1mg/ml. The DiI/ethanol solution was diluted in a 1:3 ratio with tetraglycol for injection. The DiI solution was injected into the lateral plate mesoderm at HH-stage 8-12 with fine glass capillaries. The embryos were re-incubated at 38°C and checked them with fluorescence microscope.

2.2.3 *In ovo* Electroporation

DNA plasmid solution, re-suspended in RNase-free water at 5-10ng/µl supplemented with 0.2% fast green, was injected into the coelom of HH-stage 11 embryos at specific level by using a glass capillary. The embryos were electroporated dorsally by putting the anode on top and cathode underneath the embryos and parallel to each other. Subsequently, one pulse on high voltage, 70V, 0.01ms with 99.9ms interval and two pulses on low voltage, 7V 50ms with 200ms interval were applied with an electroporator (CUY21EDIT II). The un-electroporated contralateral side and the electroporation of EGFP-containing vector were used as controls. The effect of electroporation was assessed after re-incubation still HH-stages 20-22 by direct observation with a microscope and by *in situ* hybridization.

2.2.4 Preparation of template DNA plasmids

1µl plasmid DNA was added to 10µl competent cells, mixed gently and incubated on ice. After 30min incubation, cells were given a heat shock at 42℃ for 35 seconds, cooled on ice for 2min, mixed with 500µl LB medium and incubated 1 hour at 37℃ with shaking. 50-100µl of the solution was spread on a pre-warmed culture plate and incubated for 16 hours at 37℃ for the colonies to grow. A single colony from a streaked plate was used to inoculate 200ml of LB medium with appropriate antibiotics. The culture was grown over night at 37°C with vigorous shaking and then transferred into specific centrifuge tubes. The NucleoBond® Xtra Midi DNA preparation kit was used to isolate DNA from these cultures (Table 3).

Tab. 3: The protocol for DNA preparation kit

Harvest	Centrifuge 30min, at 4000g, 4℃
Cell lysis	8 ml buffer LYS (storage in 4℃)
Equilibration of the column and filter	12ml buffer EQU, vertically drop to the filter
Neutralization	8ml buffer NEU, mix thoroughly until colorless
Clarification and loading of the lysate	Invert the tube 3 times, load lysate on the filter
First wash	5ml buffer EQU, vertically drop to the filter
Filter removal	
Second wash	8ml buffer WASH
Elusion	8ml buffer ELU to a new 15ml tube
Precipitation	3.5ml isopropanol, vortex, 12000g, 4℃, 30min
Washing and drying	2ml 70% ethanol, 12000g, RT, 5min; air drying
Reconstitution	Appropriate volume of TE buffer, check the concentration, storage at -20℃

2.2.5 Linearization of plasmids and template purification

The plasmid DNA was linearized in the reaction system with specific enzyme and specific reaction buffer after overnight digestion at specific temperature related to the enzyme. The linearized DNA was at first purified by extracting using phenol/chloroform (1:1) to remove proteins. The top aqueous layer was then isolated and extracted with 100µl of chloroform to remove the phenol carry-over. 10µl of 3M sodium acetate (pH 5.2) was added, followed by 220µl ethanol. The sample was mixed and transferred to -80°C for 30 minutes before centrifuging at 12,000 x g for 45 minutes at 4°C. The resulting pellet was washed in 100µl cold 70% ethanol which was again centrifuged at 12000 g for 30 minutes. The pellet was air dried and re-suspended in 20µl water. The DNA concentration was determined using a NanoPhotometer (IMPLEN).

2.2.6 RNA probes for *in situ* hybridization

The RNA probes were the cleaved products of the DNA plasmids using restriction enzymes, and some RNA probes were produced by PCR and subsequently transcription using a DIG-RNA labeling Kit with T3/T7/SP6 polymerases. The purified linearized DNA and purified PCR product were concentrated and prepared for transcription using a commercial kit (Table 4).

Table 4: Protocol for RNA probes preparation kit

Add 1µg purified DNA to a sterile, RNase-free reaction vial, then add enough water to make the volume up to 13µl.	
Place the reaction vial on ice, then add the following reagent:	
10 X NTP labeling mixture	2µl
10 X transcription buffer	2µl
Protector RNase inhibitor	1µl
RNA polymerase SP6/T3/T7	2µl
Mix gently and centrifuge briefly.	
Incubate for 2 hours at 37°C.	
Add 2µl DNase I, RNase-free to remove template DNA.	
Incubate for 15min at 37°C.	
Stop the reaction by adding 2µl 0.2M EDTA (pH 8.0). The RNA probes were aliquoted in 10µl each tube and storage in -80°C.	

2.2.7 Whole mount *in situ* hybridization (ISH)

Prepare embryos for hybridization	
Dissection of embryos in PBT	
Fixation in 4% PFA with PBT	overnight, 4℃
Wash in PBT	10-20 min, 4℃
Dehydration in 100% methanol	20-30min, 4℃
(embryos can be stored in -20℃ for several months)	
Rehydration with PBT	10-20min x2, 4℃
Proteinase K in PBT, stock solution 20mg/ml	1min/stage, RT
1:1000, final 20ug/ml	
Wash in PBT	10min x3, 4℃
Fixation in 1% Glutaraldehyde in 4% PFA in PBT	30min x2, 4℃
Wash in PBT	30min, 4℃
Pre-hybridization with Hybridization buffer	1-2hour, 65℃
Replacement with fresh Hybridization buffer	overnight (18 hours), 65℃
Adding 1ul RNA probe to hybridization buffer	**2days, 65℃**
Washing	
2 X SSC without CHAPS	20min, 65℃
2 X SSC with CHAPS（1:50）	2x20min, 65℃
0.2 X SSC with CHAPS（1:50）	2x20min, 65℃
(solution should be preheated in 65℃)	
Replacement with KTBT	5min, RT
Immunocytochemical detection of the probe	
Preblocking with 10% FCS in KTBT	4 hours, RT
Incubation with antibody	overnight , 4℃
(anti-DIG 1:2000 in 10% FCS)	
Wash with KTBT	2 hours ,6 times, RT,
	overnight, 4℃
Wash in AP-buffer	15min,x 2, RT
Incubation in the dark with Staining-solution	

200µl stock solution to 10ml AP buffer	variable, RT
Rewash in AP-buffer	variable, RT
Refix in 4% PFA	overnight, 4℃

2.2.8 Photographic documentation and data analysis

Samples were photographed by using a Nikon digital camera DXM1200C connected to a Nikon SM21500 fluorescence microscope. Images were assembled and annotated using ImageJ and Adobe Photoshop CS3.

2.2.9 mRNA-sequencing analysis

The lateral plate mesoderm and overlying ectoderm of the neck field, ectopic wing buds induced by Hoxa6 ectopic expression, and the endogenous wing buds from HH-stage 22 embryos were dissected and collected. Total RNA was isolated with miRNeasy Micro Kit (QIAGEN). DNase digested total RNA samples used for transcriptome analyses were quantified (Qubit RNA HS Assay, Thermo Fisher Scientific) and the quality measured by capillary electrophoresis using the Fragment Analyzer and the 'Total RNA Standard Sensitivity Assay' (Agilent Technologies, Inc. Santa Clara, USA). All samples in this study showed good RNA Quality Numbers (RQN; median = 8.1). The library preparation was performed according to the manufacturer's protocol using the 'VAHTS™ Universal RNA-Seq Library Prep Kit for Illumina® V6 with mRNA capture module'. 500 ng total RNA were used for mRNA capturing, fragmentation, synthesis of cDNA, adapter ligation and library amplification. Bead purified libraries were normalized and finally sequenced on the HiSeq 3000/4000 system (Illumina Inc. San Diego, USA) with a read setup of 1x150 bp. The bcl2fastq tool was used to convert the bcl files to fastq files as well for adapter trimming and demultiplexing.

2.2.10 Statistical analysis

Data analyses on fastq files were conducted with CLC Genomics Workbench (version 21.0.4, QIAGEN, Venlo. NL). The reads of all probes were adapter trimmed (Illumina TruSeq) and quality trimmed (using the default parameters: bases below Q13 were trimmed from the end of the reads, ambiguous nucleotides maximal 2). Mapping was done against the *Gallus gallus* (GRCg6a) (March 19, 2021) genome sequence. Statistical differential expression tests were determined using the 'Differential Expression for RNA-Seq' tool (version 2.4) (Qiagen

Inc. 2021). The resulting *P* values were corrected for multiple testing by FDR and Bonferroni-correction. A *P* value of ≤ 0.05 was considered significant. The RNA expression level was indicated by reads per kilobase of transcript per million mapped reads (RPKM) and the statistical analyses between three groups were done by two-way ANOVA, using GraphPad Prism v6 (San Diego, CA, USA). Data are presented as means ± SEM. And the level of statistical significance was set at *p≤0.05.

3. Results

In order to investigate our hypothesis that *Hox PG 6-7* genes are involved in anterior boundary formation of the wing bud, at first, I studied gene expression in the prospective wing region and compared the expression patterns of *Tbx5* and *Hox* genes in chicken embryos. Next, I chose HH-stage 11 embryos to perform electroporation with *Hox PG 6-7* overexpression plasmids or a plasmid containing the dominant-negative form of *Hoxb4*. The observed effects on wing bud development clearly indicated morphogenetic functions of *Hox* genes and the *Hox* code for forelimb initiation and positioning.

3.1 Identification of the prospective wing region

In order to investigate the function of *Hox* genes on wing bud induction, at first, I wanted to identify the axial level of the prospective wing field at stages before wing bud induction. Two cellular-tracing methods were used to label the forelimb-forming LPM cells. For embryos at HH-stage 10-12, I carried out electroporation with EGFP plasmid to label mesodermal cells. This was done because at these stages, the somatic and splanchnic LPM are separated by the coelom, into which DNA solution can be injected. Then, plasmids were uni-directionally introduced into the dorsal layer of mesoderm. For younger embryos from HH-stage 8 to 10, I performed injection with DiI solution to label cells directly. Embryos were studied after re-incubation periods when the wing bud was already present.

3.1.1 Identification of the prospective wing region using DiI

To label the prospective wing-forming mesoderm at HH-stage 8 to 10, I performed *in ovo* injections with DiI solution into LPM at three axial levels: i.) anterior end of the presomitic mesoderm (PSM), ii.) anterior to and iii.) posterior to Hensen's node. The embryos were subsequently re-incubated till HH-stage 19, when the early wing bud was formed. Embryos were studied under a fluorescence microscope.

DiI injection into HH-HH-stage 8 embryos

After injection at the level posterior to Hensen's node of HH-stage 8 embryos with 3-5 somites, the DiI was located within the preliminary wing bud at HH-stage 19 (n=12) (Fig. 12A). The DiI injected at the level anterior to the Hensen's node level of HH-stage 8 embryos was located at the level of somite 8-13 at HH-stage 19 (n=15). This region with DiI was anterior to the wing bud. The embryos injected with DiI at the level of the anterior end of

PSM displayed red fluorescence at the level of somite 4-10 (n=5). Based on these results, it could be concluded that the prospective wing region is restricted to the level posterior to the Hensen's node of HH-stage 8 embryos.

DiI injection into HH-stage 9 embryos

The LPM cells which were located at the level posterior to the Hensen's node at HH-stage 8 were found anterior to it at HH-stage 9 (with 6-8 somites). Hence, I chose the level anterior to Hensen's node for DiI injection with HH-stage 9 embryos. And I observed that the preliminary wing bud was labeled (n=13) (Fig. 12B). LPM cells at the level of the anterior end of PSM were now located adjacent to somites 7-13 (n=6). These results indicated that cells of the LPM located anterior to the Hensen's node at HH-stage 9 are determined for wing bud formation.

DiI injection into HH-stage 10 embryos

As described above, the wing field of HH-stage 10 embryos are expected to be located at a level more anterior to Hensen's node than in HH-stage 9. Hence, the DiI injection was now performed at the level of the anterior end of PSM. When checked embryos at HH-stage 19, the red color was located anterior to the wing bud but and some adjacent to the anterior part of the wing bud (n=18) (Fig. 12C). This indicated that the prospective wing region is located around the level of the anterior part of PSM at HH-stage 10.

As Hensen's node regresses, the wing bud-forming LPM cells remain at the same axial level during HH-stages 8 to 10. At HH-stage 8, it was located at the level posterior to Hensen's node. At HH-stage 9, it was situated at the level anterior to Hensen's node, and at HH-stage 10, it was restricted to the level of the anterior part of PSM. Due to diffusion of DiI solution, the labeled domain can be much broader than the injected region, which raises a problem of reduced specificity. EGFP electroporation is one way to partially solve this problem partially and give a much clearer indication of the position of the pre-wing field. Therefore, I performed electroporation to further narrow down the location of the wing field.

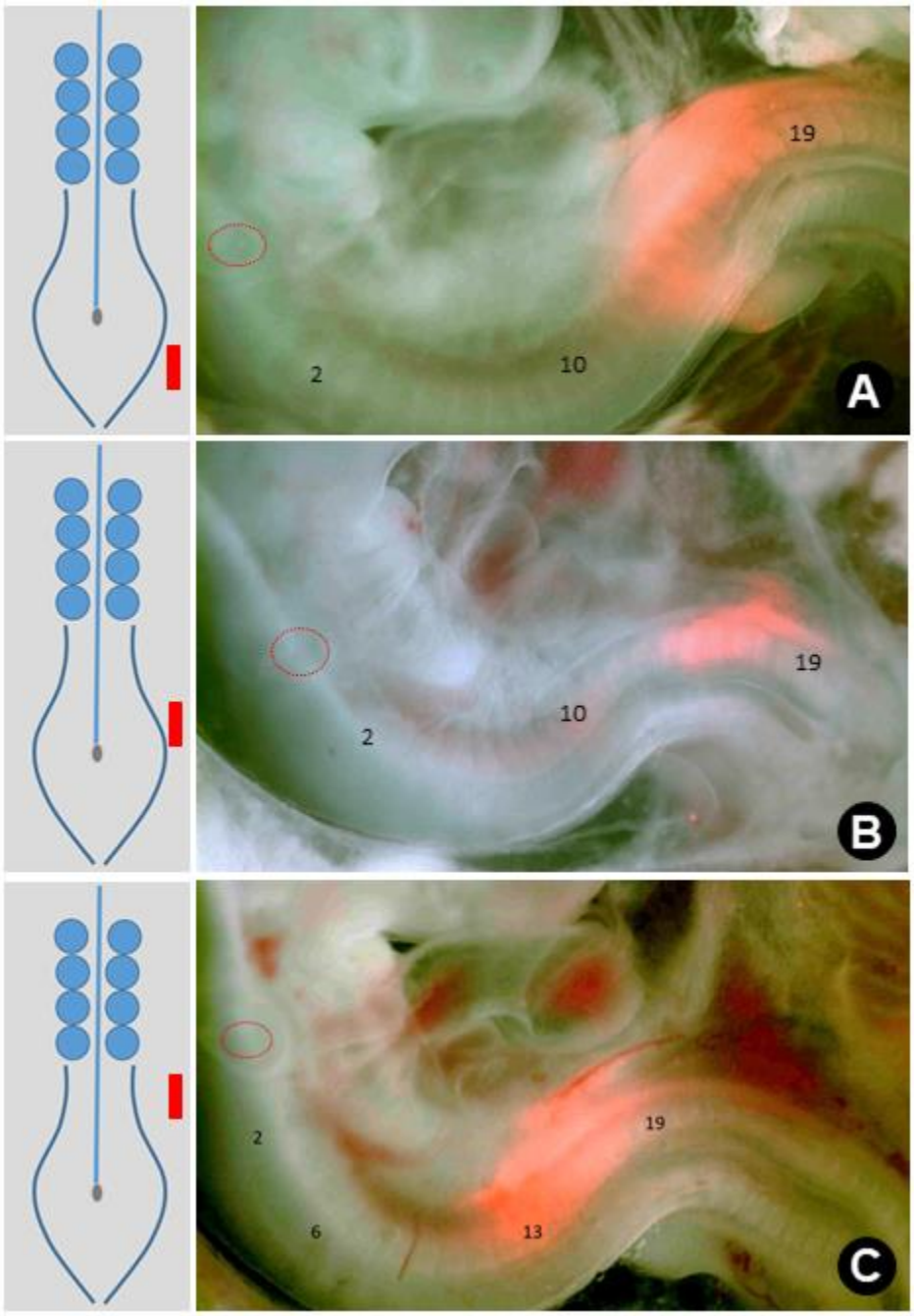

Fig. 12: Prospective wing field as demonstrated by DiI labelling. The DiI injected region is shown by red bars in embryos at HH-stage 8 (**A**), HH-stage 9 (**B**), and HH-stage 10 (**C**). The position of DiI was tracked at HH-stage 19 in injected chick embryos. The otic vesicle is shown by red dotted circle. Somites are marked by numbers.

3.1.2 Identification of the prospective wing field using EGFP electroporation

In the set of experiments, I performed EGFP-electroporation to trace the prospective wing region from HH-stage 10 to 12 (embryos of 9 to 17 somites). Results from DiI labelling showed that at HH-stage 10, the wing-forming LPM was located around the level of the anterior part of PSM. Accordingly, I performed electroporation at the level of the anterior end of PSM at these three stages. After re-incubation, embryos were checked at HH-stage 22 under the fluorescence microscope.

EGFP electroporation of HH-stage 10 embryos

At HH-stage 22, the green fluorescence was located at the level anterior to the wing bud with or without labelling of the anterior part of the wing bud (n=8) (Fig. 13A). This variation may be due to minor differences of the injection level, which covered the length of several somites. It was concluded that the prospective wing field is located immediately posterior to the rostral end of PSM of HH-stage 10 embryos. The cells at the anterior end of PSM at HH-stage 10 were found at the level of somite 12, which was consistent with the results from the DiI injections at HH-stage 10.

EGFP electroporation of HH-stage 11 embryos

After electroporation at the level of the anterior end of PSM at HH-stage 11, it was surprising that EGFP was always located in the anterior part of the wing bud, even the entire bud (n=9) (Fig. 13B). The cells of the anterior end of PSM at HH-stage 11 were found at the level of somite 15. This indicated that the prospective wing region is located at the level of the anterior part of PSM, and anterior boundary of the prospective wing bud is situated at the level of the anterior end of PSM in HH-stage 11 embryos.

EGFP electroporation of HH-stage 12 embryos

Chicken embryos at HH-stage 12 have 15-17 somites, and the wing bud is situated adjacent to somites 15-20 (Burke et al., 1995). This implies that electroporation at the level of the last new-formed somite and the anterior end of the PSM would entirely cover the wing field. Indeed, after electroporation and two days of re-incubation, the EGFP signal was restricted to the wing bud (Fig. 13C). Hence, at HH-stage 12, the wing field had reached its final axial level.

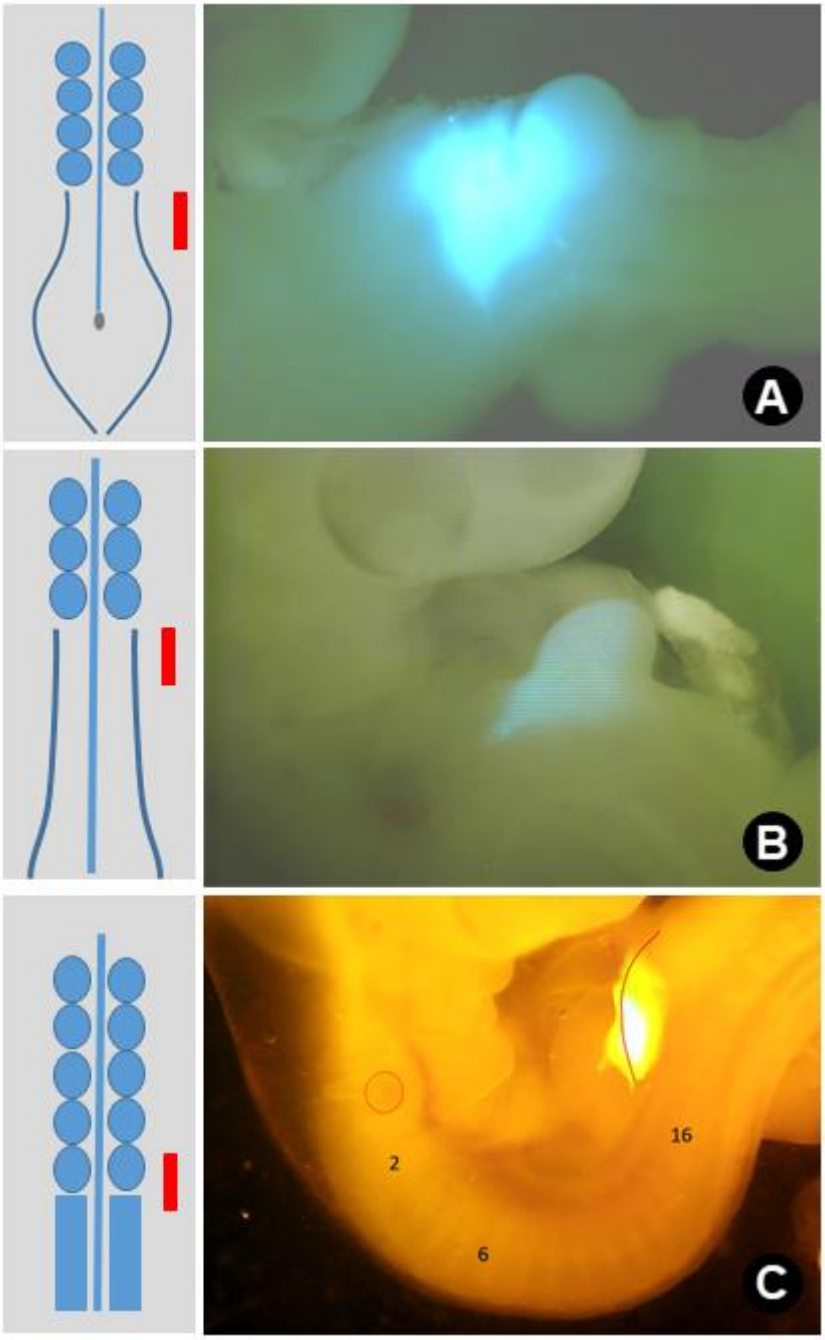

Fig. 13: The prospective wing fields at HH-stages 10 to 12 after EGFP electroporation. Electroporate area is shown schematically by red bars at HH-stage 10 (**A**), HH-stage 11 (**B**), and HH-stage 12 (**C**). EGFP was followed into HH-stage 20-22 chick embryos. In C) the otic vesical is shown by red circle and somite numbers are shown. The wing bud is shown with red dotted line.

Taken together, the LPM cells at the level of the anterior end of PSM of HH-stage 10 embryos can later be found anterior to the wing bud and within the anterior portion of the wing bud when injected at HH-stage 11. Since the level of the anterior end of PSM corresponds to somite 12 at HH-stage 10 and somite 15 at HH-stage 11, it can be concluded that the anterior boundary of the wing bud is always located at the somite 15 level and the prospective wing region maintains its position during embryonic development. Furthermore, the anterior boundary of the wing bud is located perfectly at the level of the anterior end of PSM of HH-stage 11 chick embryos. This is the anatomical land mark for the electroporation experiments to study effects of *Hox* genes within or adjacent to the prospective wing region.

3.2 Expression patterns of *Hox* genes related to the wing bud

As we hypothesized above, *Hox PG 6-7* genes may contribute to wing bud formation, together with *Hox PG 4-5* genes. Therefore, the expression patterns of *Hox PG 4-7* genes were compared to the *Tbx5* expression in the wing bud-forming region (Fig. 14).

As shown above, the prospective wing region was found at the level of the anterior part of PSM at HH-stage 11. The *in situ* hybridization (ISH) with *Hoxb4* and *Hoxa6* RNA probes shows that, in the LPM, *Hoxb4* was expressed from somite 5/6 level posteriorly (Fig. 14A) and *Hoxa6* from somite 10/11 level posteriorly (Fig. 14B). The specific wing bud marker, Tbx5, was first detected at the level of somites 12-20 of HH-stage 13 embryos (Fig. 14E). When the wing bud started to grow out at HH-stage 17, *Tbx5* was expressed adjacent to somites 16-21 (Fig. 14H). At both of the HH-stages, *Hoxb4* was expressed in LPM posterior from somite 1 (Fig. 14C, F), and the *Hoxa6* expression was extended posteriorly from the level of somite 13 (Fig. 14D, G). Expression domains of both *Hoxb4* and *Hoxa6* overlapped with the *Tbx5*. Moreover, *Hoxa6* was more closed to it. These results were in line with our hypothesis that Hox PG 4-7 genes have functions on the wing bud induction.

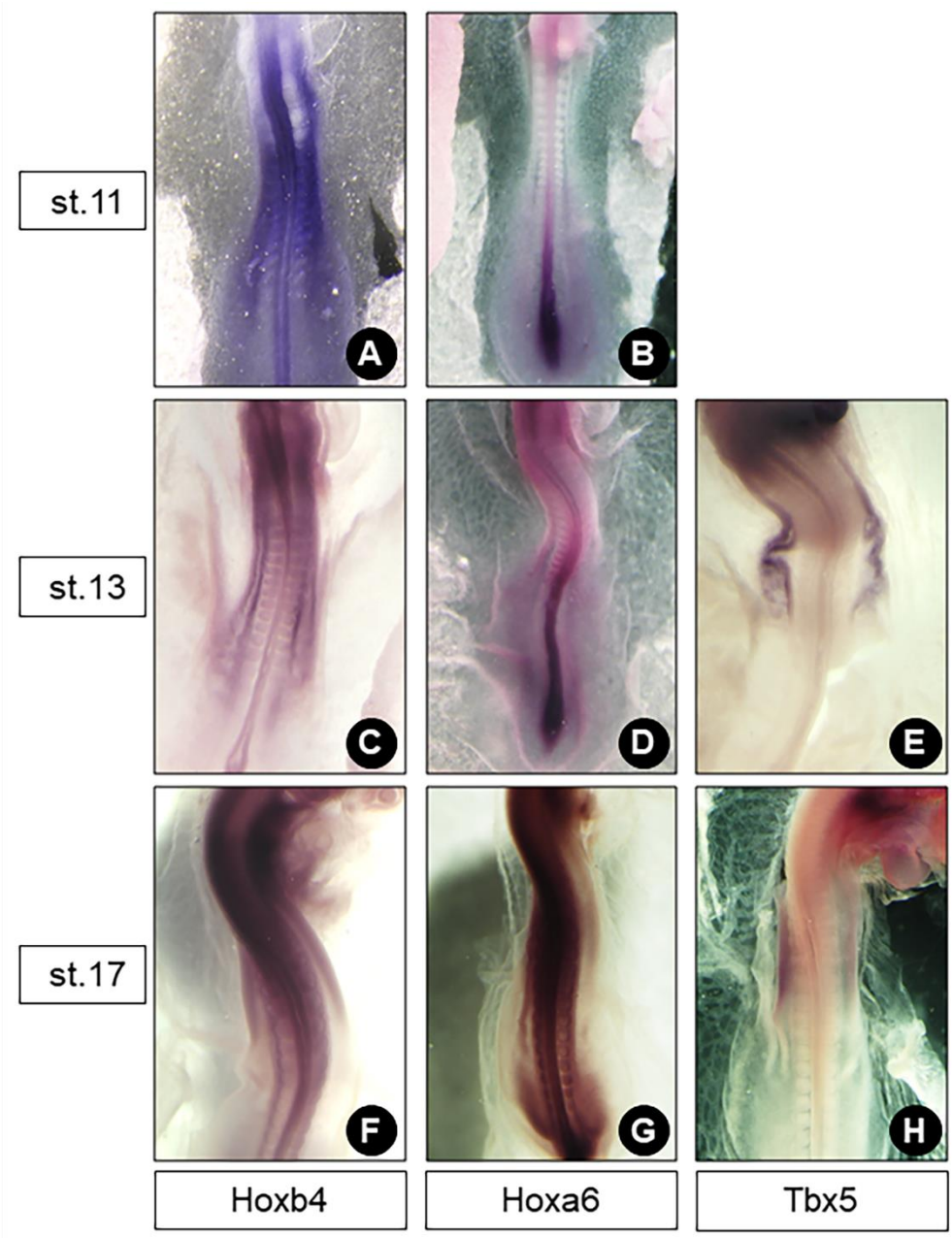

Fig. 14: The expression patterns of *Hoxb4*, *Hoxa6*, and *Tbx5* in chicken embryos. The first row shows the expression of *Hoxb4* (A) and *Hoxa6* (B) at HH-stage 11 embryos. The second row shows the expression of *Hoxb4* (C), *Hoxa6* (D), and *Tbx5* (E) at HH-stage 13, and the third row shows *Hoxb4* (F), *Hoxa6* (G), and *Tbx5* (H) expression at HH-stage 17.

3.3 Ectopic *Hox PG 6-7* induces additional wing buds

To pursue our hypothesis further, I induced ectopic expression of *Hox PG 6-7* genes anterior to the prospective wing region at HH-stage 11 of chicken embryos. We first chose *Hoxa6* as a typical representative for *Hox PG 6-7* genes. The operated embryos were analyzed after one to two days of re-incubation.

3.3.1 Ectopic *Hoxa6* induces expression of wing genes

After one day of re-incubation, the *Tbx5* expression domain extended anteriorly from its endogenous expressing domain and overlapped with the *Hoxa6* electroporation field (Fig. 15D). Control embryos with EGFP control vector injection did not show ectopic *Tbx5* expression (Fig. 15C). This indicated the ectopic expression of *Hoxa6* activated *Tbx5* expression.

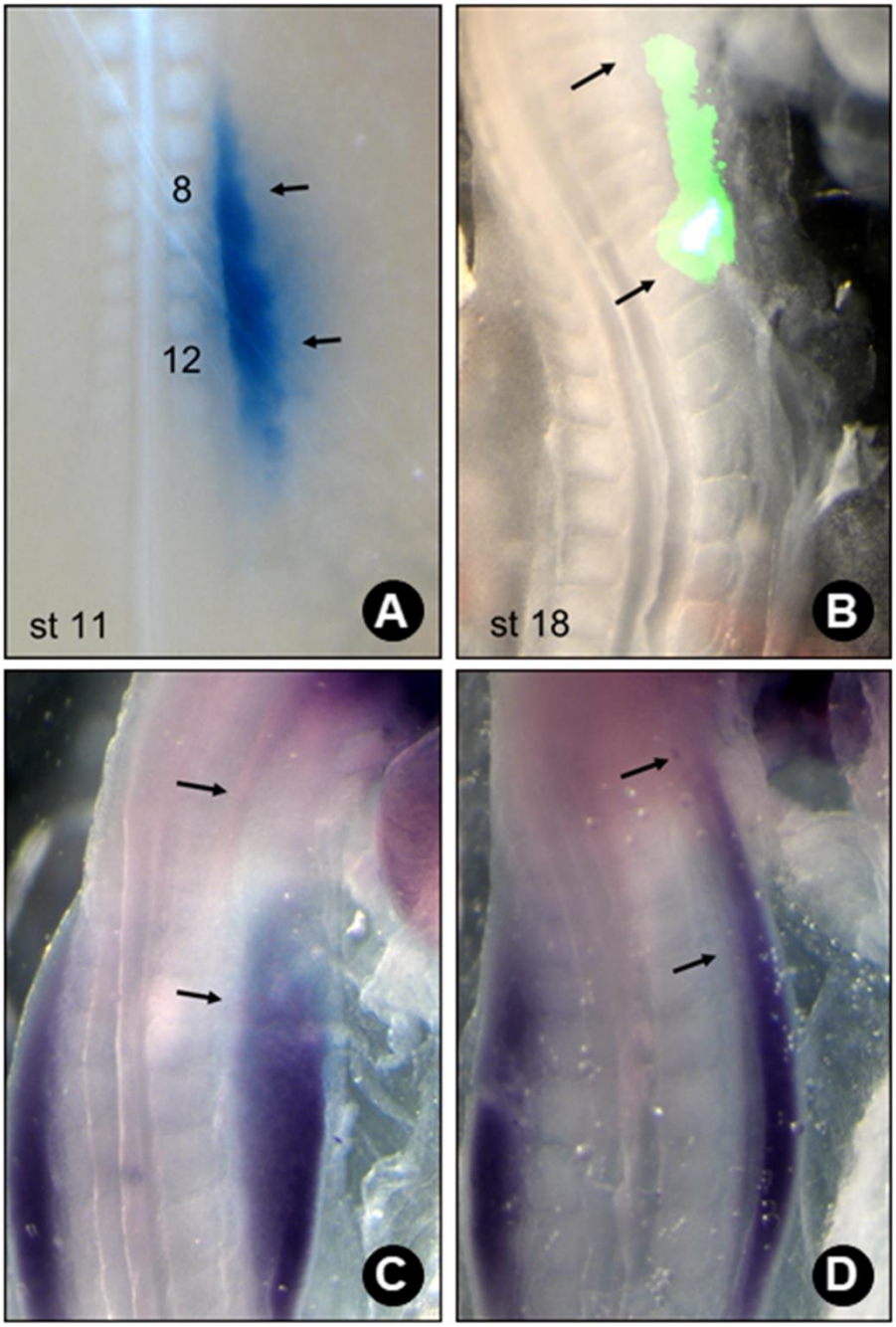

Fig. 15: Ectopic *Hoxa6* expression increased *Tbx5* expression. A) The photo for electroporation region at HH-stage 11 embryos. B) *Hoxa6* injection site is shown with fluorescence marker at HH-stage 18. C) *Tbx5* expression domain at HH-stage 18 corresponds to EGFP control electroporation. D) Ectopic *Tbx5* expression at HH-stage 18. Numbers in A indicate the somite level. Space between arrows indicates the electroporation region.

In line with ectopic *Tbx5* expression, *Fgf10* and *Fgf8* were also activated, although the expression level *Fgf10* was lower than the endogenous one (Fig. 16A). *Tbx5* is the key regulator for wing bud induction (Gibson-Brown et al., 1996). *Fgf10* expression is *Tbx5* dependent (Gros and Tabin, 2014). *Fgf8* expression in the ectoderm is activated by *Fgf10* from the mesoderm (Ohuchi et al., 1997). Both *Fgf10* and *Fgf8* contribute to wing bud outgrowth (Tickle, 2015). In the embryos with ectopic *Hoxa6* expression, additional expression of *Tbx5*, *Fgf10*, and *Fgf8* indicates an inductive potential of *Hoxa6*.

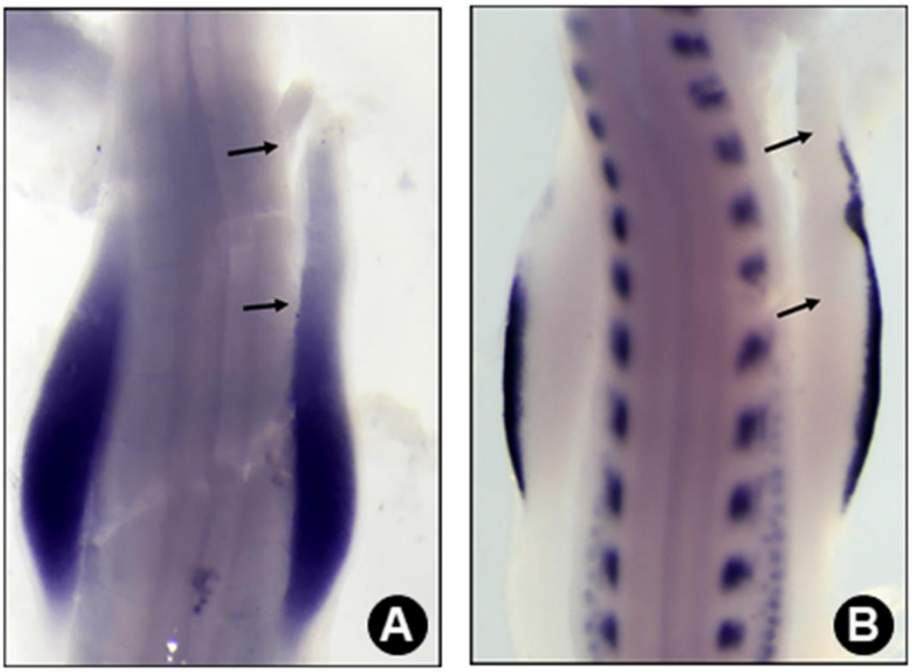

Fig. 16: Ectopic *Hoxa6* expression increased *Fgf10* and *Fgf8* expression. Ectopic *Hoxa6* expression increased *Fgf10* (A) and *Fgf8* (B) expression anteriorly. The arrows indicate the electroporation region.

3.3.2 Ectopic *Hoxa6* induces additional wing buds

To further investigate the function of *Hoxa6* during wing bud formation, I studied the embryos two days after electroporation. Surprisingly, I found a small ectopic bud anterior to the endogenous wing bud (Fig. 17A). In the ectopic bud, *Tbx5* was expressed as strong as in the natural one (Fig. 17B). This indicated that *Hoxa6* potently activated *Tbx5* expression and thus wing bud formation. However, in the ectopic bud, there was only weak *Fgf10* expression (Fig. 17C), and no *Fgf8* expression (Fig. 17D). This showed that the feedback loop between *Fgf10* and *Fgf8* failed to establish. Because the formation of the AER is *Fgf8* dependent (Crossley et al., 1996). There was no AER formed in the ectopic bud. Without *Fgf8* maintenance, *Fgf10* expression was kept at low level in the ectopic bud.

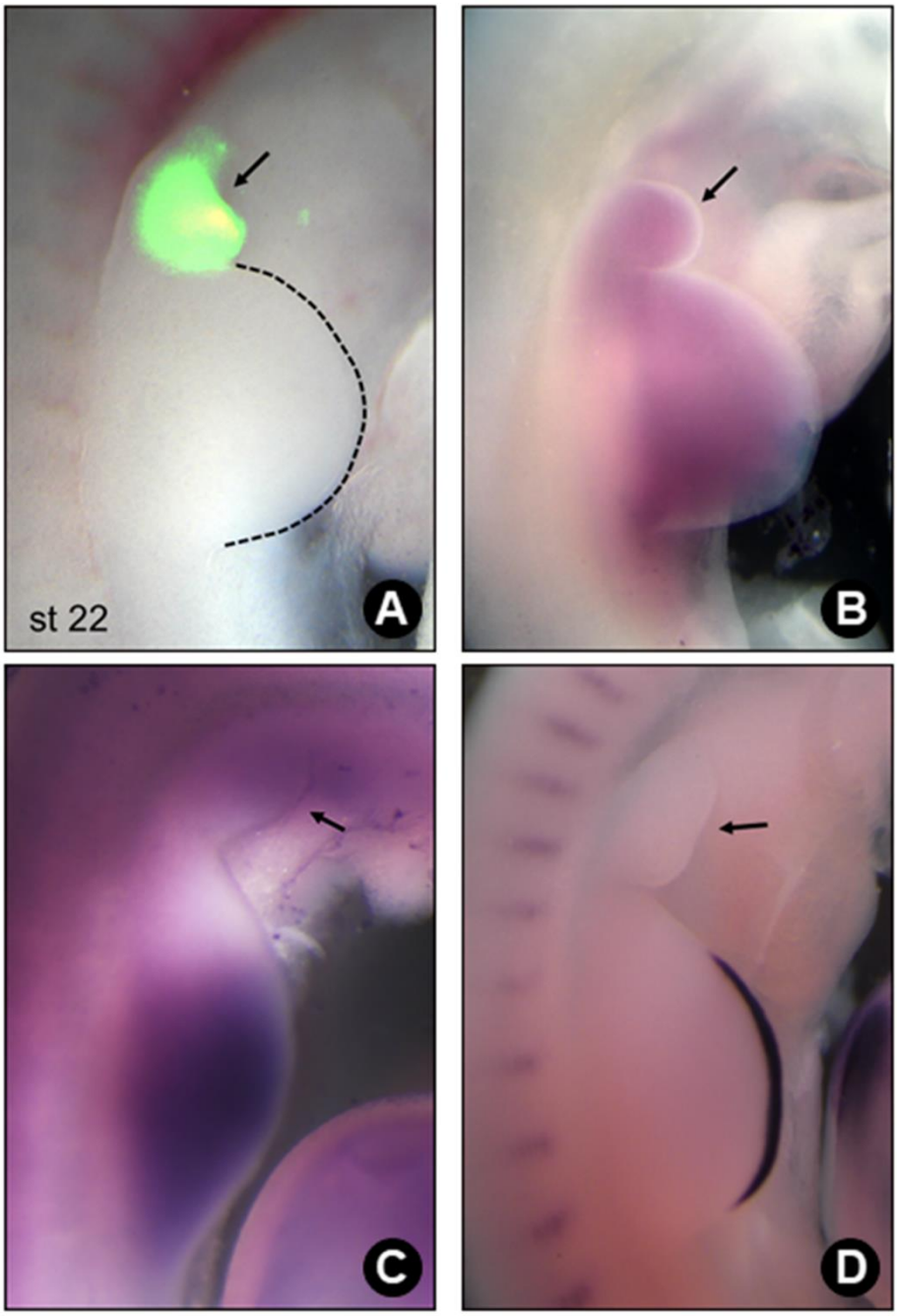

Fig. 17: *Hoxa6* induces ectopic buds anterior to the nature wing bud in HH-stage 22 embryos. A) Ectopic *Hoxa6* induced an ectopic bud with EGFP marker expression (arrow) anterior to the endogenous wing bud (black dotted line). B) *Tbx5* is expressed in the ectopic bud (arrow). C) *Fgf10* expression (arrow) in the ectopic bud. D) *Fgf8* is not expressed in the ectopic bud (arrow).

The wing bud is a three-dimensional structure. For the AP polarity of wing buds, *Fgf8* in the ectoderm activates *Shh* expression in posterior region of wing mesoderm (Riddle et al., 1993). Because of the lack of *Fgf8*, there was no *Shh* expression in the ectopic buds, therefore no ZPA formation was observed (Fig. 18A). The DV polarity of the wing bud is controlled through Wnt7a, Lmx1, and En1 (Tickle, 2002). The dorsal mesoderm marker, *Lmx1*, was detected in the ectopic bud (Fig. 18B), implying the dorsal polarity of the wing bud was formed in the ectopic bud. In summary, *Hoxa6* ectopic expression induced an additional small bud with the expression of *Tbx5*, *Fgf10*, and *Lmx1*, but not *Shh*.

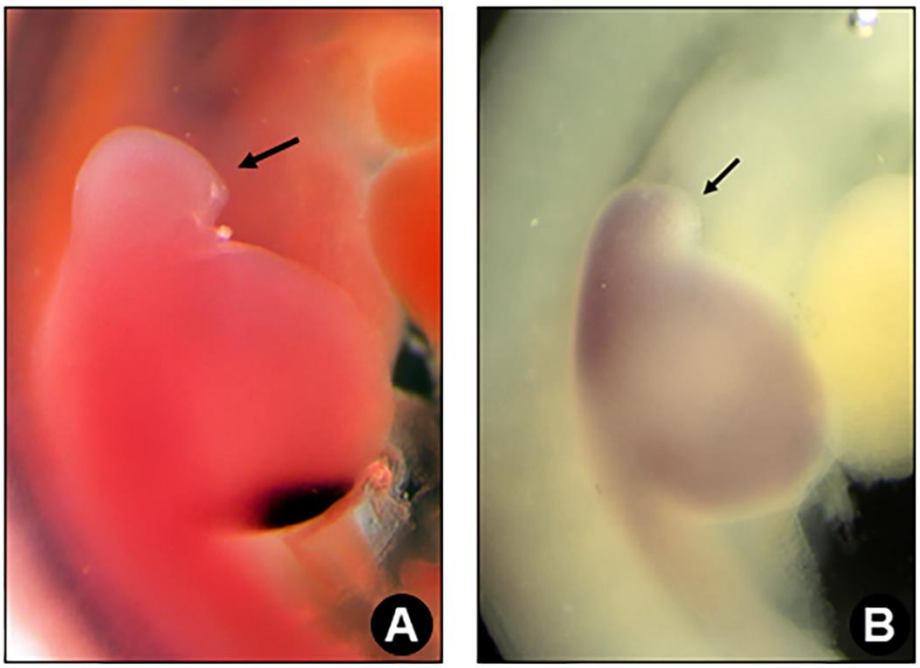

Fig. 18: *Hoxa6* induces *Lmx1* expression but not *Shh* in ectopic buds. **A**) Ectopic *Hoxa6* expression does not induce *Shh* expression in ectopic buds (arrow). **B**) *Hoxa6* induces *Lmx1* expression in ectopic buds (arrow).

3.3.3 Gene expression profiles in ectopic buds

In order to analyze the global function of *Hoxa6* on wing gene expression at HH-stage 22, I collected ectopic buds from *Hoxa6*-treated embryos, neck tissues anterior to the wing bud of normal embryos and endogenous wing buds from untreated embryos for mRNA sequencing (mRNA-seq) analysis. Gene expression profiles were compared among these three groups. The expression profiles were in line with the results from ISH. The *Tbx5* expression level in the ectopic bud was higher than that of the neck, but lower than that of the normal bud (Fig. 19). *Fgf10* and *Fgf8* expression patterns were generally the same as *Tbx5*, but at lower levels (Fig. 19). The results suggested that the gene expression patterns of the induced ectopic buds were highly similar to that of the natural wing buds.

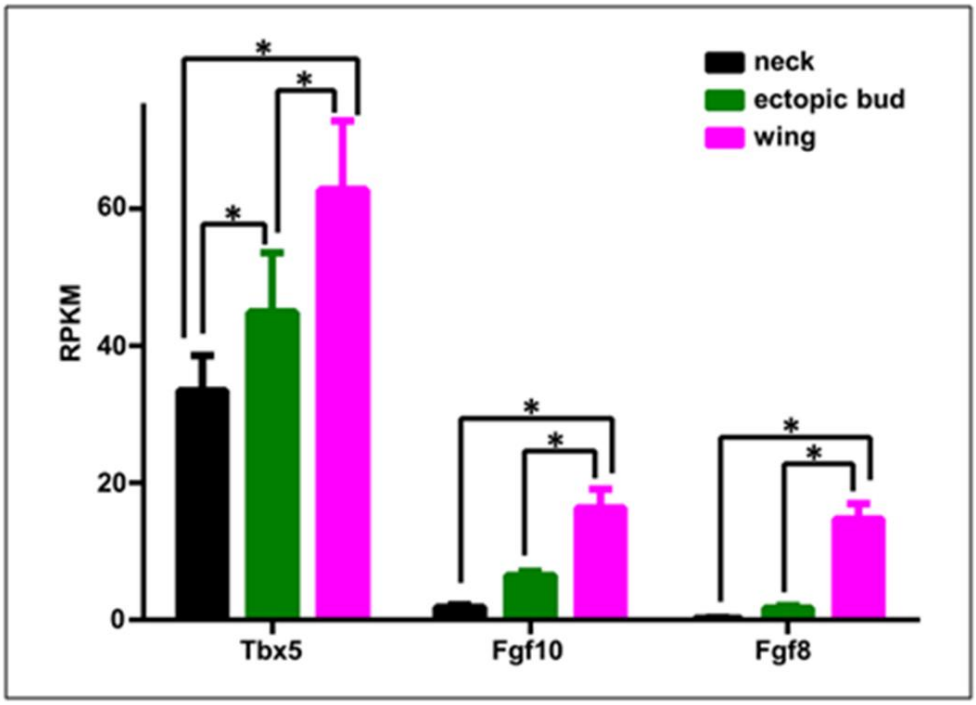

Fig. 19: Comparison of *Tbx5*, *Fgf10*, and *Fgf8* expression by mRNA sequencing. Data are presented as mean ± SEM. RPKM, Reads per Kilobase of transcipt per Million mapped reads. *p < 0.05

In line with the disappearance of *Fgf8* in the ectopic buds at HH-stage 22, *Wnt3a*, the signal that bridges mesodermal *Fgf10* to ectodermal *Fgf8*, was not expressed in the ectopic buds (Fig. 20). Also, other ectodermal signaling molecules such as *Bmp2*, *Fgf2*, and *Fgf4* were not expressed (Fig. 20), suggesting that neither the Fgf10-Fgf8 loop nor the AER formed in the ectopic buds.

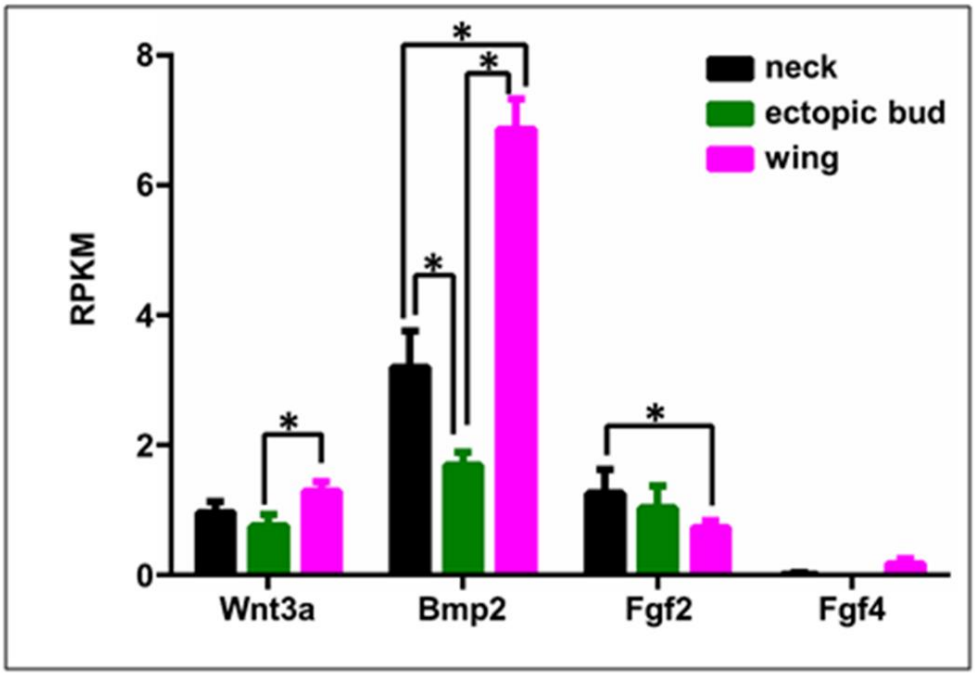

Fig. 20: Comparison of *Wnt3a*, *Bmp2*, *Fgf2*, and *Fgf4* expression by mRNA sequencing. Data are presented as mean ± SEM. RPKM, Reads per Kilobase of transcipt per Million mapped reads. *$p < 0.05$

Lmx1 was expressed in the ectopic bud as observed by ISH. The mRNA-seq expression profiles showed that *Lmx1* was expressed significantly higher in the ectopic bud than in the neck, and equally strong when compared to the natural wing bud (Fig. 21). Furthermore, *Wnt7a* expression level was higher than that of the neck and similar to that of the normal wing bud (Fig. 21). In contrast to the normal bud, no *En1* expression was found in the ectopic bud (Fig. 21). The high expression of *Lmx1* and *Wnt7a* but absence of *En1* expression suggested that the ectopic bud was predominantly dorsalized, whereas ventralization signals were missing.

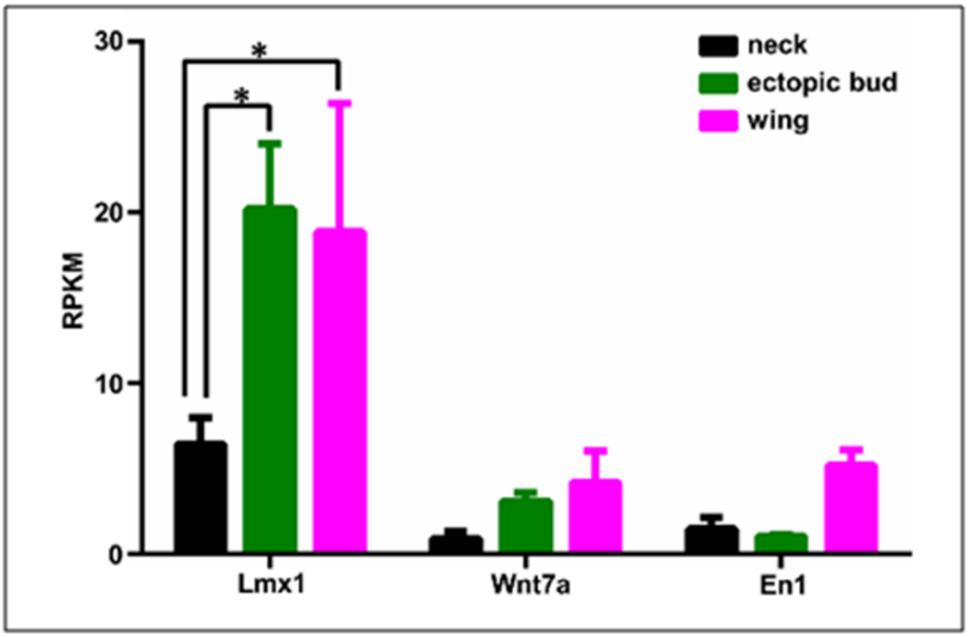

Fig. 21: Comparison of *Lmx1*, *Wnt7a*, and *En1* expression by mRNA sequencing. Data are presented as mean ± SEM. RPKM, Reads per Kilobase of transcipt per Million mapped reads. *p < 0.05

Intriguingly, some of the Hox genes related to the PD patterning of wing buds were expressed in the ectopic buds, including Hox PG 9-11 genes (Fig. 22). There was, however, no Hox PG 12-13 expression. These are expressed in the most distal part of the wing bud, indicating that *Hoxa6*-induced ectopic buds possessed only proximal fate.

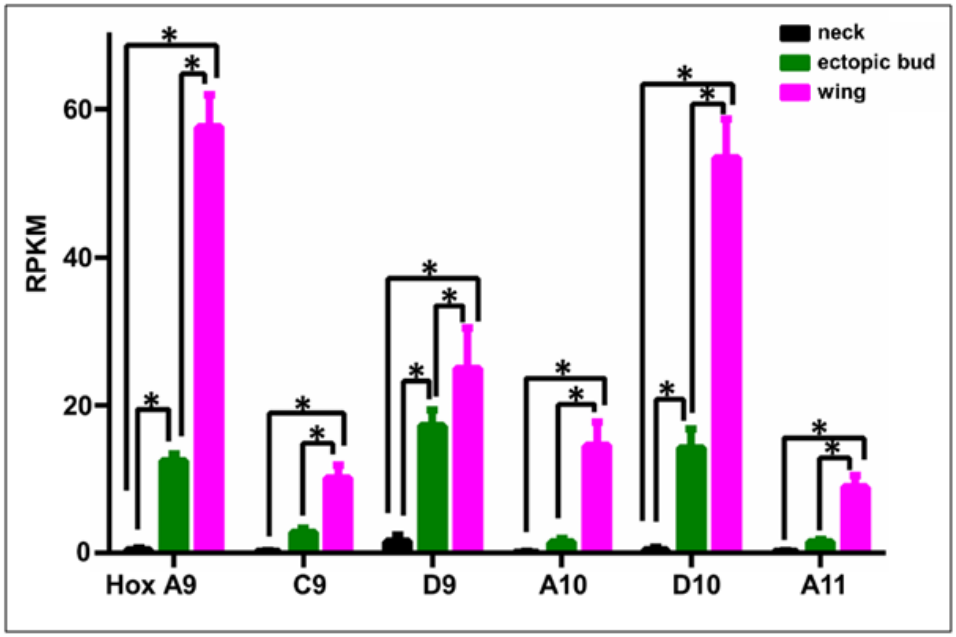

Fig. 22: Comparison of Hox PG 9-11 expression by mRNA sequencing. Data are presented as mean ± SEM. RPKM, Reads per Kilobase of transcipt per Million mapped reads. *p < 0.05

3.3.4 All of the *Hox PG 6-7* genes can induce ectopic buds

The other *Hox PG 6* members, *Hoxb6* and *Hoxc6*, have similar expression pattern as *Hoxa6* in chicken embryos. *Hoxa6* was able to induce an ectopic bud in the cervical region. To determine whether *Hoxb6* and *Hoxc6* have the same function, I performed electroporation using the same protocol as for *Hoxa6*. After 2 days of re-incubation, it was observed that both *Hoxb6* and *Hoxc6* induced ectopic buds anterior to the endogenous wing bud (Fig. 23). Thus, all of the *Hox PG 6* genes are able to induce ectopic buds anterior to the endogenous wing.

In general, the expression of *Hox PG 7* genes greatly overlaps with the wing field and is found just one vertebra caudal to the *Hox PG 6* expression domain, and *Hox PG 7* may have redundant functions. To study this, *Hoxa7* and *Hoxb7* expression plasmids were transfected into the LPM following the same protocol as for *Hoxa6*. Again, both *Hoxa7* and *Hoxb7*

induced ectopic bud formation anterior to the endogenous wing bud (Fig. 23). Together, ectopic expression of all members of *Hox PG 6* and *Hox PG 7* can induce ectopic buds in the cervical region.

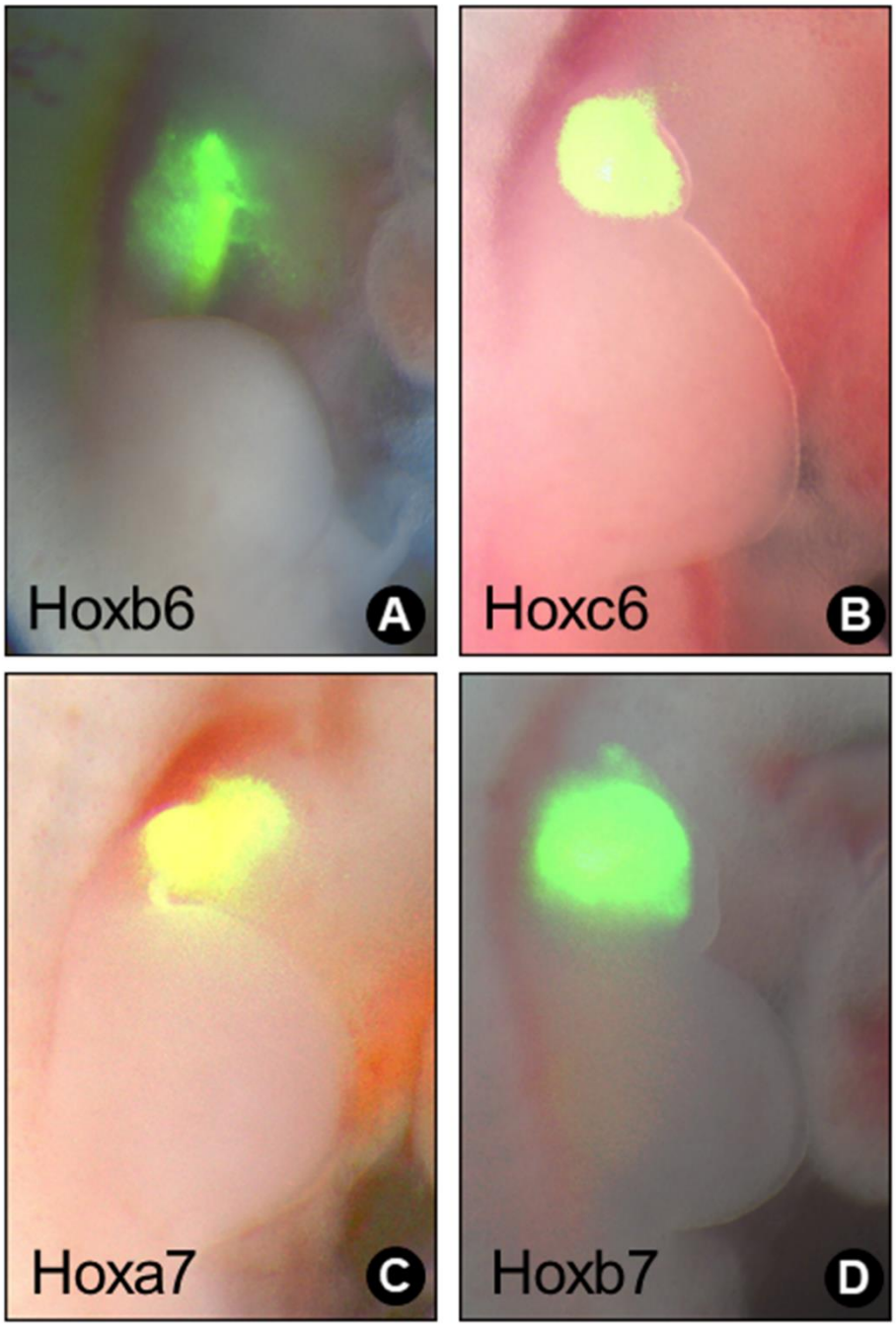

Fig. 23: Other Hox PG 6/7 genes can also induced ectopic buds, as shown in HH-stage 22 embryos. Ectopic expression of *Hoxb6* (**A**), *Hoxc6* (**B**), *Hoxa7* (**C**), and *Hoxb7* (**D**) induced ectopic buds anterior to the endogenous wing bud.

3.4 *Hox PG 4-5* genes are necessary for wing bud formation

After I observed the ectopic bud formation induced by *Hox PG 6-7* expression, we asked whether *Hox PG 6-7* genes are sufficient to induce wing bud formation. Since *Hox PG 6-7* expression domains overlap with that of *Hox PG 4-5* in the cervical region, we investigated whether the wing bud can form under the absence of *Hox PG 4-5* genes in the wing region. *Hoxb4* was chosen as a representative of this paralogous group. A dominant-negative form of *Hoxb4* (*Hoxb4dn*) plasmid was electroporated into the LPM cells of the anterior part of the prospective wing region at HH-stage 11 chicken embryos, which were studied after one or two days of re-incubation.

3.4.1 *Hoxb4dn* down-regulates expression of wing genes

After electroporation of *Hoxb4dn* and one day of re-incubation, the expression domain of *Tbx5* was shorter than that in the contralateral side (Fig. 24D). In the control plasmid electroporation domain indicated by EGFP, *Tbx5* expression was detected (Fig. 24C). The result shows that Hoxb4dn down-regulated *Tbx5* transcription during the stages of wing bud induction and initiation.

In addition to *Tbx5*, the expression of *Fgf10* and *Fgf8* was also repressed in the *Hoxb4dn* expression region (Fig. 25). In summary, Hoxb4dn affected the wing bud formation by inhibiting *Tbx5*, *Fgf10*, and *Fgf8* expression. To determine whether this repression by Hoxb4dn affected the further wing bud development, I also studied the subsequent wing bud formation.

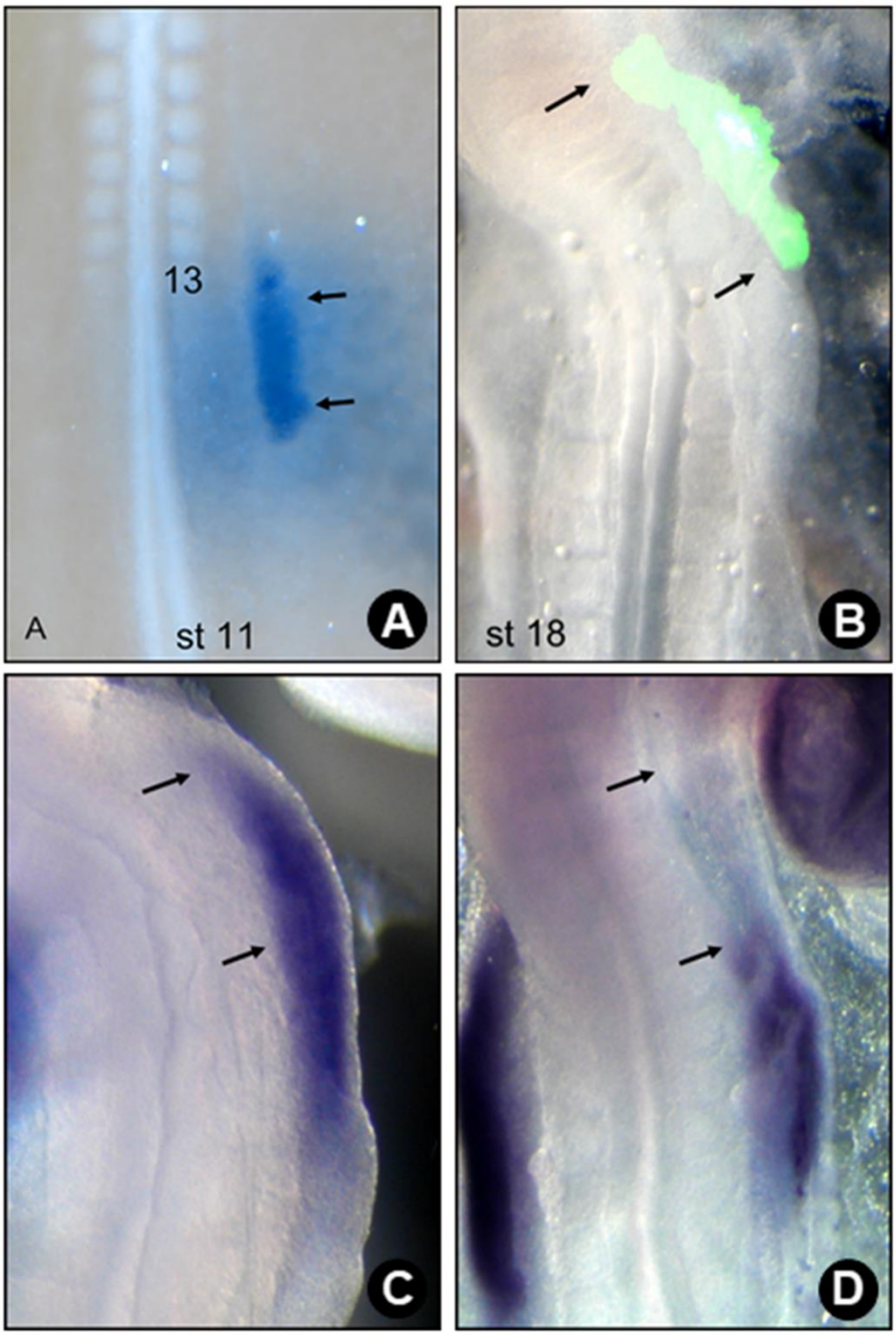

Fig. 24: *Hoxb4dn* expression down-regulates *Tbx5* expression. A) The photo showing the electroporation region (arrows) of HH-stage 11 embryos. Number indicates somite 13. B) Hoxb4dn position is shown with fluorescence maker (arrows) at HH-stage 18. C) *Tbx5* expression at HH-stage 18 after control EGFP electroporation is normal. D) *Tbx5* expression at HH-stage 18 after *Hoxb4dn* is reduced in the electroporation region (arrows).

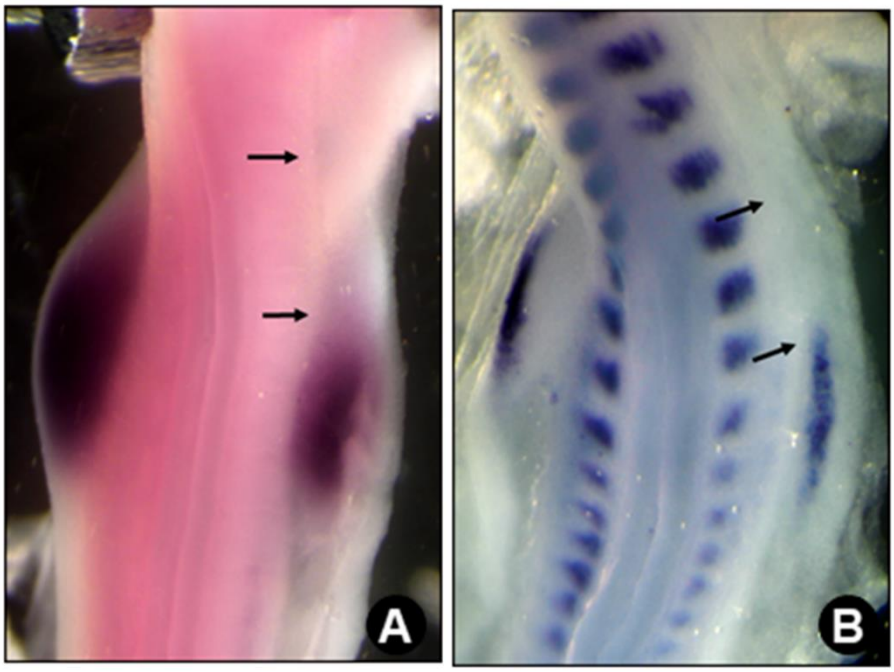

Fig.25: *Hoxb4dn* expression down-regulates *Fgf10* and *Fgf8* expression. Hoxb4dn expression down-regulated *Fgf10* (A) and *Fgf8* (B) expression anteriorly, corresponding to the electroporation region (arrows).

3.4.2 *Hoxb4dn* induces a flattening of the wing bud

After electroporation and two days of re-incubation, the wing bud formation was significantly affected by *Hoxb4dn*. The anterior part of the wing bud with *Hoxb4dn* was flattened, while the posterior part appeared to have a normal volume (Fig. 16B). The wing bud with control EGFP did not show this phenomenon, excluding the side effects of electroporation process (Fig. 16A). This flattened anterior wing bud indicated that *Hoxb4dn* delayed the outgrowth of the anterior wing bud.

The expression levels of *Fgf10*, *Fgf8*, and *Lmx1* in the anterior part of the wing bud were reduced in comparison to the posterior part and the contralateral side (Fig. 26, Fig. 27A), indicating prolonged effects of Hoxb4dn during wing bud development, although the *Tbx5* expression showed only a very weak decrease at HH-stage 22 (Fig. 27B). Therefore, the dominant-negative expression of Hoxb4 repressed *Tbx5* during wing bud induction, *Fgf10* and *Fgf8* during wing bud initiation and outgrowth and *Lmx1* during dorsal-ventral patterning. Hence, *Hoxb4* is necessary for multiple processes of wing bud formation.

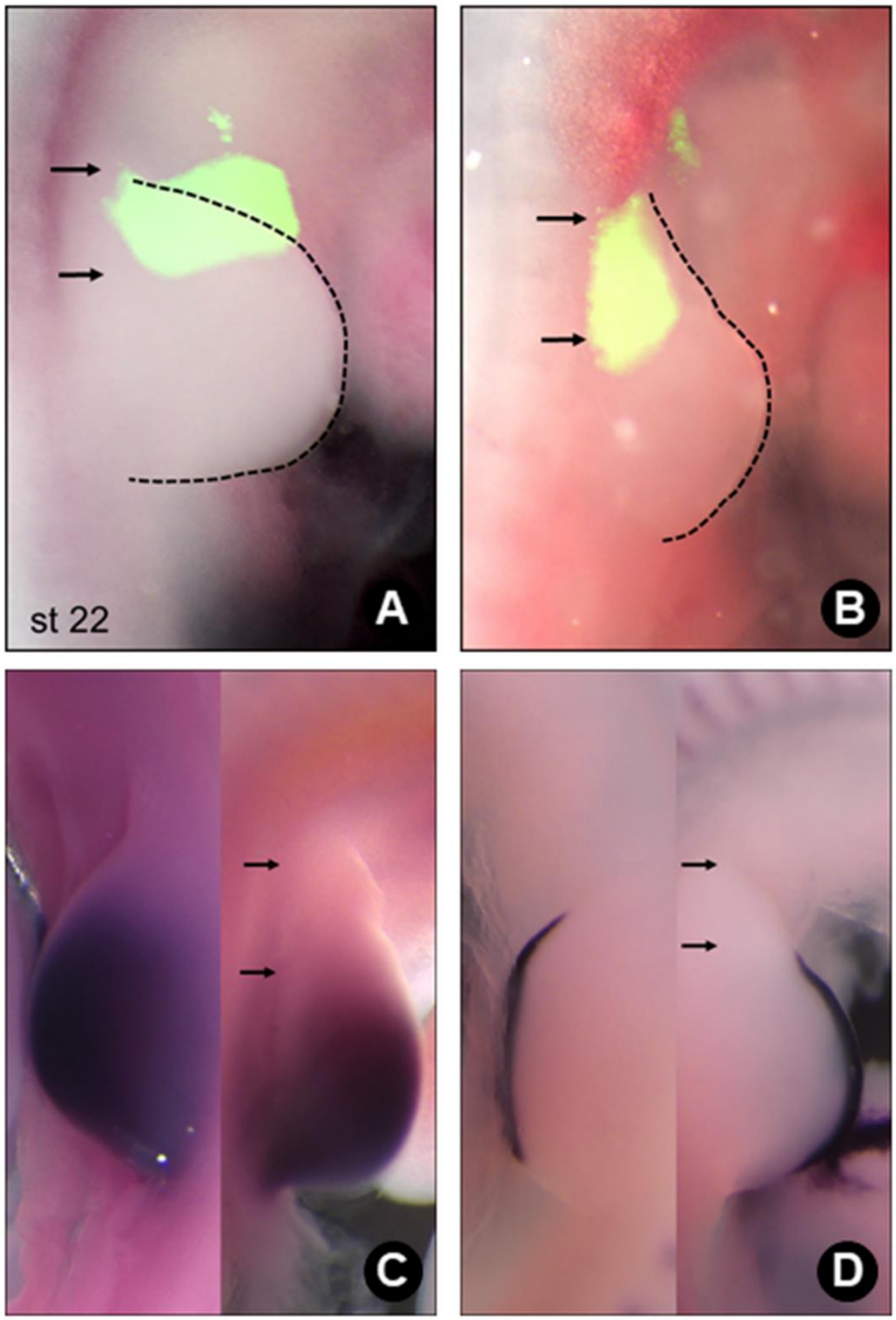

Fig. 26: *Hoxb4dn* expression induced a flat wing bud. *Hoxb4dn* expression resulted in a flat wing bud (B) compared to control (A) with EGFP plasmid. *Hoxb4dn* down-regulated *Fgf10* (C) and *Fgf8* (D) expression in the electroporation region (arrows).

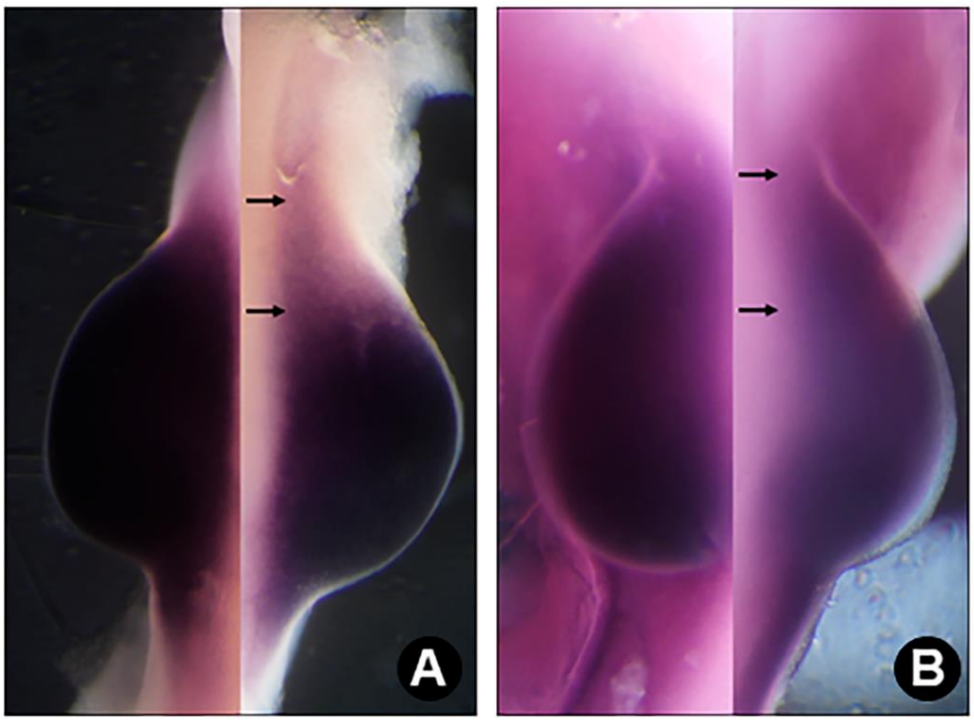

Fig. 27: *Hoxb4dn* expression down-regulates expression of wing genes. *Hoxb4dn* clearly down-regulated *Lmx1* (A) expression. *Tbx5* (B) showed a weak down-regulation expression in the electroporation region (arrows).

3.5 Summary

(1) The prospective wing region maintains its axial level throughout HH-stage 8 to 12 of chick embryos.

(2) The expression patterns of *Hox PG 4-5* and *Hox PG 6-7* overlap with the prospective wing region, which gave rise to the hypothesis that *Hox PG 6-7* is involved in the determination of the forelimb position.

(3) Ectopic expression of *Hox PG 6-7* in the cervical region induces *Tbx5*, the master gene for wing bud induction. *Hox PG 6-7* genes are sufficient for forelimb induction.

(4) The ectopic expression of *Hox PG 6-7* in the cervical region induces additional wing buds anterior to the endogenous one (Fig. 28A) and expression of a number of typical wing genes. *Hox PG 6-7* genes are sufficient for wing bud induction and initiation. They are positive activators of forelimb development.

(5) Repression of *Hoxb4* with a dominant-negative approach within the prospective wing region down-regulates wing bud induction, initiation, and outgrowth (Fig. 28B). Hence, *Hox PG 4-5* is necessary and indispensable for the development of the forelimb.

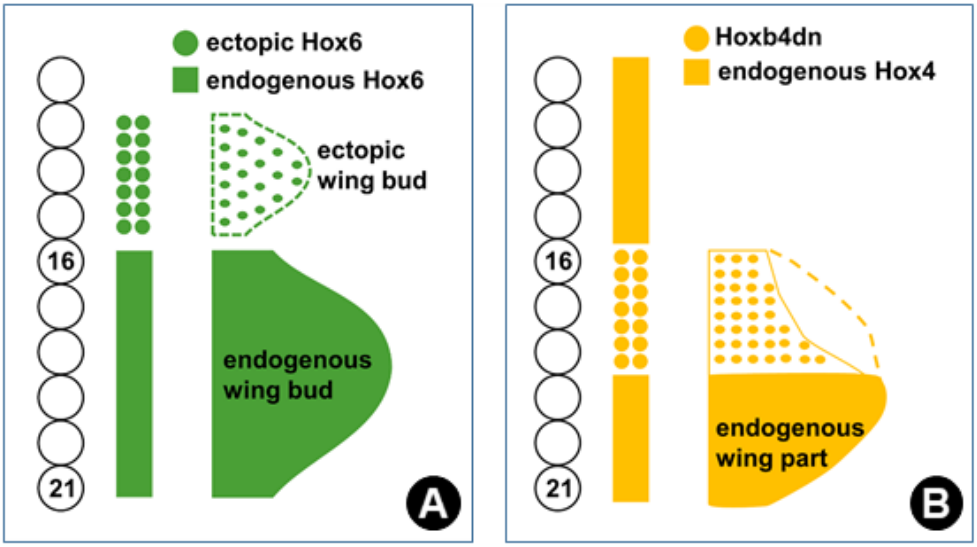

Fig. 28: Schemes summarizing the results of *Hox PG 6-7* and *Hoxb4dn* effects during wing bud formation. The left scheme shows the ectopic bud induction by ectopic *Hox PG 6-7* expression anterior to the endogenous expression domain (A). The right scheme shows the flattening of the anterior part of wing bud by *Hoxb4dn* (B).

4. Discussion

4.1 The prospective forelimb maintains its axial level

The precursor cells for the lateral plate mesoderm (LPM) is located in the posterior part of the primitive streak (PS) in gastrulation chick embryos ((Iimura and Pourquie, 2006; Sweetman et al., 2008). Formation of the LPM takes place between HH-stages 4-10. The prospective forelimb cells are generated around HH-stage 4-5 (Moreau et al., 2019), and the temporal collinear activation of *Hox PG 4/7/9* correlates with the axial position of the prospective limbs. For example, the timing for *Hoxb4* activation perfectly correlates with the ingression of the forelimb precursor cells (Moreau et al., 2019). Therefore, the axial position of limbs is determined during gastrulation under the regulation of the collinearity of *Hox* gene expression. First, *Hox* genes temporally determine the early formation of forelimbs and late the formation of hindlimbs and then, spatially restrict the axial position of forelimbs anterior to the hindlimbs.

It has already been described the prospective wing is located at the level of somite 15-20 of HH-stage 13 chick embryos. Chaube (1959) demonstrated the gradual expansion and positioning of the prospective wing by color-tracing methods (Chauber, 1959). He labelled the right part of embryos throughout the HH-stages 7-12 during *ex ovo* incubation. Thereby, HH-stage 7-9 embryos were re-incubated until HH-stage 11/12, and HH-stage 10-12 embryos were collected at HH-stage 17-19. The prospective wing region was at a level posterior to the Hensen's node at HH-stage 7 to HH-stage 8. But its position continuously changed in relation to the node and it was located at a level anterior to the node at the later stages (Chauber, 1959). My results were in line with his observation. However, in contrast to his *ex ovo* experiment, my *in ovo* LPM cell-tracing using DiI injection and EGFP electroporation allowed normal embryonic growth and minimize damage until the wing bud formation.

My cell-tracing results from HH-stage 8 to HH-stage 12 indicated that the prospective wing region maintains its axial level during wing induction. Somite 15 was a landmark of the anterior boundary of the wing bud (Fig. 29). In HH-stage 8 embryos, the 'pre-somite' 15 was located at the level immediately posterior to the Hensen's node. While, at HH-stage 9, it was located at the level anterior to the Hensen's node. At HH-stage 10 with 9-11 somites, the pre-somite 15 was found at a level clearly anterior to the Hensen's node.

Typically, the LPM at the level of the anterior end of presomitic mesoderm (PSM) in HH-stage 11 embryos was the subsequent anterior boundary of the wing bud. HH-stage 11 embryos have 12 to 14 somites, indicating that the anterior end of PSM would form somite 15 perfectly. At HH-stage 12, the anterior boundary of the wing bud was found at the newly formed somite. In conclusion, the prospective wing maintains its axial position through HH-stage 8 to HH-stage 12 (Fig. 29). Because of the homologous expression pattern of *Hox* genes, this maintenance of the forelimb position appears to be conserved in other animals during evolution, from fish to amphibians, to birds and mammals ((Burke et al., 1995; Jeannotte et al., 1993; Molven et al., 1990; Moreau et al., 2019). These differences in the forelimb position during evolutionary development would be a result of the reprogramming of the expression patterns of homologous *Hox* genes. To further verify this, fate mapping of the limb bud in other species would be necessary.

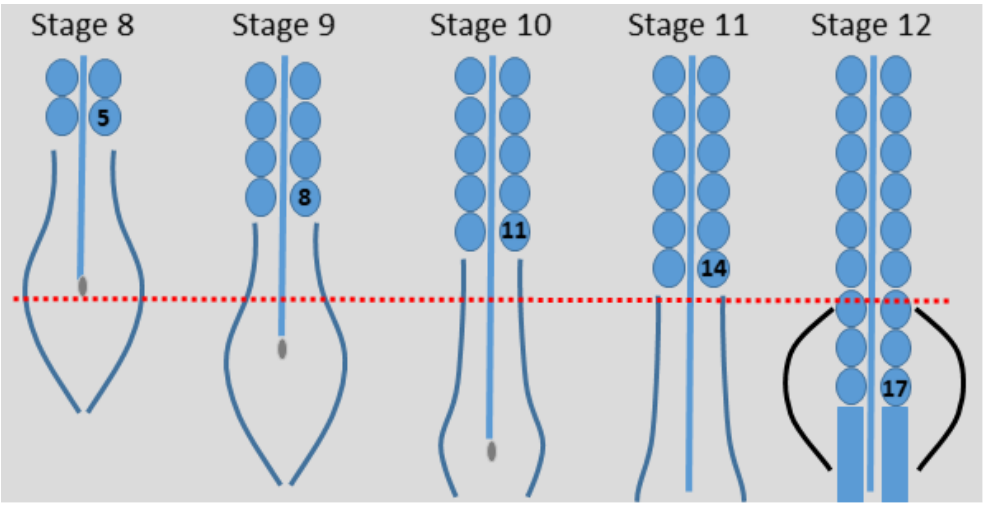

Fig. 29: Fate map of HH-stage 8-12 chick embryos. Somites are shown as circles with numbers. The wing bud is shown as a black line. The red dotted line indicates the axial level of the prospective somite 15 as a landmark of the anterior boundary of the wing bud.

4.2 Function of mesodermal *Hox PG 6-7* expression during wing bud formation

My data shows that ectopic expression of *Hox PG 6-7* genes induced additional wing buds anterior to the endogenous ones, confirming my hypothesis. They could participate in the wing bud formation, besides *Hox PG 4-5* genes, and they are sufficient for early wing bud formation.

4.2.1 Mesodermal *Hox PG 6-7* expression is sufficient for wing bud induction and initiation

The data shows that ectopic expression of *Hoxa6* in the cervical region induced *Tbx5* expression anterior to the preliminary endogenous preliminary wing bud. Its expression level was similar to the endogenous one. These results indicate that *Hoxa6* is able to induce wing bud by activating *Tbx5* transcription. The ectopic expression of *Tbx5* subsequently induced *Fgf10*, which started the wing bud initiation. The ectopic expression of *Tbx5* and *Fgf10* was maintained at later stages, showing a constant function of *Hoxa6* during wing bud initiation. Normally, there is no *Hoxa6* expression and no *Tbx5* expression in the cervical region anterior to the wing bud. Therefore, ectopic *Hoxa6* can activate the pathway for wing bud induction and initiation anterior to the natural wing bud. The formation of ectopic buds induced by other members of *Hox PG 6-7* indicate that all of these *Hox PG 6-7* genes are sufficient to activate wing bud formation.

Taken together, the function of *Hox PG 6-7* to activate *Tbx5* expression overrules the functions of *Hox PG 4-5* in the cervical region. It is common sense that the functions of more posterior *Hox* genes are stronger than those of more anterior ones, owing to their collinear expression pattern.

4.2.2 Mesodermal *Hox PG 6-7* cannot induce wing bud outgrowth

In my experiments, ectopic *Hoxa6* expression induced the small additional bud in the cervical region. However, in the ectopic bud, there was no *Fgf8* expression in the overlying ectoderm. Therefore, the feedback loop between *Fgf10* and *Fgf8* did not form. The distal *Fgf8*-expressing ectoderm in limb buds of normal embryos forms the apical ectodermal ridge (AER), which is essential for the outgrowth of the limb bud (Tickle, 2015). In the ectopic buds, there was no expression of signals related to AER. Therefore, the AER was not formed, resulting in a discontinuation of mesenchymal outgrowth and formation of a small wing bud.

Considering the small size of the ectopic bud a comparison with the wing in the *limbless* chick mutant is obvious. The *limbless* chick is based on an autosomal recessive mutation (Prahlad et al., 1979). There is no *Fgf8* expression in the ectoderm, and no AER is formed (Grieshammer et al., 1996; Noramly et al., 1996; Ros et al., 1996). Therefore, the wing in the

limbless chick mutant remains small. Hence, wing bud outgrowth does not occur in both the *limbless* chick and the ectopic bud induced by *Hoxa6*.

However, the question remains why the wing bud outgrowth not take place in the ectopic bud induced by *Hoxa6*? An ectopic limb could be induced in the flank region after application of FGFs or by the transplantation of prospective limb cells with all of the signaling characteristics of normal limbs (Cohn et al., 1995; Lours and Dietrich, 2005). The flank mesoderm and ectoderm possess the entire potential for limb bud initiation and outgrowth. Flank cells are competent for limb formation. In contrast, the same type of operations in the neck region cannot induce ectopic limb formation (Lours and Dietrich, 2005). In my study, *Hoxa6* ectopic expression in the neck region gave similar results to those after FGF induction or transplantation of the prospective limb mesoderm in the neck region. Only deformed buds develop in the neck region as compared to the ectopic limbs in the flank region. Accordingly, one must conclude that there are differences between the flank and the neck, which cause different bud formation.

There is one theory that may explain this phenomenon. The incomplete formation of ectopic wing buds in the neck is due to the interruption of the *Fgf10-Fgf8* signaling cascade via the MAPK pathway (Lours and Dietrich, 2005). As a consequence, the feedback loop between *Fgf10* and *Fgf8* fails to form and no AER and no limb bud forms in the neck region (Fig. 30). *Fgf10* in the neck LPM cannot through the MAPK pathway to activate *Fgf8* expression in the overlying ectoderm; *Fgf8* in the neck ectoderm cannot activate Fgf10 expression in the neck mesoderm, although it passes the MAPK pathway (Lours and Dietrich, 2005). The neck is limb-incompetent (Lours and Dietrich, 2005). There must be some other yet unknown signaling mechanisms that interrupts this cascade.

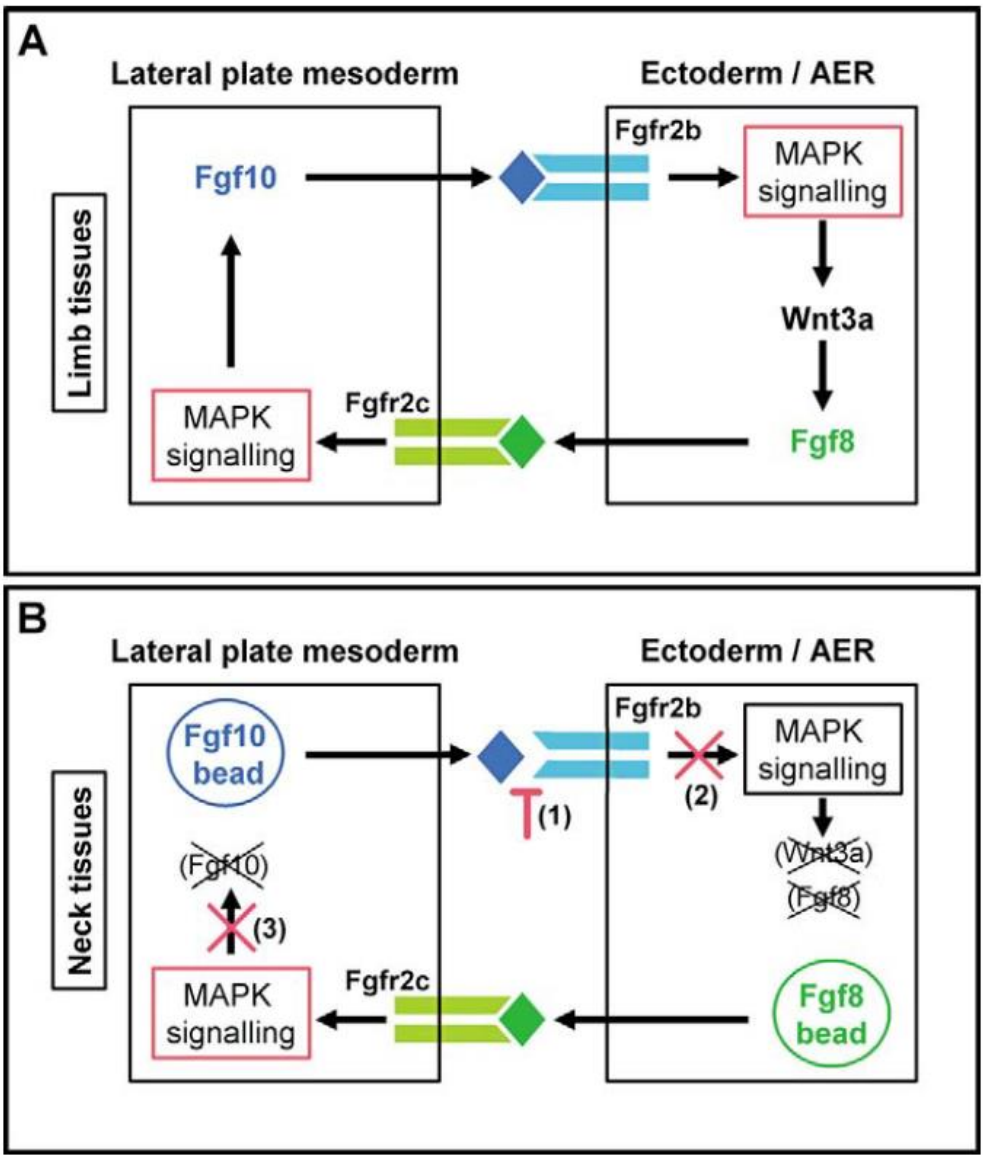

Fig. 30: The Fgf10-Fgf8 cascade through MAPK pathway in limb tissues and neck regions (Lours and Dietrich, 2005).

Although *Hoxa6* ectopic expression induced *Tbx5* and *Fgf10* expression in the neck mesoderm. With the theory of the neck limb-incompetent, because of the MAPK interruption, it was not able to activate the ectodermal *Fgf8* expression. Therefore, no Fgf10-Fgf8 feedback loop formed and no AER formation resulted in a small limb bud. Hence, the ectopic bud induced by *Hoxa6* only underwent the induction and initiation phases. From another aspect, *Hoxa6* ectopic expression did induce *Tbx5* and *Fgf10* expression, indicating that *Hoxa6* can induce the neck mesoderm transfer into limb-fate mesoderm.

Intriguingly, *Fgf8* was transiently expressed after ectopic *Hoxa6* expression in the preliminary bud, but disappeared very soon. Why can the neck ectoderm express *Fgf8* transiently?

According to Lours and Dietrich (2005), there should not be Fgf8 expression in the neck ectoderm. It is probable that *Fgf10* at early stages induced Fgf8 expression, but this was not sufficient for constant *Fgf8* activation, and *Fgf8* may need additional signals for its maintenance. Alternatively, the disappearance of *Fgf8* at the later stages did not maintain *Fgf10* expression, following which *Fgf10* expression level decreased and was too low to activate *Fgf8*. Both scenarios would explain the absence of the positive feedback loop in the ectopic bud.

4.2.3 *Hox PG 6-7* cannot induce wing bud AP patterning

In the *Hoxa6*-induced ectopic bud, I observed neither *Shh* expression nor the zone of polarizing activity (ZPA) formation. Therefore, anterior-posterior (AP) patterning of the wing bud was not activated. A similar phenomenon is seen in the *limbless* chick mutant. Because of the missing *Fgf8* expression to induce *Shh* expression, the ZPA formation failed. FGF8-soaked beads could induce *Shh* expression in the wing of the *limbless* chick mutant, and also, AER removal experiments prove *Fgf8* from AER is the endogenous inducer of *Shh* expression during normal limb bud patterning (Grieshammer et al., 1996; Johnson et al., 1994). *Shh* has all properties for the AP patterning of the limb bud (Tickle and Towers, 2017). The ectopic expression of *Hox PG 6-7* cannot ensure *Shh* expression and ZPA formation, therefore, no AP patterning was seen, similar to that of the *limbless* wing bud. As FGF8-soaked bead can induce *Shh* expression in the *limeless* mutant, I would suspect that it could also cause the same expression and ZPA formation in the ectopic buds induced by *Hox PG 6-7*.

4.2.4 Ectopic wing buds induced by *Hoxa6* is dorsalized

The dorsal-ventral (DV) polarity of the limb bud progressively develops during limb bud initiation (Tickle, 2002). In the *Hoxa6*-induced ectopic buds, I observed strong *Lmx1* and *Wnt7a* expressions. Moreover, the *Lmx1* expression level was even higher than that of the endogenous wing bud. However, the ventral ectoderm marker, *En1*, was poorly expressed in ectopic buds. These results suggest the ectopic bud was predominantly dorsalized. Similarly, a pure dorsal polarity also develops in the *limbless* mutant with *Wnt7a* and *Lmx1* expression (Grieshammer et al., 1996). This dorsalization is also seen in chick embryos after

transplantation of prospective forelimb cells into the neck region (Lours and Dietrich, 2005).The reasons for the dorsalization of the ectopic wing bud could, in part, be due to the absence of the AER similar to the *limbless* mutant (Grieshammer et al., 1996; Noramly et al., 1996).

4.2.5 *Hox PG 6-7* induces wing bud PD patterning

Ectopic *Hoxa6* induced *Hox PG 9-11* expression in the ectopic buds. *Hox PG 9-13* genes are expressed in a gradient along the proximal-distal (PD) axis and are required for the PD patterning of the wing bud (Tickle, 2002). Expression of only *Hox PG 9-11* in ectopic buds indicates that the ectopic wing bud processes only the stylopodium and zeugopodium but not autopodium. In contrast, in the *limbless* mutant, expression of H*oxd11 - 13* suggests the distal part patterning of the limb bud is occurred (Noramly et al., 1996). Therefore, mechanisms for PD patterning in the *limbless* wing bud and the *Hoxa6*-induced ectopic bud must be different. Usually, *Shh* expression has the potential for limb PD patterning (Tickle and Towers, 2017). However, *Shh* is neither expressed in the *limbless* mutant nor the *Hoxa6*-induced ectopic bud, indicating that PD patterning is partly independent of *Shh*.

4.3 *Hox PG 4-5* genes are dispensable for wing bud induction

Hox PG 4-5 genes are expressed in LPM along the cervical region, and they can activate Tbx5 transcription in chicken embryos (Minguillon et al., 2012). *Hox PG 4-5* mutant mice have vertebral transformations at the cervical-thoracic interface, where the forelimb is located. So, *Hox PG 4-5* genes seem to be necessary for wing bud formation. However, because they have a broader expression region than the wing field, the anterior boundary of the wing bud cannot be determined by them. So, I drew my attention to *Hox PG 6-7* genes. Indeed, ectopic expression of *Hox PG 6-7* resulted in ectopic wing bud formation. However, considering the Hox genes' collinearity expression pattern, *Hox PG 4-5* is activated ahead of *Hox PG 6-7*.

Therefore, the question remains whether *Hox PG 6-7* genes can regulate the normal wing bud formation without the expression of *Hox PG 4-5*. First, the negative expression of *Hoxb4* firstly down-regulated *Tbx5* expression. Then, with decreased *Tbx5* expression, the wing bud initiation detected by *Fgf10* expression was affected. As a result, the wing bud outgrowth was failed, showing neither the Fgf10-Fgf8 feedback loop nor the AER was formed. The wing bud was flattened. Hence, the negative expression of *Hoxb4* affected first the wing bud induction

and subsequently the initiation and outgrowth. Similarly, *Hoxb4dn* during gastrulation could shorten *Tbx5* expression region (Moreau et al., 2019). On the contrary, overexpression of *Hoxb4* at the flank could extend the wing bud posteriorly (Moreau et al., 2019). In conclusion, *Hox PG 4-5* genes are necessary, while *Hox PG 6-7* genes alone are not sufficient for wing bud induction.

4.4 *Hox* code

The *Hox* code is named as the combinatory functions of several *Hox* genes together and it is contributing to the specific body plan of embryos morphologically (Duboule and Dollé, 1989; Kessel and Gruss, 1991). Previous studies as well as my investigations show that the forelimb position and its induction are regulated by a *Hox* code. Furthermore, I proposed that *Hox* code for forelimb would be also conserved in other vertebrates.

4.4.1 *Hox* code for forelimb induction

Hox PG 6-7 expression in the neck region induced ectopic wing buds and negative expression of *Hoxb4* caused the wing bud fail to form as distal as the endogenous one. These genes are essential during forelimb/wing formation. The contribution of *Hox* genes to the forelimb is to initiate the induction process through activating *Tbx5* transcription in the prospective forelimb cells. After the activation of *Tbx5* for induction, the next step for bud formation would follow. Previous studies show that *Hox PG 9* genes stop the forelimb formation by inhibiting *Tbx5* expression. They play repress functions also in the forelimb bud induction process. Hence, the *Hox* code for the forelimb bud induction should include an activating component, including *Hox PG 4-5* and *Hox PG 6-7* genes, and an inhibiting component, the *Hox PG 9* genes. At first, *Hox PG 4-5* genes initiate *Tbx5* transcription, and then, *Hox PG 6-7* genes maintain its expression in the prospective forelimb region. Finally, *Hox PG 9* genes cease the posterior extension of *Tbx5* expression, determining the posterior boundary of the forelimb bud.

Further, I proposed that the anterior boundary of the forelimb would be determined by *Hox PG 6-7* genes. At first, the expression of *Tbx5* is activated by *Hox PG 4-5* in a broad cervical region. At the cervical-thoracic interface, *Tbx5* expression is maintained by *Hox PG 6-7* genes. This mechanism is underpinned by comparison of the expression pattern of *Hoxb4*, *Hoxa6*, and *Tbx5* at HH-stage 13-17 chicken embryos. The expression of *Hoxa6* at HH-stage 11 is perfectly started at the level of the anterior end of PSM, which is identified as the anterior

boundary of the prospective wing bud. Hence, the anterior boundary of forelimb is determined by *Hox PG 6-7* genes.

4.4.2 *Hox* code for forelimb lateral motor column

In the developing chicken embryos, a certain population of motor neurons (MN) in the spinal cord that innervate the limb muscles forms the lateral motor column (LMC). This level of the spinal cord is called the brachial spinal cord, which is posterior to the cervical spinal cord after forelimb formation. Previous studies have identified that the brachial spinal cord is congruent with the expression region of *Hoxc6* and the posterior end of the brachial spinal cord is determined by *Hoxc9*. *Hoxc9* has a function on the repression of LMC posteriorly extension (Dasen et al., 2005). This repression of *Hoxc9* on LMC is similar to that of the *Tbx5* expression for the forelimb bud formation. This cooperation of *Hoxc6* and *Hoxc9* on LMC formation is similar to that on the forelimb bud induction. I assumed this would be another instance to interpret the regulation of Hox code to the forelimb development.

The LMC formation is regulated by the combinatory functions of *Hox PG 4-7* genes. And its anterior end is determined by *Hox PG 6-7*. At HH-stage 18 of chicken embryos, *Hox PG 4-5* genes are permissive to the development of LMC in the entire cervical spinal cord (Mukaigasa et al., 2017). However, in absence of *Hox PG 6-7*, LMC in the cervical region undergoes apoptosis from HH-stage 23 up to HH-stage 27, exclusively restricting the LMC in the brachial region (Mukaigasa et al., 2017). Ectopic expression of *Hox PG 6-7* in the cervical spinal cord can repress apoptosis and result in the LMC being kept in the non-brachial region (Mukaigasa et al., 2017).

In conclusion, the LMC is determined by the Hox code. It consists of *Hox PG 4-5* genes, activating LMC formation permissively in the entire cervical region; *Hox PG 6-7* genes, maintaining LMC development in the brachial region; and *Hox PG 9* genes, limiting the posterior end of LMC (Dasen et al., 2005; Mukaigasa et al., 2017). This *Hox* code determines the specific position of LMC, corresponding to the axial level of the forelimb.

4.4.3 *Hox* code for forelimb position

A study showed recently, a comparison among three bird species with different axial levels of their wings further identified the contribution of *Hox* code to the forelimb formation. In birds, no matter where the wing is located posterior to a long neck or a short neck, the *Hoxb4*/*Hoxb9* expression interface is always corresponding to the posterior boundary of the wing (Moreau et al., 2019). This is consistent to that *Hox PG 9* limits the posterior end of the forelimb bud. Thus, the Hox code for wing bud formation in zebra finch and ostrich would be the same as that in chicken. So, I would like to conclude that the *Hox* code for forelimb position is conserved within the different species of birds.

The forelimb is always formed in the cervical and thoracic interface regions. Hox PG 6 has functions on the determination of the cervical-thoracic transition and this is consistent with its expression starting from the first thoracic vertebrae (Burke et al., 1995). Its expression pattern is conserved to be correlated with morphologies in chicken and mouse embryos which have distinct axial formulas. Besides chicken and mouse, *Hoxc6* also has the same expression pattern in domestic goose, zebra fish, lizard, turtle and crocodile (Böhmer, 2017; Böhmer et al., 2015a; Burke et al., 1995; Mallo et al., 2010; Molven et al., 1990; Ohya et al., 2005). Therefore, *Hox PG 6* would be a member of the *Hox* code for forelimb formation that is conserved from fish to mammals.

4.5 Permissive and decisive roles of *Hox* code genes

During forelimb induction regulated by *Hox* code, *Hox PG 9* genes are inhibitors for Tbx5 expression and stop the forelimb formation. And *Hox PG 4-5* and *Hox PG 6-7* are activators to activate *Tbx5* expression for the forelimb bud induction. The ectopic expression of *Hox PG 6-7* was able to induce additional wing bud, while repression of *Hoxb4* affected wing bud formation. As observed during the LMC formation, there is a cooperation between *Hox PG 4-5* and *Hox PG 6-7*.

Considering the spatial and temporal collinearity expression pattern of Hox genes, at first *Hox PG 4-5* genes induce *Tbx5* transcription along their expression region. This is a much broader region than the forelimb field. Subsequently, *Hox PG 6-7* genes maintain *Tbx5* expression in the prospective forelimb field.

Meanwhile, at the anterior cervical region where only *Hox PG 4-5* are expressed, *Tbx5* is silenced. Finally, *Tbx5* is only concentrated in the forelimb region and contributes to the forelimb induction.

Hence, *Hox PG 4-5* and *Hox PG 6-7* genes are necessary and indispensable for forelimb induction. The lack of either of them cannot promote forelimb formation. However, their functions are different. *Hox PG 4-5* genes induce a broad permissive region, where *Hox PG 6-7* genes decisively instruct the forelimb induction, determining the forelimb anterior boundary. Similarly, during LMC formation in the cervical spinal cord, *Hox PG 4-5* also plays the permissive role to initiate LMC formation, and then, *Hox PG 6-7* decisively restricts the LMC in the brachial spinal cord. Therefore, the permissive and decisive roles of *Hox* code genes would be a common feature during the determination of axial identities of vertebrate animals.

4.6 Conclusion

(1) The prospective forelimb position, which is determined by *Hox* genes during gastrulation, maintains its axial level during embryonic development. The differences in the forelimb position among vertebrates is owing to the reprogramming of the expression patterns of homologous *Hox* genes during evolutionary development.

(2) *Hox PG 6-7* genes are sufficient for the forelimb induction (Fig. 31A).

(3) *Hox PG 4-5* genes are indispensable for the forelimb induction (Fig. 31B).

(4) The anterior boundary of the forelimb is regulated by functionally distinct *Hox* code genes. *Hox PG 4-5* genes, playing as the permissive role, activate *Tbx5* transcription. While, *Hox PG 6-7* genes, playing as the decisive role, maintain *Tbx5* expression for the forelimb induction (Fig. 31C).

(5) Because of the homologous *Hox* genes among vertebrates during evolutionary development, the permissive and decisive roles of *Hox* genes would be a general mechanism for the combinatory functions of *Hox* genes for morphogenesis and organogenesis.

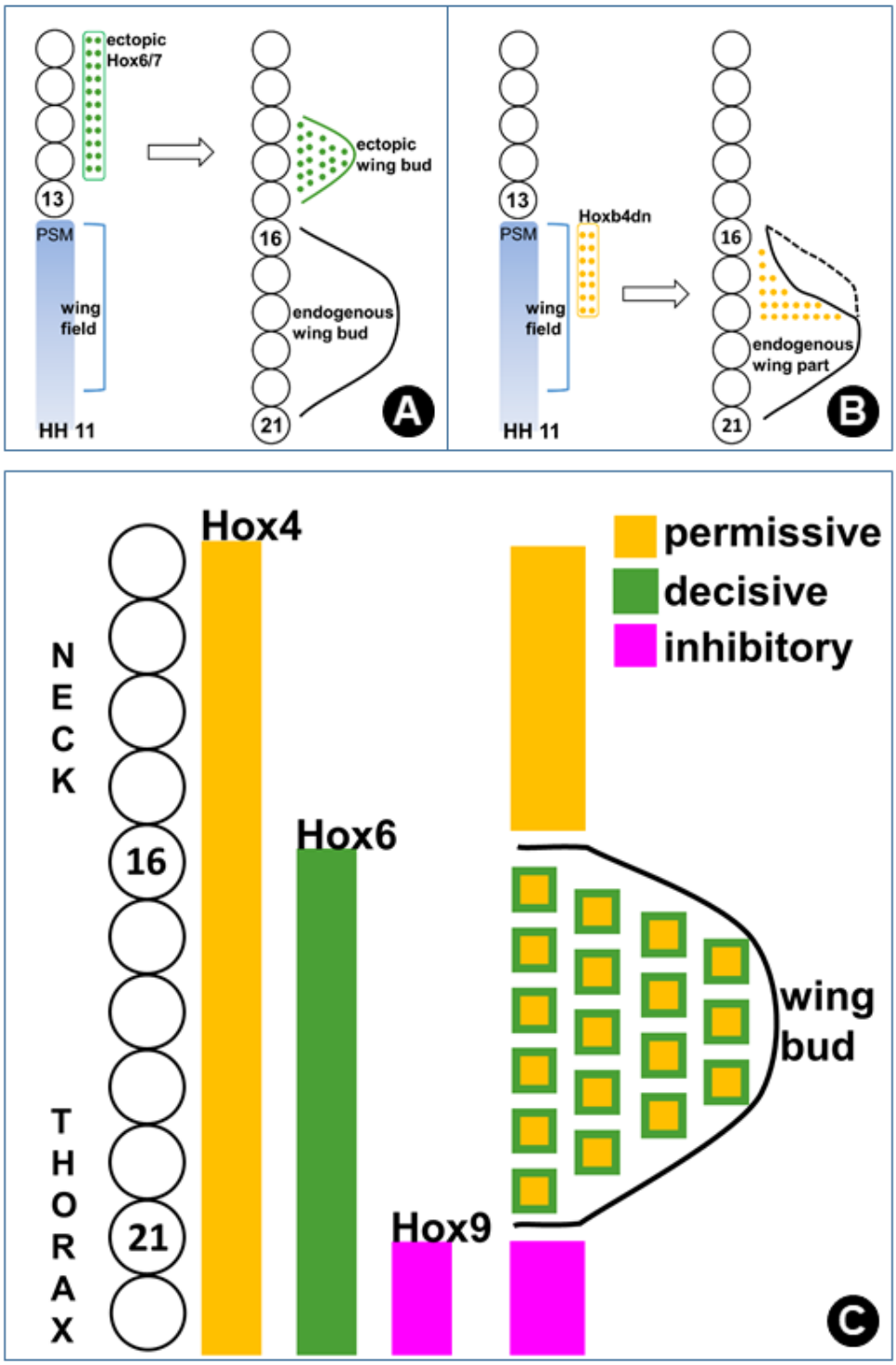

Fig. 31: Diagrams for the experiments and the *Hox* code. A) Ectopic *Hox PG 6-7* induced ectopic buds in the neck region. B) *Hoxb4dn* down-regulated wing bud formation. C) The *Hox* code for forelimb includes *Hox PG 4-5* with permissive, *Hox PG 6-7* with instructive, and *Hox PG 9* with inhibitory roles.

5. References

Agarwal, P., Wylie, J.N., Galceran, J., Arkhitko, O., Li, C., Deng, C., Grosschedl, R., and Bruneau, B.G. (2003). Tbx5 is essential for forelimb bud initiation following patterning of the limb field in the mouse embryo. Development 130, 623-633.

Altabef, M., Clarke, J.D., and Tickle, C. (1997). Dorso-ventral ectodermal compartments and origin of apical ectodermal ridge in developing chick limb. Development 124, 4547-4556.

Aulehla, A., and Pourquie, O. (2009). More than patterning--Hox genes and the control of posterior axial elongation. Developmental cell 17, 439-440.

Barak, H., Preger-Ben Noon, E., and Reshef, R. (2012). Comparative spatiotemporal analysis of Hox gene expression in early stages of intermediate mesoderm formation. Developmental Dynamics 241, 1637-1649.

Barrow, J.R., Thomas, K.R., Boussadia-Zahui, O., Moore, R., Kemler, R., Capecchi, M.R., and McMahon, A.P. (2003). Ectodermal Wnt3/beta-catenin signaling is required for the establishment and maintenance of the apical ectodermal ridge. Genes Dev 17, 394-409.

Basson, C.T., Bachinsky, D.R., Lin, R.C., Levi, T., Elkins, J.A., Soults, J., Grayzel, D., Kroumpouzou, E., Traill, T.A., Leblanc-Straceski, J., et al. (1997). Mutations in human TBX5 [corrected] cause limb and cardiac malformation in Holt-Oram syndrome. Nat Genet 15, 30-35.

Begemann, G., Schilling, T.F., Rauch, G.J., Geisler, R., and Ingham, P.W. (2001). The zebrafish neckless mutation reveals a requirement for raldh2 in mesodermal signals that pattern the hindbrain. Development 128, 3081-3094.

Bel-Vialar, S., Itasaki, N., and Krumlauf, R. (2002). Initiating Hox gene expression: in the early chick neural tube differential sensitivity to FGF and RA signaling subdivides the HoxB genes in two distinct groups. Development 129, 5103-5115.

Bellairs, R., and Osmond, M. (2005). Atlas of chick development (Elsevier).

Böhmer, C. (2017). Correlation between Hox code and vertebral morphology in the mouse: towards a universal model for Synapsida. Zoological letters 3, 8.

Böhmer, C., Rauhut, O.W., and Wörheide, G. (2015a). Correlation between Hox code and vertebral morphology in archosaurs. Proceedings Biological sciences 282.

Böhmer, C., Rauhut, O.W., and Wörheide, G. (2015b). New insights into the vertebral Hox code of archosaurs. Evolution & development 17, 258-269.

Boulet, A.M., Moon, A.M., Arenkiel, B.R., and Capecchi, M.R. (2004). The roles of Fgf4 and Fgf8 in limb bud initiation and outgrowth. Dev Biol 273, 361-372.

Burke, A.C. (2000). Hox genes and the global patterning of the somitic mesoderm. Current topics in developmental biology 47, 155-181.

Burke, A.C., Nelson, C.E., Morgan, B.A., and Tabin, C. (1995). Hox genes and the evolution of vertebrate axial morphology. Development 121, 333-346.

Chambers, D., Wilson, L., Maden, M., and Lumsden, A. (2007). RALDH-independent generation of retinoic acid during vertebrate embryogenesis by CYP1B1. Development 134, 1369-1383.

Charrier, J.B., and Teillet, M.A. (1999). [Regression of Hensen's node and axial growth of the embryo]. Journal de la Societe de biologie 193, 237-241.

Chaube, S. (1959). On axiation and symmetry in transplanted wing of the chick. Journal of Experimental Zoology 140, 29-77.

Chen, F., Greer, J., and Capecchi, M.R. (1998). Analysis of Hoxa7/Hoxb7 mutants suggests periodicity in the generation of the different sets of vertebrae. Mech Dev 77, 49-57.

Chen, J.W., Zahid, S., Shilts, M.H., Weaver, S.J., Leskowitz, R.M., Habbsa, S., Aronowitz, D., Rokins, K.P., Chang, Y., Pinnella, Z., et al. (2013). Hoxa-5 acts in segmented somites to regulate cervical vertebral morphology. Mech Dev 130, 226-240.

Chuai, M., and Weijer, C.J. (2008). The mechanisms underlying primitive streak formation in the chick embryo. Current topics in developmental biology 81, 135-156.

Chuai, M., and Weijer, C.J. (2009). Regulation of cell migration during chick gastrulation. Curr Opin Genet Dev 19, 343-349.

Coelho, C.N., Sumoy, L., Kosher, R.A., and Upholt, W.B. (1992). GHox-7: a chicken homeobox-containing gene expressed in a fashion consistent with a role in patterning events during embryonic chick limb development. Differentiation; research in biological diversity 49, 85-92.

Cohn, M.J., Izpisúa-Belmonte, J.C., Abud, H., Heath, J.K., and Tickle, C. (1995). Fibroblast growth factors induce additional limb development from the flank of chick embryos. Cell 80, 739-746.

Cohn, M.J., Patel, K., Krumlauf, R., Wilkinson, D.G., Clarke, J.D., and Tickle, C. (1997). Hox9 genes and vertebrate limb specification. Nature 387, 97-101.

Crossley, P.H., Minowada, G., MacArthur, C.A., and Martin, G.R. (1996). Roles for FGF8 in the induction, initiation, and maintenance of chick limb development. Cell 84, 127-136.

Dasen, J.S., Tice, B.C., Brenner-Morton, S., and Jessell, T.M. (2005). A Hox regulatory network establishes motor neuron pool identity and target-muscle connectivity. Cell 123, 477-491.

DeRuiter, Corinne,, Doty, Maria, "Gastrulation in Gallus gallus (Domestic Chicken)". *Embryo Project Encyclopedia* (2011-06-21). ISSN: 1940-5030

de Santa Barbara, P., and Roberts, D.J. (2002). Tail gut endoderm and gut/genitourinary/tail development: a new tissue-specific role for Hoxa13. Development 129, 551-561.

Denans, N., Iimura, T., and Pourquié, O. (2015). Hox genes control vertebrate body elongation by collinear Wnt repression. eLife 4.

Downs, K.M. (2009). The enigmatic primitive streak: prevailing notions and challenges concerning the body axis of mammals. BioEssays : news and reviews in molecular, cellular and developmental biology 31, 892-902.

Duboule, D., and Dollé, P. (1989). The structural and functional organization of the murine HOX gene family resembles that of Drosophila homeotic genes. Embo j 8, 1497-1505.

Fernandez-Teran, M., and Ros, M.A. (2008). The Apical Ectodermal Ridge: morphological aspects and signaling pathways. The International journal of developmental biology 52, 857-871.

Fromental-Ramain, C., Warot, X., Lakkaraju, S., Favier, B., Haack, H., Birling, C., Dierich, A., Doll e, P., and Chambon, P. (1996a). Specific and redundant functions of the paralogous Hoxa-9 and Hoxd-9 genes in forelimb and axial skeleton patterning. Development 122, 461-472.

Fromental-Ramain, C., Warot, X., Messadecq, N., LeMeur, M., Dollé, P., and Chambon, P. (1996b). Hoxa-13 and Hoxd-13 play a crucial role in the patterning of the limb autopod. Development 122, 2997-3011.

Garcia-Gasca, A., and Spyropoulos, D.D. (2000). Differential mammary morphogenesis along the anteroposterior axis in Hoxc6 gene targeted mice. Developmental dynamics: an official publication of the American Association of Anatomists 219, 261-276.

Gaunt, S.J., and Strachan, L. (1996). Temporal colinearity in expression of anterior Hox genes in developing chick embryos. Dev Dyn 207, 270-280.

Gehring, W.J., Müller, M., Affolter, M., Percival-Smith, A., Billeter, M., Qian, Y.Q., Otting, G., and Wüthrich, K. (1990). The structure of the homeodomain and its functional implications. Trends in genetics : TIG 6, 323-329.

Gibson-Brown, J.J., Agulnik, S.I., Chapman, D.L., Alexiou, M., Garvey, N., Silver, L.M., and Papaioannou, V.E. (1996). Evidence of a role for T-box genes in the evolution of limb morphogenesis and the specification of forelimb/hindlimb identity. Mech Dev 56, 93-101.

Gouveia, A., Marcelino, H.M., Gonçalves, L., Palmeirim, I., and Andrade, R.P. (2015). Patterning in time and space: HoxB cluster gene expression in the developing chick embryo. Cell cycle (Georgetown, Tex) 14, 135-145.

Grieshammer, U., Minowada, G., Pisenti, J.M., Abbott, U.K., and Martin, G.R. (1996). The chick limbless mutation causes abnormalities in limb bud dorsal-ventral patterning: implications for the mechanism of apical ridge formation. Development 122, 3851-3861.

Gros, J., and Tabin, C.J. (2014). Vertebrate limb bud formation is initiated by localized epithelial-to-mesenchymal transition. Science 343, 1253-1256.

Hamburger, V., and Hamilton, H.L. (1951). A series of normal stages in the development of the chick embryo. Journal of morphology 88, 49-92.

Hasson, P., Del Buono, J., and Logan, M.P. (2007). Tbx5 is dispensable for forelimb outgrowth. Development 134, 85-92.

Horan, G., Ramírez-Solis, R., Featherstone, M.S., Wolgemuth, D.J., Bradley, A., and Behringer, R.R. (1995a). Compound mutants for the paralogous hoxa-4, hoxb-4, and hoxd-4 genes show more complete homeotic transformations and a dose-dependent increase in the number of vertebrae transformed. Genes & development 9, 1667-1677.

Horan, G., Wu, K., Wolgemuth, D.J., and Behringer, R.R. (1994). Homeotic transformation of cervical vertebrae in Hoxa-4 mutant mice. Proceedings of the National Academy of Sciences 91, 12644-12648.

Horan, G.S., Kovàcs, E.N., Behringer, R.R., and Featherstone, M.S. (1995b). Mutations in paralogous Hox genes result in overlapping homeotic transformations of the axial skeleton: evidence for unique and redundant function. Developmental biology 169, 359-372.

Iimura, T., and Pourquie, O. (2006). Collinear activation of Hoxb genes during gastrulation is linked to mesoderm cell ingression. Nature 442, 568-571.

Jeannotte, L., Lemieux, M., Charron, J., Poirier, F., and Robertson, E. (1993). Specification of axial identity in the mouse: role of the Hoxa-5 (Hox1. 3) gene. Genes & development 7, 2085-2096.

Jin, L., Wu, J., Bellusci, S., and Zhang, J.S. (2018). Fibroblast Growth Factor 10 and Vertebrate Limb Development. Frontiers in genetics 9, 705.

Johnson, R.L., Riddle, R.D., Laufer, E., and Tabin, C. (1994). Sonic hedgehog: a key mediator of anterior-posterior patterning of the limb and dorso-ventral patterning of axial embryonic structures. Biochemical Society transactions 22, 569-574.

Kawakami, Y., Capdevila, J., Buscher, D., Itoh, T., Rodriguez Esteban, C., and Izpisua Belmonte, J.C. (2001). WNT signals control FGF-dependent limb initiation and AER induction in the chick embryo. Cell 104, 891-900.

Kengaku, M., Capdevila, J., Rodriguez-Esteban, C., De La Pena, J., Johnson, R.L., Izpisua Belmonte, J.C., and Tabin, C.J. (1998). Distinct WNT pathways regulating AER formation and dorsoventral polarity in the chick limb bud. Science 280, 1274-1277.

Kessel, M., and Gruss, P. (1990). Murine developmental control genes. Science 249, 374-379.

Kessel, M., and Gruss, P. (1991). Homeotic transformations of murine vertebrae and concomitant alteration of Hox codes induced by retinoic acid. Cell 67, 89-104.

Kostic, D., and Capecchi, M.R. (1994). Targeted disruptions of the murine Hoxa-4 and Hoxa-6 genes result in homeotic transformations of components of the vertebral column. Mechanisms of development 46, 231-247.

Krumlauf, R. (2016). Hox Genes and the Hindbrain: A Study in Segments. Current topics in developmental biology 116, 581-596.

Lawson, A., Colas, J.F., and Schoenwolf, G.C. (2001). Classification scheme for genes expressed during formation and progression of the avian primitive streak. The Anatomical record 262, 221-226.

Lim, A.A., Karakla, D.W., and Watkins, D.V. (1999). Osteoradionecrosis of the cervical vertebrae and occipital bone: a case report and brief review of the literature. American journal of otolaryngology 20, 408-411.

Liu, X., Zhang, Y., Liu, W., Li, Y., Pan, J., Pu, Y., Han, J., Orlando, L., Ma, Y., and Jiang, L. (2022). A single-nucleotide mutation within the TBX3 enhancer increased body size in Chinese horses. Curr Biol 32, 480-487.e486.

Lours, C., and Dietrich, S. (2005). The dissociation of the Fgf-feedback loop controls the limbless state of the neck. Development 132, 5553-5564.

Mahmood, R., Bresnick, J., Hornbruch, A., Mahony, C., Morton, N., Colquhoun, K., Martin, P., Lumsden, A., Dickson, C., and Mason, I. (1995). A role for FGF-8 in the initiation and maintenance of vertebrate limb bud outgrowth. Curr Biol 5, 797-806.

Mallo, M. (2018). Reassessing the Role of Hox Genes during Vertebrate Development and Evolution. Trends in genetics : TIG 34, 209-217.

Mallo, M., Wellik, D.M., and Deschamps, J. (2010). Hox genes and regional patterning of the vertebrate body plan. Dev Biol 344, 7-15.

Marigo, V., Laufer, E., Nelson, C.E., Riddle, R.D., Johnson, R.L., and Tabin, C. (1996). Sonic hedgehog regulates patterning in early embryos. Biochem Soc Symp 62, 51-60.

McIntyre, D.C., Rakshit, S., Yallowitz, A.R., Loken, L., Jeannotte, L., Capecchi, M.R., and Wellik, D.M. (2007). Hox patterning of the vertebrate rib cage. Development 134, 2981-2989.

McQueen, C., and Towers, M. (2020). Establishing the pattern of the vertebrate limb. Development 147.

Michaud, J.L., Lapointe, F., and Le Douarin, N.M. (1997). The dorsoventral polarity of the presumptive limb is determined by signals produced by the somites and by the lateral somatopleure. Development 124, 1453-1463.

Mikawa, T., Poh, A.M., Kelly, K.A., Ishii, Y., and Reese, D.E. (2004). Induction and patterning of the primitive streak, an organizing center of gastrulation in the amniote. Dev Dyn 229, 422-432.

Min, H., Danilenko, D.M., Scully, S.A., Bolon, B., Ring, B.D., Tarpley, J.E., DeRose, M., and Simonet, W.S. (1998). Fgf-10 is required for both limb and lung development and exhibits striking functional similarity to Drosophila branchless. Genes Dev 12, 3156-3161.

Minguillon, C., Nishimoto, S., Wood, S., Vendrell, E., Gibson-Brown, J.J., and Logan, M.P. (2012). Hox genes regulate the onset of Tbx5 expression in the forelimb. Development 139, 3180-3188.

Molven, A., Wright, C.V., Bremiller, R., De Robertis, E.M., and Kimmel, C.B. (1990). Expression of a homeobox gene product in normal and mutant zebrafish embryos: evolution of the tetrapod body plan. Development 109, 279-288.

Moreau, C., Caldarelli, P., Rocancourt, D., Roussel, J., Denans, N., Pourquie, O., and Gros, J. (2019). Timed Collinear Activation of Hox Genes during Gastrulation Controls the Avian Forelimb Position. Curr Biol 29, 35-50 e34.

Mortlock, D.P., and Innis, J.W. (1997). Mutation of HOXA13 in hand-foot-genital syndrome. Nat Genet 15, 179-180.

Mukaigasa, K., Sakuma, C., Okada, T., Homma, S., Shimada, T., Nishiyama, K., Sato, N., and Yaginuma, H. (2017). Motor neurons with limb-innervating character in the cervical spinal cord are sculpted by apoptosis based on the Hox code in chick embryo. Development 144, 4645-4657.

Nakamura, T., Gehrke, A.R., Lemberg, J., Szymaszek, J., and Shubin, N.H. (2016). Digits and fin rays share common developmental histories. Nature 537, 225-228.

Nelson, C.E., Morgan, B.A., Burke, A.C., Laufer, E., DiMambro, E., Murtaugh, L.C., Gonzales, E., Tessarollo, L., Parada, L.F., and Tabin, C. (1996). Analysis of Hox gene expression in the chick limb bud. Development 122, 1449-1466.

Neumann, C.J., Grandel, H., Gaffield, W., Schulte-Merker, S., and Nüsslein-Volhard, C. (1999). Transient establishment of anteroposterior polarity in the zebrafish pectoral fin bud in the absence of sonic hedgehog activity. Development 126, 4817-4826.

Ng, J.K., Kawakami, Y., Buscher, D., Raya, A., Itoh, T., Koth, C.M., Rodriguez Esteban, C., Rodriguez-Leon, J., Garrity, D.M., Fishman, M.C., et al. (2002). The limb identity gene Tbx5 promotes limb initiation by interacting with Wnt2b and Fgf10. Development 129, 5161-5170.

Nishimoto, S., Minguillon, C., Wood, S., and Logan, M.P. (2014). A combination of activation and repression by a colinear Hox code controls forelimb-restricted expression of Tbx5 and reveals Hox protein specificity. PLoS Genet 10, e1004245.

Nishimoto, S., Wilde, S.M., Wood, S., and Logan, M.P. (2015). RA Acts in a Coherent Feed-Forward Mechanism with Tbx5 to Control Limb Bud Induction and Initiation. Cell Rep 12, 879-891.

Noramly, S., Pisenti, J., Abbott, U., and Morgan, B. (1996). Gene expression in the limbless mutant: polarized gene expression in the absence of Shh and an AER. Dev Biol 179, 339-346.

Nowicki, J.L., and Burke, A.C. (2000). Hox genes and morphological identity: axial versus lateral patterning in the vertebrate mesoderm. Development 127, 4265-4275.

Nüsslein-Volhard, C., and Wieschaus, E. (1980). Mutations affecting segment number and polarity in Drosophila. Nature 287, 795-801.

Nüsslein-Volhard, C., Wieschaus, E., and Kluding, H. (1984). Mutations affecting the pattern of the larval cuticle inDrosophila melanogaster. Wilhelm Roux's archives of developmental biology 193, 267-282.

Ohuchi, H., Nakagawa, T., Yamamoto, A., Araga, A., Ohata, T., Ishimaru, Y., Yoshioka, H., Kuwana, T., Nohno, T., Yamasaki, M., et al. (1997). The mesenchymal factor, FGF10, initiates and maintains the outgrowth of the chick limb bud through interaction with FGF8, an apical ectodermal factor. Development 124, 2235-2244.

Ohya, Y.K., Kuraku, S., and Kuratani, S. (2005). Hox code in embryos of Chinese soft-shelled turtle Pelodiscus sinensis correlates with the evolutionary innovation in the turtle. Journal of experimental zoology Part B, Molecular and developmental evolution 304, 107-118.

Pick, L. (2016). Hox genes, evo-devo, and the case of the ftz gene. Chromosoma 125, 535-551.

Prahlad, K.V., Skala, G., Jones, D.G., and Briles, W.E. (1979). Limbless: a new genetic mutant in the chick. The Journal of experimental zoology 209, 427-434.

Rallis, C., Bruneau, B.G., Del Buono, J., Seidman, C.E., Seidman, J.G., Nissim, S., Tabin, C.J., and Logan, M.P. (2003). Tbx5 is required for forelimb bud formation and continued outgrowth. Development 130, 2741-2751.

Ramfrez-Solis, R., Zheng, H., Whiting, J., Krumlauf, R., and Bradley, A. (1993). Hoxb-4 (Hox-2.6) mutant mice show homeotic transformation of a cervical vertebra and defects in the closure of the sternal rudiments. Cell 73, 279-294.

Rancourt, D.E., Tsuzuki, T., and Capecchi, M.R. (1995). Genetic interaction between hoxb-5 and hoxb-6 is revealed by nonallelic noncomplementation. Genes & Development 9, 108-122.

Riddle, R.D., Johnson, R.L., Laufer, E., and Tabin, C. (1993). Sonic hedgehog mediates the polarizing activity of the ZPA. Cell 75, 1401-1416.

Ros, M.A., Dahn, R.D., Fernandez-Teran, M., Rashka, K., Caruccio, N.C., Hasso, S.M., Bitgood, J.J., Lancman, J.J., and Fallon, J.F. (2003). The chick oligozeugodactyly (ozd) mutant lacks sonic hedgehog function in the limb. Development 130, 527-537.

Ros, M.A., López-Martínez, A., Simandl, B.K., Rodriguez, C., Izpisua Belmonte, J., Dahn, R., and Fallon, J.F. (1996). The limb field mesoderm determines initial limb bud anteroposterior asymmetry and budding independent of sonic hedgehog or apical ectodermal gene expressions. Development 122, 2319-2330.

Scotti, M., Kherdjemil, Y., Roux, M., and Kmita, M. (2015). A Hoxa13:Cre mouse strain for conditional gene manipulation in developing limb, hindgut, and urogenital system. Genesis (New York, NY : 2000) 53, 366-376.

Sekine, K., Ohuchi, H., Fujiwara, M., Yamasaki, M., Yoshizawa, T., Sato, T., Yagishita, N., Matsui, D., Koga, Y., Itoh, N., et al. (1999). Fgf10 is essential for limb and lung formation. Nat Genet 21, 138-141.

Sheeba, C.J., Andrade, R.P., and Palmeirim, I. (2016). Getting a handle on embryo limb development: Molecular interactions driving limb outgrowth and patterning. Seminars in cell & developmental biology 49, 92-101.

Stainton, H., and Towers, M. (2022). Retinoic acid influences the timing and scaling of avian wing development. Cell Rep 38, 110288.

Stratford, T., Horton, C., and Maden, M. (1996). Retinoic acid is required for the initiation of outgrowth in the chick limb bud. Curr Biol 6, 1124-1133.

Sweetman, D., Wagstaff, L., Cooper, O., Weijer, C., and Münsterberg, A. (2008). The migration of paraxial and lateral plate mesoderm cells emerging from the late primitive streak is controlled by different Wnt signals. BMC developmental biology 8, 63.

Takeuchi, J.K., Koshiba-Takeuchi, K., Suzuki, T., Kamimura, M., Ogura, K., and Ogura, T. (2003). Tbx5 and Tbx4 trigger limb initiation through activation of the Wnt/Fgf signaling cascade. Development 130, 2729-2739.

Tam, P.P., and Behringer, R.R. (1997). Mouse gastrulation: the formation of a mammalian body plan. Mech Dev 68, 3-25.

Tickle, C. (2002). Molecular basis of vertebrate limb patterning. American journal of medical genetics 112, 250-255.

Tickle, C. (2015). How the embryo makes a limb: determination, polarity and identity. Journal of anatomy 227, 418-430.

Tickle, C., and Towers, M. (2017). Sonic Hedgehog Signaling in Limb Development. Frontiers in cell and developmental biology 5, 14.

van den Akker, E., Fromental-Ramain, C., de Graaff, W., Le Mouellic, H., Brûlet, P., Chambon, P., and Deschamps, J. (2001). Axial skeletal patterning in mice lacking all paralogous group 8 Hox genes. Development 128, 1911-1921.

Vilches-Moure, J.G. (2019). Embryonic Chicken (Gallus gallus domesticus) as a Model of Cardiac Biology and Development. Comparative medicine 69, 184-203.

Vogel, A., Rodriguez, C., and Izpisúa-Belmonte, J.-C. (1996). Involvement of FGF-8 in initiation, outgrowth and patterning of the vertebrate limb. Development 122, 1737-1750.

Wellik, D.M. (2007). Hox patterning of the vertebrate axial skeleton. Developmental dynamics: an official publication of the American Association of Anatomists 236, 2454-2463.

Wellik, D.M. (2009). Hox genes and vertebrate axial pattern. Current topics in developmental biology 88, 257-278.

Wellik, D.M., and Capecchi, M.R. (2003). Hox10 and Hox11 genes are required to globally pattern the mammalian skeleton. Science 301, 363-367.

Xu, B., Hrycaj, S.M., McIntyre, D.C., Baker, N.C., Takeuchi, J.K., Jeannotte, L., Gaber, Z.B., Novitch, B.G., and Wellik, D.M. (2013). Hox5 interacts with Plzf to restrict Shh expression in the developing forelimb. Proc Natl Acad Sci U S A 110, 19438-19443.

Xu, B., and Wellik, D.M. (2011). Axial Hox9 activity establishes the posterior field in the developing forelimb. Proc Natl Acad Sci U S A 108, 4888-4891.

Young, J.J., Grayson, P., Edwards, S.V., and Tabin, C.J. (2019). Attenuated Fgf Signaling Underlies the Forelimb Heterochrony in the Emu Dromaius novaehollandiae. Curr Biol 29, 3681-3691.e3685.

Young, T., Rowland, J.E., van de Ven, C., Bialecka, M., Novoa, A., Carapuco, M., van Nes, J., de Graaff, W., Duluc, I., Freund, J.N., et al. (2009). Cdx and Hox genes differentially regulate posterior axial growth in mammalian embryos. Developmental cell 17, 516-526.

Zakany, J., and Duboule, D. (2007). The role of Hox genes during vertebrate limb development. Current opinion in genetics & development 17, 359-366.

6 Acknowledgement

At the end of my doctoral study, I would like to look back on my academic career and give my gratitude to everyone who has provided me with so much help over these years. Firstly, I appreciate to my supervisor Prof. Dr. med. Ruijin Huang, for giving me the opportunity to work with him at the University of Bonn. His consideration, encouragement and patience, especially his professionalism, gave me confidence in my work and in my four years of life abroad. Thanks to the help of Prof. Huang, I have not only improved my skills in academic research but also enriched my life in Germany and even Europe.

I would like to thank all of my colleagues in the Institute of Anatomy, especially the Neuroanatomy group. I thank the encouragement from Prof. Dr. Thomas Franz, Prof. Dr. Karl Schilling and Prof. Dr. Stephan Baader. I thank Maik Hintze for the instruction on my experiments and the advice for writing the paper. I thank Prof. Jinbao Wang who gave me confidence and helped me with my experiments even when I wanted to give up. I thank the cooperation from Hengxun Tao, Peng Zhou, Longfei Cheng and Qin Pu, and thank Ms. Sandra Gräfe, Ms. Rau Birgit, Ms. Angelica Zoons, Ms. Birgit Blanck, Ms. Marion Michels for the daily lab assistance. I thank Mr. Heinz Bioernsen and the Institute of Animal Science, Agriculture Faculty for delivering experimental materials. I would also like to thank Prof. Jörg Wilting and Dr. Rittika Chunder who put effort to improve the writing of my thesis. Finally, I want to thank Prof. Stefanie Kürten for her support in several aspects.

I would like to thank the following institutions for their financial support, including the China Scholarship Council (CSC), DFG, DAAD and the Institute of Anatomy. Thank you for supporting my study and life in Germany.

Besides the help during these four years, I would also like to acknowledge Prof. Yanfang Wang and Prof. Cong Tao. They are the leaders in my scientific career. Their self-discipline and rigorous attitude influenced me to put in the effort and stay focused on the details. Their influence allowed me to be objective to analyze and solve problems and to be interested in as well as enjoy the research. The motivation and consideration of my colleagues in the Institute of Animal Science, Chinese Academy of Agricultural Sciences also positively influenced me to go ahead.

At last, I would like to wholeheartedly thank my family. Although my parents were worried about me, they still stood by me when I insisted to study in Germany. It was just like that, that I was focused on the entrance examination for the master's study, although they were afraid of my failure without a chance for further study. Maybe sometimes we need to take chances and have a last stand. As Jack Ma said, you still need to have a dream, what if it came true? During my four years of study, the communication between me and my parents has been improved. And the encouragement and understanding of my parents are the origins of my motivation. I thank them from my heart. Even my younger brother gave me company. Several months later, he will take part in the national college entrance examination. I hope he knows it is not too late to study hard now and this challenge is not going to dictate the outcome of his life; it is just a crossing during his long life.

The end of my doctoral study means a new beginning to the next journey of my life. The experience gained during this phase encourages me to be powerful and optimistic about my future.